

NUMERICAL SIMULATION OF THE BASE-LEVEL BUFFERS  
AND BUTTRESSES CONCEPTUAL MODEL  
OF FLUVIAL SYSTEMS

by

RONNIE TOOYAK TINGOOK

Presented to the Faculty of the Graduate School of  
The University of Texas at Arlington in Partial Fulfillment  
of the Requirements  
for the Degree of

DOCTOR OF PHILOSOPHY

THE UNIVERSITY OF TEXAS AT ARLINGTON

May 2012

Copyright © by Ronnie Tooyak Tingook 2012

All Rights Reserved

## ACKNOWLEDGEMENTS

First and foremost I would like to acknowledge the constant support and guidance offered me by my advisor, Dr. John Holbrook. From the first day I met him whilst considering the pursuit of a Ph.D., it was his voice of encouragement that led me to apply to the UTA. I look forward to working with Dr. Holbrook in the decades to come in the pursuit of the ultimate message the rocks give us: "...it is", ours is the task of discerning what is there.

There are others in the department of geoscience at the UTA that I would like to acknowledge as well for their support and assistance along the way, including my committee members Dr. John Wickham, Dr. Merlynd Nestell, Dr. Max Hu, and Dr. James Grover from the biology department. Dr. John McEnery, Dr. Harry Rowe, and Dr. Andrew Hunt were readily available to answer questions and otherwise chat about my work.

I would like to acknowledge my grandparents, parents, brothers and sister and other extended family who have also encouraged me to pursue higher education. Finally, I would like to acknowledge the loving support my dear wife, Parisa Lotfi, whose constant support throughout my time at the UTA have kept the goal of finishing alive, even at times when quitting and going back to work in industry looked very attractive.

April 20, 2012

## ABSTRACT

# NUMERICAL SIMULATION OF THE BASE-LEVEL BUFFERS AND BUTTRESSES MODEL OF FLUVIAL SYSTEMS

Ron Tingook, PhD

The University of Texas at Arlington, 2012

Supervising Professor: John M. Holbrook

A “buffer” in fluvial stratigraphy is a surface which defines either: a) the lowest possible depth to which streams will incise; or b) the maximum elevation to which aggradation will occur; together, these surfaces define a buffer zone. The buffer zone is tied down profile to a “buttress” which defines base level for the system. A buttress shift, e.g., change in sea-level or shoreline-trajectory (*sensu* Catuneanu et al., 2009), will effect a change as to where the buffer zone exists for a fluvial system at a particular point in time.

This work expounds upon the base level buffers and buttresses concepts by running a numerical model of landscape evolution, the Channel-Hillslope Integrated Landscape Development model (CHILD) (Tucker et al., 2001). Simulation of aggradation/degradation cycles using the CHILD Model shows that the buffer zone increases in thickness from a zero-thickness at the drainage divide, remains thin through provenance bed-rock streams, thickens through alluvial rivers to a maximum near the junction(s) of major tributaries and the basin’s primary trunk river, then thins downstream to one-channel thickness at the strand. Furthermore, an examination of existing literature shows that for periods of buttress stability and quiescent

tectonics, buffer zones can attain thicknesses of over 150m due to climate variations, supporting local incision of valleys to comparable scale.

Channel scour at confluences and sharp bends in the streams were also present in the model and it shown that a local increase in discharge is the primary driver in the creation of fluvial scour.

This work has important implications on reservoir characterization and subsurface data interpretation, in that fluvial-valley geometries can be implied laterally away from a bore-hole. This also implies that deep valleys can be carved during falling and lowstand phases without significant buttress drop.

## TABLE OF CONTENTS

ACKNOWLEDGEMENTS.....	iii
ABSTRACT.....	iv
LIST OF ILLUSTRATIONS.....	ix
LIST OF TABLES .....	xv
Chapter .....	Page
1. INTRODUCTION.....	1
1.1 Fluvial Landscapes.....	1
1.1.1 Fluvial Valleys.....	3
1.1.1.1 Structural Valley.....	3
1.1.1.2 Denudation Valley.....	4
1.1.1.3 Buttress Valley .....	5
1.1.1.4 Buffer Valley.....	6
1.2 Landscape Evolution Model (LEM) .....	8
1.3 Base-Level Buffers and Buttresses .....	9
1.3.1 Upstream versus Downstream Controls.....	11
2 FLUVIAL VALLEYS .....	13
2.1 Buffer Valley Extents.....	13
2.1.1 River Incision and Aggradation .....	14
2.1.2 Quaternary Buffer Valleys .....	15
2.1.2.1 Colorado River .....	15
2.1.2.2 Upper Thames River, U.K.....	17
2.1.2.3 Gibbler Gulch, Colorado .....	20

	2.1.2.4 Rio Diamante, Argentina.....	22
	2.1.2.5 Texas Gulf Coast .....	24
	2.1.3 Discussion .....	27
3	LANDSCAPE EVOLUTION MODELING.....	28
	3.1 Channel-Hillslope Integrated Landscape Development Model.....	28
	3.1.1 Triangulated Irregular Network (TIN).....	29
	3.1.2 Governing Equations .....	31
	3.1.2.1 Conservation of Mass .....	32
	3.1.2.2 Climate Inputs .....	32
	3.1.2.3 Surface Runoff .....	34
	3.1.2.4 Hillslope Process .....	35
	3.1.2.5 Bed Load Transport Equations .....	36
	3.1.2.5.1 Meyer-Peter and Muller .....	37
	3.1.2.6 Dynamic Vegetation.....	41
	3.1.2.7 Slope Area Relationship .....	43
	3.1.3 Running CHILD .....	44
	3.1.3.1 Simplicity of Mass Transport Laws .....	46
	3.2 Methods .....	47
	3.2.1 Aggradation of Sediment in Valleys .....	56
	3.3 Discussion .....	70
4	RIVER SCOUR.....	74
	4.1 Scour Types .....	74
	4.1.1 Characteristic Fluid Flow at Confluences .....	75
	4.1.2 Flume Studies and Field Investigations.....	77
	4.2 Methods .....	81

5	CHAPTER FIVE.....	85
	5.1 Conclusions.....	85
	REFERENCES .....	87
	BIOGRAPHICAL INFORMATION .....	109



## LIST OF ILLUSTRATIONS

Figure	Page
1 Example of a structural valley. The figure shows a high altitude regional view of the Dead Sea Transform fault system which created the Jordan Rift valley and the Dead Sea basin. The structural low of the valley confines the fluvial systems laterally. <a href="http://woodshole.er.usgs.gov/project-pages/dead_sea/images/DSgenMaptopo.jpg">http://woodshole.er.usgs.gov/project-pages/dead_sea/images/DSgenMaptopo.jpg</a> .....	4
2 Arial view of the Colorado River in Canyonlands National Park near Moab, Utah. The river has created a denudation valley as the Colorado Plateau geologic province has uplifted over the past ~6Myr .....	5
3 Diagrammatic depiction of the initiation of a buttress valley formed by headward knickpoint migration after a significant drop in elevation of the buttress. A is the system sea level at time one (T1), and B is the system after sea level drops at time two (T2) .....	6
4 Diagram of a buffer valley on a landscape that is otherwise in equilibrium with sea level (the buttress). Internal complexity of the buffer valley due to multiple episodes of aggradation and incision are shown by the terraces .....	7
5 Diagram of a buffer valley and a landward migrating buttress valley formed from a drop in elevation of the buttress at time two; in time the two valleys will merge in the vicinity of the buffer valley and a complex valley will be created by controls from the two processes .....	8
6 Visual representation of the Buffers and Buttresses concept of Holbrook et al. (2006). Fluvial system's channel elevations are lowest at the buttress but may exhibit an instantaneous profile (black) of any geometry within the buffer zone based on upstream controls. Elevations to which the instantaneous profiles attain through time (red lines) define the preservation space of the system. The buffer zone narrows downstream to one channel thickness at the buttress. After (Holbrook et al., 2006) .....	11
7 Watershed of the Colorado River (red stippled line), Southwestern United States. Area of interest for this paper is from the Lake Mead area south to the United States/Mexico border. From <a href="http://www.usbr.gov/lc/images/maps/crbsnmap.gif">http://www.usbr.gov/lc/images/maps/crbsnmap.gif</a> .....	16

8 Map of Upper Thames River from Stermerdink et al., 2010, (their Figure 1) showing their study location at “A”. The Legend shows ground elevation in meters .....	18
9 Stermerdink et al. (2010) figure showing Marine Isotope Stages (Emiliani, 1955). (A) Modeled elevations of beds using the Fluver2 model, and (B) actual heights of beds from field data .....	19
10 Gibbler Gulch in western Colorado near Moab, Utah where incision / aggradational cycles are present. (a) Map of drainage basin, (b) larger scale map showing extent of the Qt2 terrace .....	21
11 Cross-section and longitudinal profile of the Gibbler Gulch in western Colorado. (A) Initial surface beneath Qt2 is a denudation valley, very likely produced by uplift of the Colorado Plateau; aggradation above that surface produces the Qt2 terrace. The Qt2 terrace is subsequently incised, then aggradation occurs to produce the Qt1 terrace, and finally incising to the present day elevation. (B) Dip cross sectional view of the Qt2 terrace. From Jones et al. (2010) .....	22
12 Area studied by Baker, et al., 2010, showing the location of the cross-section in Figure 13. Notice that their study area is in a region of uplift mostly responsible for the deep incision of the Rio Diamante River. Because the location is at a latitude that produces a rain shadow, we expect that only desert vegetation existed there in the recent past. Modified from Baker et al., 2010 .....	23
13 Cross-section of the Rio Diamante River, in the piedmont area of Argentina, showing overall incision with intervals of aggradation. This is shown to illustrate the aggradation of the Qt2 terrace, which is built upon the Qt2 strath terrace. From Baker et al., 2010.....	24
14 Map of fluvial valleys along the Texas Gulf Coast. From Blum and Aslan, 2006.....	25
15 Figure modified from Blum, 1993, showing schematic cross section of Holocene terraces ~ 10m thick in the Colorado River Drainage, Texas gulf coast. (A) Relationship of EH incising into LP; (B) LH incising into EH; (C) LH aggrading over EH; (D) modern river incising into LH .....	26
16 Example of a 3D surface created by CHILD and displayed with MATLAB software. Dimensions are in meters .....	28

17 Nodes, Delauny Triangles (Black lines), Voronoi Polygons (gray lines), and flow lines (arrows) of the TIN. Modified from Tucker et al., 2001 .....	29
18 Mesh types used to begin a new run in CHILD. We used the Perturbed Hexagonal Mesh for runs in this work .....	30
19 Example of various boundary types that CHILD can implement. ....	31
20 Distribution of rainfall from a single storm event. From Tucker et al., 2001, modified after Eagleson, 1978 .....	33
21 Variation among common bed-load transport equations .....	38
22 Graph from Lick et al. (2004), showing critical shear stress for various quartz grain sizes. Their Figure 6. Boxes are data points for a mixture of sand and 2% bentonite; x's are quartz grains only. Notice that 1000 micrometers (1 mm), critical shear stress is set at 0.4 newton's per square meter .....	39
23 Modified after Miller et al. (1977), showing a critical shear stress value of 70 dynes per cm <sup>2</sup> for a 1 mm sand grain. When converted, 70 dynes per cm <sup>2</sup> is equal to seven Pascals .....	40
24 Graph produced by the U.S. Bureau of Reclamation showing critical tractive force required to entrain a sand grain; notice that for a 1mm grain the force ranges from 170 – 450 g/m <sup>2</sup> , which converts to 1.66 to 4.41 pascals .....	41
25 Shear stresses which different types of vegetation are able to withstand in lbs / sq ft. Modified from Fischenich, 2001 .....	43
26 Display of channel slope vs. catchment area on log-log plot showing a constant regression. It is normal for there to be variation of slope for small drainage areas when landscapes are at equilibrium .....	44
27 Example of the computer interface initiating a run of the CHILD model.....	45
28 Flow chart showing how CHILD iterates though a run. Modified after Tucker et al., 2001 .....	46
29 Original surface topography for which changes in vegetation shear stresses and climate parameters were changed to initiate aggradation .....	48
30 Display of original surface showing slope angles of the drainage basin .....	49

31 Histogram showing distribution of Dip angles for original surface; max = 46.73 degrees; mean = 19.53 degrees; standard deviation = 10.55. Percent of total data points (Y axis) and angle in degrees (X axis).....	50
32 Satellite image from GoogleEarth showing the location of the Black Mountains in New Mexico, United States .....	51
33 GoogleEarth image of a drainage basin considered comparable to the one created by CHILD in this study located near the Black Mountains of New Mexico, United States .....	52
34 DEM data from the USGS of North and South Black Mountains, NM. Black polygon shows area that was initially clipped and used for statistical analysis .....	53
35 Flipped drainage basin on the western flanks of the Black Mountains, NM .....	54
36 Comparable basin from New Mexico (clear). Though the drainage basin is slightly steeper with a greater range of elevations, we consider it to be a comparable basin in drainage density and hillslope angles .....	55
37 Histograms showing distributions of hillslope dip angles for surfaces in Figure 35. Right Histogram: max = 46.73 degrees; mean = 19.53 degrees; standard deviation = 10.55. Left Histogram: max = 52.13 degrees; mean = 27.21 degrees; standard deviation = 8.13. Percent of total data points (Y axis) and angle in degrees (X axis).....	56
38 Comparison of original surface and the modified landscape after 10 years of climate and vegetation change. Notice that erosion occurs at the headlands of first-order valleys whilst deposition occurs in the higher-order valley bottoms.....	58
39 Isopach between the original surface and a 10 year surface which represents 10 years of model run at new climate and vegetation parameters .....	59
40 Isopach map between Original surface and 10 year surface of aggradation. Bold contours from the original surface colored according to z-values are superimposed. This display shows the distribution of the eroded areas, which represent areas where the change in vegetation was most susceptible to erosion.....	60
41 3D view from above and south of the resultant surface after 100 years of aggradation .....	61

42 Hillslope dip angles for the final surface of aggradation. Notice that the landscape overall is denuded, with low hillslope dip angles and relatively flat valley floors.....	62
43 Histogram showing distribution of hillslope angles for the final surface of aggradation. Percent of total data points (Y - axis) and dip angle in degrees (X - axis) .....	63
44 Original surface and final surface of aggradation .....	64
45 Histograms showing the distribution of hillslope dip angles for the original surface (left) and final surface of aggradation (right). Original Surface: max = 46.73 degrees; mean = 19.53 degrees; standard deviation = 10.55. Final Surface: max = 30.72 degrees; mean = 11.16 degrees; standard deviation = 4.67 .....	65
46 Location of cross section A - A' which is run from the furthestmost first-order valley through the higher-order valleys to the outlet point of the drainage basin .....	66
47 Cross section of a buffer zone, showing the original surface (cyan) at the bottom, 10 year time steps (black), and the highest surface (light brown) at the top. 2X vertical exaggeration.....	67
48 View from above and west showing the location of a North - South cross section near the center of the drainage basin.....	68
49 North to South cross section of the landscape. Cyan line represents the original surface, light brown line represents the upper-most surface of aggradation, and black lines are 10 years steps of time .....	68
50 Isopach showing aggradation due to deposition in the valleys after 100 years of climate change. Cyan polygon outline is the position of zero thickness; outside of this polygon the surface would show negative thickness, representing erosion and denudation of the landscape .....	69
51 Log - log plot for the landscape at each time when the climate and vegetation parameters were changed. Original landscape (Blue); 10 years aggradation (Red); 20 years aggradation (Green); 40 years aggradation (Magenta); 100 years aggradation (Black) .....	70
52 Types of channel scour recognized in river systems. From Gibling (2006) .....	74

53 Flow dynamics at channel junctions. Notice the presence of zones of stagnation, flow separation, and maximum velocity. This work was originally examined by Taylor (1944) and expounded upon in subsequent years. From Best (1987) .....	76
54 Velocity vectors of stream flow at channel junctions. From Best (1987) .....	77
55 Channel scour in a modern braided stream. From Best and Ashworth, (1997) .....	78
56 Diagrams showing fluid flow dynamics at a stream channel junction (a) location of scour hole in relation to streams, and locations of cross sections A-A', and B-B'; (b) mixing of stream channel waters view from above; (c) cross section A-A' showing fluid flow dynamics (d) cross section B-B' showing fluid flow dynamics. From Mosely, (1976) .....	79
57 Depiction of helicoidal flow as shown by Paola (1987) .....	80
58 Original landscape used in this study with a red outline showing the location of both channel-bend scour and confluence scour examined in the following figures.....	81
59 Water discharge across the basin in cubic meters per minute; color bar adjusted to show slight increases at channel-bends and at confluences .....	82
60 Water discharge in cubic meters per minute shown in white; contours of elevation shown in black. Notice that a slight increase in discharge exists at the bend in the channel to 46.99 .....	83
61 Shear stresses in pascals shown in white at nodes comprising the surface. Elevations shown in black. Notice that at the channel-bend where an increase in water discharge exists, an increase in bed shear stress does not necessarily exist (the value of 90.64 at the bend, down from 92.84 just upstream).....	84

LIST OF TABLES

Table	Page
1.1 Parameters used in the CHILD Model.....	70

## CHAPTER 1

### INTRODUCTION

#### 1.1 Fluvial Landscapes

Aggradation and incision of sediment in alluvial valleys are generally understood to result from the ratio of sediment discharge ( $Q_s$ ) to water discharge ( $Q_w$ ) in the valley stream channel(s). When more sediment is available than the streams can move, i.e.  $Q_s > Q_w$ , aggradation will occur; incision ensues when the reverse is true, i.e., the streams ability to transport sediment exceeds the sediment available for transport. This idea is not new and can be dated back to the early days of earth science. However, there is a lack of literature explicitly stating how sediment is removed from, or fills valleys. This work investigates the cut and fill of fluvial valleys by virtually aggrading and incising valleys using a numerical model and examines if the model parameters required to recreate cut and fill cycles are realistic.

Grove Karl Gilbert (1877) recognized that streams tend towards a state of equilibrium with respect to water discharge and the amount of sediment they can carry and proposed the idea of an equilibrium longitudinal profile. Davis (1902) wrote about the cyclical processes of geology arguing that all landscapes advanced through stages of youthful, high-relief topography towards mature, low-relief peneplanation, only to be uplifted and the cycle repeated. The term “grade” was introduced by Davis (1902) as he described the process of evolution of landscapes which included Gilbert’s concept of an equilibrium longitudinal profile. Thus, the commonly used terms “graded profile” and “graded longitudinal profile” can be attributed to both Gilbert and Davis.

Talling (2000) suggested that streams have a tendency to maintain a Shields<sup>1</sup> Number

---

<sup>1</sup> A dimensionless number of shear stress exerted by a fluid on the surface over which it flows; used to describe the threshold (critical shields number) at which a grain will be entrained. This number incorporates bed shear stress, grain size, and grain and fluid density in a single term.



that is close to critical along stream profiles. Such a condition implies that fluvial systems tend toward an equilibrium state, commonly referred to as the “Lane Equilibrium” (Lane, 1955), where channels adjust such that there is an equilibrium between sediment load and transport capacity. However, (Phillips, 2009) suggests that such an equilibrium is “...not a goal function or attractor state”, but merely a by-product that emerges under certain conditions. My leaning in this debate is that streams do tend toward an equilibrium state.

Three primary allogenic controls of fluvial systems recognized by most workers are climate, tectonics, and sea level, which all affect the evolution of the equilibrium profile. There are autogenic controls as well. For example, local aggradation of alluvial deposits underlying a terrace formed in response to an increase in sediment from a tributary that has captured a stream up dip. There is a growing literature that examines autogenic controls on the erosion and deposition of fluvial sediment (e.g., Hajek et al., 2010; Heller et al., 2004; Pazzaglia, in press). The many processes acting on landscapes occur at various ranges of temporal and spatial scales. Though a fluvial system will always tend towards graded equilibrium, it is unlikely that equilibrium is ever achieved due to changes in the various processes affecting the system.

With the advent of sequence stratigraphy, which is a set of concepts used to interpret sediment partitioning due to processes dominantly governed by base-level (e.g., Catuneanu et al., 2009; Vail, 1977), there has been much work to place fluvial rocks in a sequence stratigraphic framework (e.g., Cross and Lessenger, 1998; Schumm and Anonymous, 1993). A significant problem in applying sequence stratigraphic concepts to fluvial strata has been the lack of appreciation for the time-transgressive nature of regional erosional surfaces preserved in alluvial rocks (Holbrook, 2001; Holbrook, 1996; Holbrook and Dunbar, 1992; Strong and Paola, 2008). Recent interest in sediment storage on the landscape, particularly with base level at maximum regression, has brought the role of valleys into focus. A brief introduction to fluvial valleys follows.

#### *1.1.1. Fluvial Valleys*

Valleys are topographic lows between highlands and are comprised of hillslopes and streams, either ephemeral or perennial. An important characteristic of a valley is that the streams remain within the valley when at flood stage. Valleys comprise drainage basins and are separated by drainage divides within the basin. Drainage basin evolution through geologic time entails the lateral migration of valleys, the denudation of the drainage divides, an increase or decrease in drainage network density, and generally an increase in the size of the drainage basin. Viewed from a geological perspective, drainage basins in general, and valleys in particular, are dynamic entities.

Four types of valleys are generally recognized: 1) structural valleys; 2) denudation valleys; 3) buttress valleys; and 4) buffer valleys.

##### *1.1.1.1. Structural Valley*

A structural valley is a topographic low that is controlled by tectonics. A typical example of such a valley is the Jordan Rift valley that marks the border between the countries of Israel and Jordan (Figure 1). Here, the topographic depression is the result of the tectonic activity at the margins of the African lithospheric plate and the Arabian plate where there has been a component of extension even though dominant motion is left-lateral strike slip (Freund et al., 1968; Klinger et al., 2000). The fluvial systems there, when active, are confined to the valley.

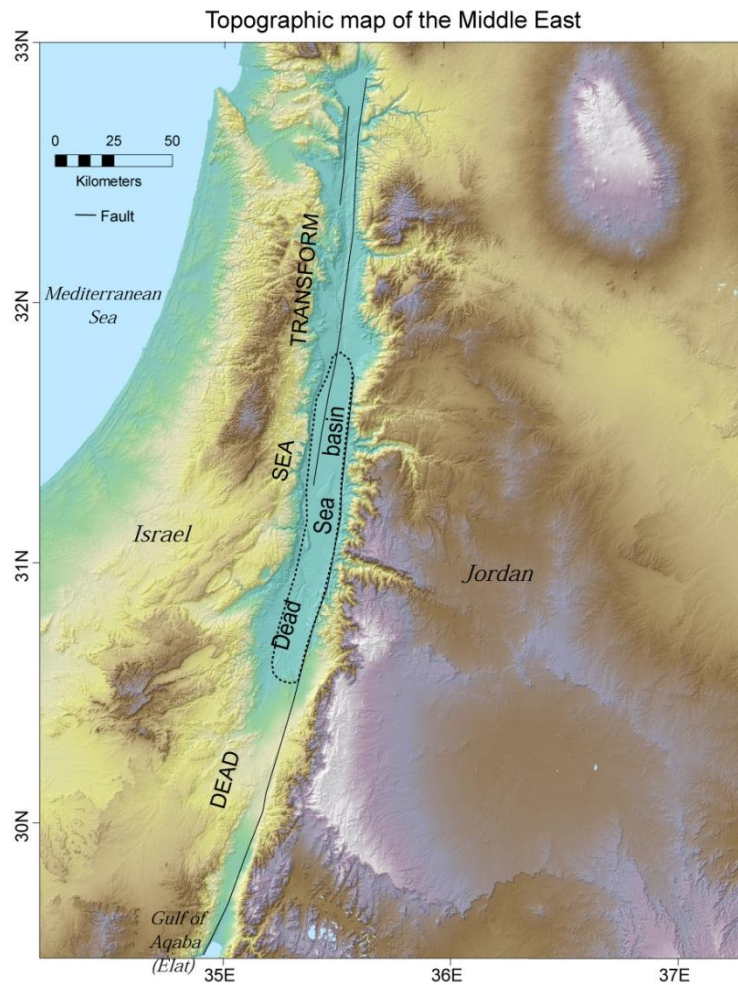


Figure 1: Example of a structural valley. The figure shows a high altitude regional view of the Dead Sea Transform fault system which created the Jordan Rift valley and the Dead Sea basin. The structural low of the valley confines the fluvial systems laterally.  
[http://woodshole.er.usgs.gov/project-pages/dead\\_sea/images/DSgenMaptopo.jpg](http://woodshole.er.usgs.gov/project-pages/dead_sea/images/DSgenMaptopo.jpg).

#### 1.1.1.2. Denudation Valley

A denudation valley is one created by streams that incise down to grade as the region over which they flow is tectonically uplifted. A classic example is the Colorado River in the vicinity of Moab, Utah (Figure 2). Here, the Colorado Plateau physiographic province has been tectonically uplifting over the past ~6Myr, presumably due to a complex convective process that

removed the upper-most mantle and asthenosphere, and replaced it with buoyant asthenosphere (Levander et al., 2011).



Figure 2: Aerial view of the Colorado River in Canyonlands National Park near Moab, Utah. The river has created a denudation valley as the Colorado Plateau geologic province has uplifted over the past ~6Myr.

#### 1.1.1.3. Buttress Valley

A buttress valley is one which owes its origin to a downward shift of a buttress (*sensu* Mackin, 1948). Briefly, a buttress is the physical feature that determines the elevation of the downstream end of a graded stream's equilibrium profile. A buttress change will render the entire profile out of equilibrium. Like the denudation valley, as the stream tends towards equilibrium after the buttress is lowered, a valley is formed; however, the mechanism for the formation of a buttress valley is the upstream migration of a knickpoint as shown in Figure 3.

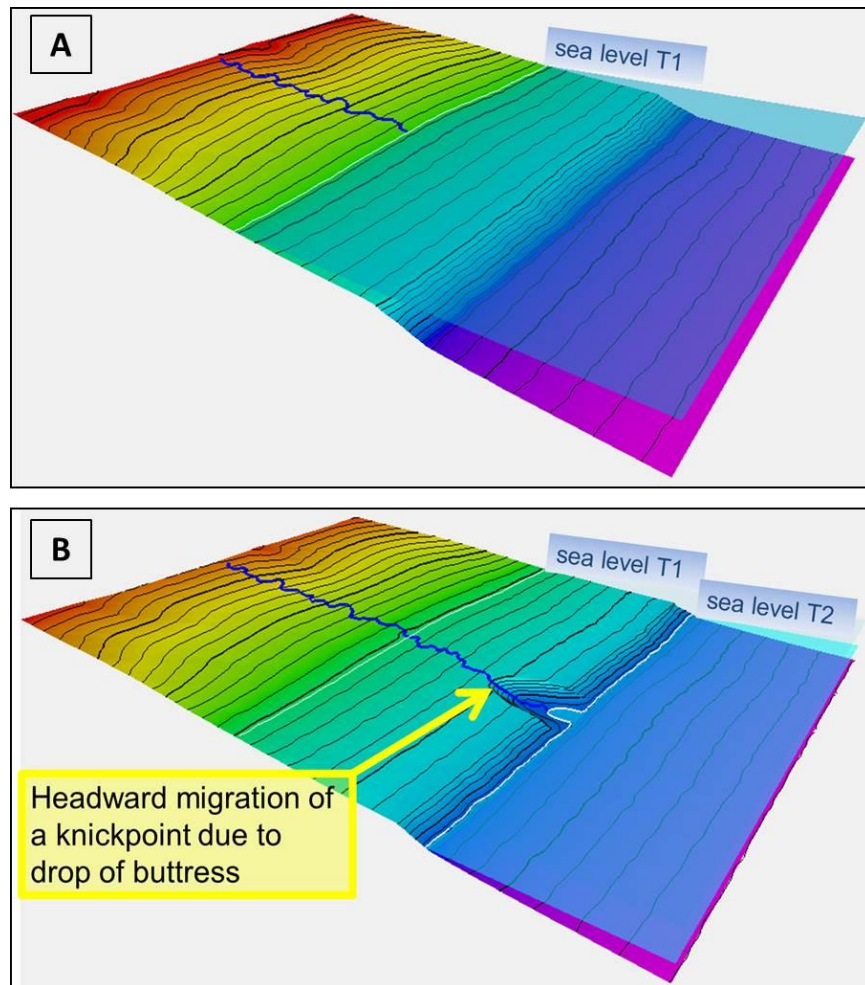


Figure 3: Diagrammatic depiction of the initiation of a buttress valley formed by headward knickpoint migration after a significant drop in elevation of the buttress. A is the system sea level at time one (T1), and B is the system after sea level drops at time two (T2).

#### 1.1.1.4. Buffer Valley

Finally, a buffer valley is created by upstream controls only. That is, incision is controlled not by a change in sea level as in the example above, but rather by processes that cause fluctuations of the incision and aggradation of alluvial streams, such as the ability of a stream to erode bedrock or entrain sediment, or controls on water discharge. These processes will be



described in detail in Chapter Three and comprise the dominant portion of this dissertation.

Figure 4 is an example of a buffer valley.

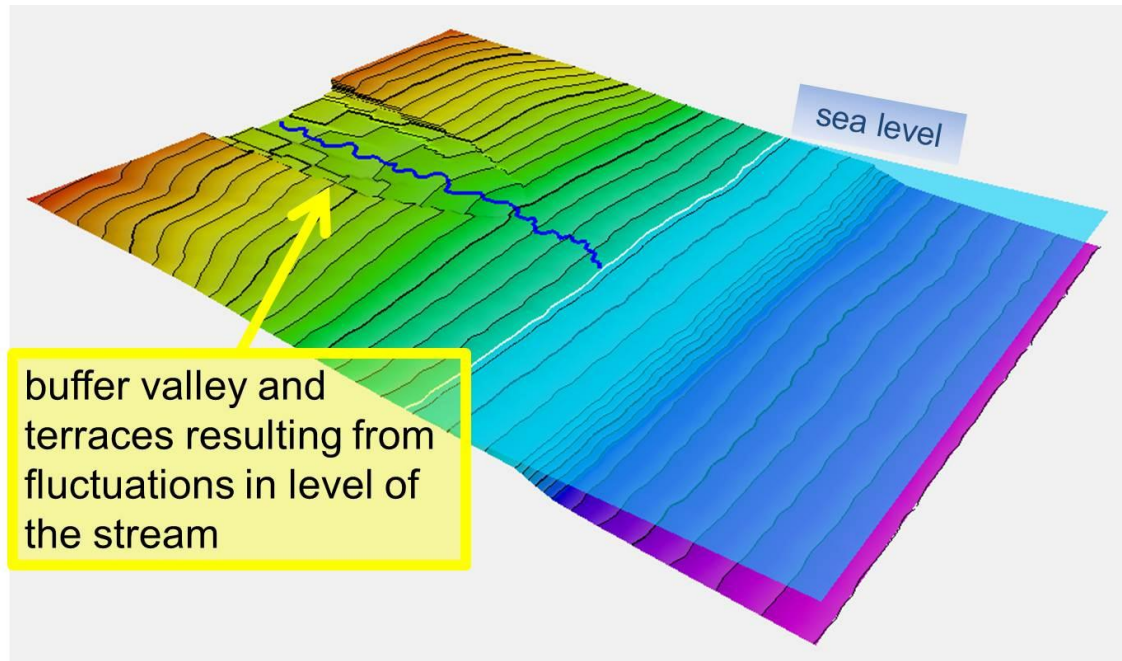


Figure 4: Diagram of a buffer valley on a landscape that is otherwise in equilibrium with sea level (the buttress). Internal complexity of the buffer valley due to multiple episodes of aggradation and incision are shown by the terraces.

The valley types introduced above are not exclusive of one another. It is more often the case that a valley is the product of two or more of the valley forming processes. For example, Figure 5 shows a buffer valley that will soon be modified to incorporate a buttress valley that is propagating into the region.

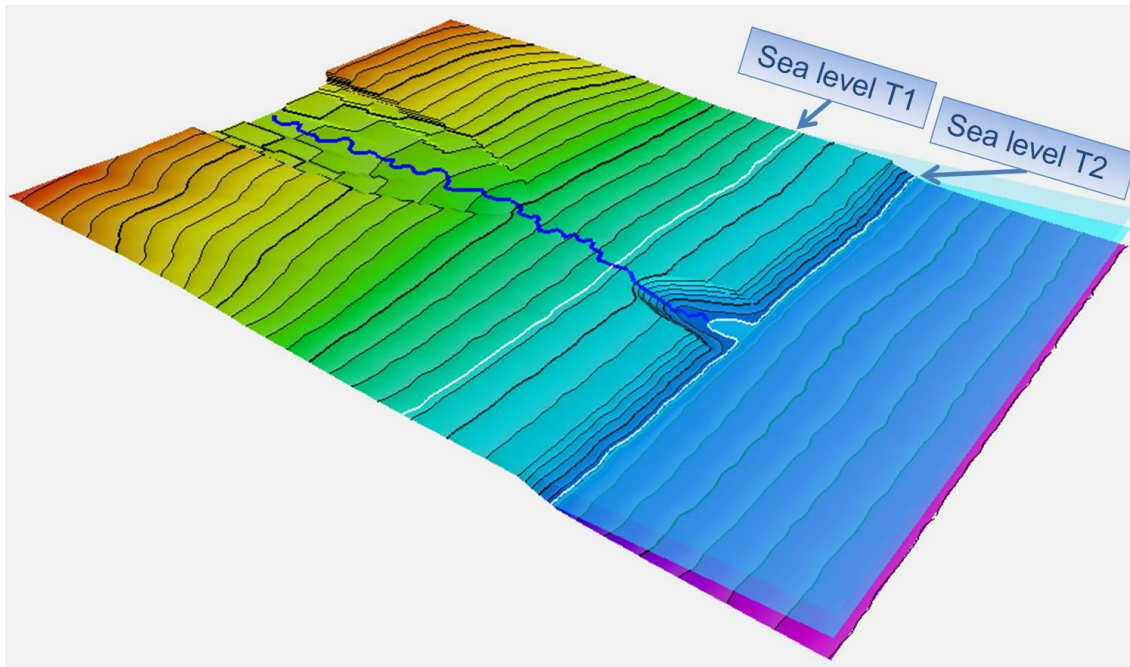


Figure 5: Diagram of a buffer valley and a landward migrating buttress valley formed from a drop in elevation of the buttress at-time two; in time the two valleys will merge in the vicinity of the buffer valley and a complex valley will be created by controls from the two processes.

## 1.2 Landscape Evolution Model (LEM)

I use a physically based LEM to investigate the parameters controlling the cut and fill of buffer valleys. This will be developed in Chapter Three; briefly, the model begins with a surface like those in figures 3-5 that is modified as the computer runs algorithms representing geomorphic processes for all grid points comprising a surface.

Numerical modeling of the evolution of landscapes using computers is a relatively recent endeavor in earth science. The work of landscape evolution modeling is in its embryonic stage and will continue to receive much attention by scientists in this century as investigators seek to recreate virtually what happens in reality, giving scientists tremendous predictive and analytical power.

The term “landscape evolution model” (LEM) itself has evolved. Tucker and Hancock (2010) explain that originally it meant a “word-picture” that described the evolution of a landscape

through time. Subsequently, the geomorphic processes were quantified empirically and equations explaining the phenomena, so the term came to include the mathematical theories describing the various geomorphic processes. With the advent of computers, which empowered investigators to run complex algorithms and solve the complex equations, the term now essentially means both underlying mathematical theories as well as the computer programs designed to solve those equations (Tucker and Hancock, 2010).

Landscape evolution modeling is of interest across many disciplines of natural science. For example, planetary geologists seek to understand extraterrestrial landscapes where liquids exist or may have existed on the surface, such as the planet Mars (Malin and Edgett, 2000) or the moon of Saturn called Titan (Hayes et al., 2011), or even extra-solar earth-like planets. To reservoir geologists from the oil and gas or water resource industries, modeling may predict where sand bodies will likely occur (Hofmann et al., 2011) and how those bodies are connected, guiding well placement and leading to better reservoir performance.

In recreating buffer valleys with a numerical model, our primary concern is to examine whether the initial and boundary conditions necessary to produce incision and aggradation are reasonable when compared to real-world data from fluvial valleys.

### 1.3 Base-Level Buffers and Buttresses

Holbrook et al. (2006) introduced the concept of base-level buffers and buttresses. Their work built on the concepts of base-level, originally proposed by Powell (1875), and the recognition that streams tend toward a graded equilibrium profile (e.g. Gilbert, 1877; Hack, 1957; Mackin, 1948; Shulits, 1972; Yatsu, 1955).

Although fluvial systems in theory will achieve a graded profile under allogenic controls over a reasonable amount of time, Holbrook et al. (2006) proposed that autogenic controls, operating at various temporal and spatial scales, will always create deviations from the graded



longitudinal profile. The deviation, however, does have some structure to it, because there is a limit to stream aggradation or incision. Those limits are termed “buffers”.

Buffers are defined as surfaces to which streams can aggrade or incise. The buffer is similar to a buffer in other sciences, like chemistry or physics, where a buffer is that which resists change, i.e. a buffer solution in chemistry can be one which maintains its pH when other solutions are added. Because the buffer in the sense of Holbrook et al. (2006) is a surface where the fluvial system can't effect a change that crosses the buffer elevation, the buffer is never actually reached by the streams of a drainage basin, it is approached, similar to an asymptote in mathematics.

Upstream controls on the system will effect changes that are confined to the buffer zone; given the variability of those controls, the buffer zone can be quite thick. Stated differently, variability of upstream controls are such that 10's of meters of preserved sediment may exist in the buffer zone as the product of incising and aggrading sediment in valleys. This variability in upstream controls may occur over relatively short periods of time, where deviations from the equilibrium profile may occur at  $10^2 - 10^5$  years (Holbrook et al., 2006).

Buffers are anchored down-profile to a buttress, where the upper buffer and the lower buffer converge to one-channel thickness. The convergence of the buffers at the buttress is the position where rivers can neither aggrade nor incise. It is the buttress that exercises primary control on buffer elevations (Figure 6).

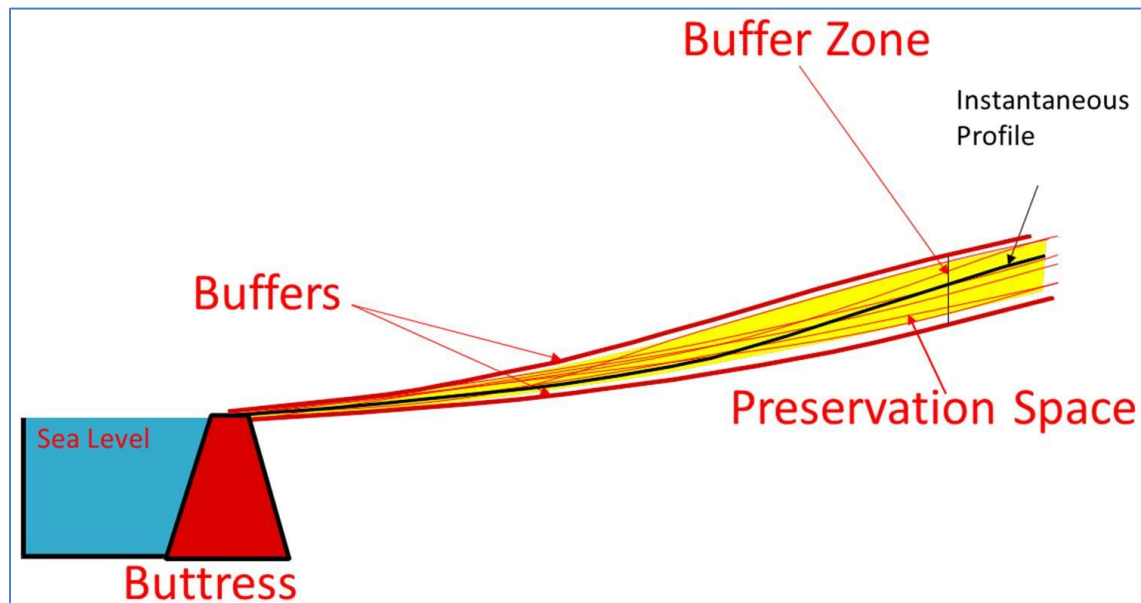


Figure 6: Visual representation of the Buffers and Buttresses concept of Holbrook et al. (2006). Fluvial system's channel elevations are lowest at the buttress but may exhibit an instantaneous profile (black) of any geometry within the buffer zone based on upstream controls. Elevations to which the instantaneous profiles attain through time (red lines) define the preservation space of the system. The buffer zone narrows downstream to one channel thickness at the buttress. After (Holbrook et al., 2006).

The strength of the buffers and buttresses model is that it cogently combines models for upstream versus downstream controls on fluvial systems, and offers a mechanism for the interpretation of fluvial strata within the framework of sequence stratigraphy, particularly with respect to architecture and connectivity of channel-deposits.

#### 1.3.1. *Upstream versus Downstream controls*

Downstream controls are simply defined as those changes which owe their origin to the buttress. For shorter periods of time, it is understood that the buttress primarily effects the distal end of the fluvial system, generally only 100 km or so inland of the strand. The buttress exercises primary control over longer periods of time, generally  $10^4 - 10^7$  years. Over those long periods of time the downstream controls affect the entire fluvial system.

Controls on the elevation of the buttress are unique to the fluvial system being examined. For example, where the streams meet the sea in a river dominated delta that is dewatering and degassing, and thus compacting, the relative sea level would rise and the system would adjust accordingly to the rise of the buttress. Another example may be where the entire distal end of the system is subject to subsidence, say, due to growth-faulting in a passive rift basin. The examples above do have a tectonic component, and a more specific description of such processes would be to label them as downstream, tectonic controls on buttress elevation. Upstream controls are understood to owe their origin to climate and tectonics. Broadly defined, upstream controls are those affecting the fluvial system anywhere in the buffer zone that is not influenced, in the short term, by the buttress.

## CHAPTER 2

### FLUVIAL VALLEYS

#### 2.1 Buffer Valley Extents

The thickness of buffer valleys is not well known. A necessary first step in the investigation of controls on buffer valleys is to gain an understanding of the potential thickness of such valleys. It is recognized that valleys migrate laterally through time as they aggrade and incise and may have different widths throughout their history; this study is more concerned about the thickness of the buffer zone. The difference in elevation between the depth of incision and the height of aggradation over some interval of time will serve as a proxy for the buffer zone thickness.

Buffer valleys—valleys owing their origins to upstream controls only—have been examined by quaternary geologists and geomorphologists for quite some time, though they were not calling the objects of their study “buffer valleys”. That being the case, there is a literature that can provide insight into buffer valley extents.

Determination of the height of aggradation requires evidence of stream elevation at some point in its history. The best evidence is the preservation of a terrace in the valley.

Two types of terraces are recognized in geomorphology. The first is a strath terrace, which is a terrace built upon a surface (the strath) eroded into bedrock (Mackin, 1937). These generally have only a few meters of alluvium deposited on the strath (Wegmann and Pazzaglia, 2002). The other type of terrace is a fill terrace, which is comprised of bedload sediments deposited by an aggrading river (Bull, 1990). The base of a fill terrace may be the base of valley that has been eroded by the stream, or another fill terrace. In my examination of Quaternary valleys in the literature I look at the relationships of terraces in a valley to determine the extent of buffer zones.

### *2.1.1. River Incision and Aggradation*

It is important to consider the causes of aggradation and incision. In the most general sense, it is understood that when sediment supply exceeds stream competence and capacity, sediment is stored and aggradation occurs (e.g., Lane, 1955; Mackin, 1948); incision occurs when the reverse is true. Workers generally cite climate as the main driver, but the specifics of how climate drives aggradation or incision isn't explicitly stated. One obvious way in which climate controls a fluvial system is its effect on base-level. It is well understood that glacial / interglacial periods drastically change sea level (e.g., Lambeck and Chappell, 2001). During glacial periods a large amount of water is stored on the continents in the form of ice, dropping sea level significantly; and vice versa for interglacial periods.

Changes in river discharge are also attributed to climate change, not only in the way precipitation changes with respect to storm intensity, duration, and return frequency in any given year, but also how water is stored and taken up by vegetation becoming unavailable for discharge (e.g., Bolton et al., 2004; Ladekarl et al., 2005). Different types of vegetation will affect how much water is available for discharge; thus a change in climate will change the vegetation type and therefore the percentage of precipitation that reaches the stream (Stemerdink et al., 2010). A change in discharge affects the shear stress on the stream bed; higher shear stresses entrain a higher volume and greater caliber of sediment. If that sediment is brought to the stream from the hillslopes it is possible that the stream would aggrade because the stream's capacity is exceeded; conversely, if the discharge in the stream and its capacity is great enough, any stored sediment there would be evacuated out of the valley and incision will occur.

A change in frequency of forest fires also plays a role (e.g., Swanson, 1981). MacDonald and Larsen (2009) state that after a forest fire sediment can be entrained in the runoff by relatively low precipitation intensities. It is well understood that vegetation anchors and binds sediment. Fires diminish the effects of vegetation to bind sediment, and therefore reduce the shear stresses required for entrainment.

I assume a continuum of climates in this study. At one end, arid climates will have less precipitation and vegetation will not bind the sediment very strongly. Such environments would also have frequent forest fires. More temperate climates have more precipitation and vegetation that binds sediment more strongly. Humid climates, at the other end of the spectrum, have high precipitation, strongly bound sediment, and a low frequency of forest fires.

Our modeling work will examine the causes of aggradation and incision and will be discussed more in Chapter Three.

### *2.1.2. Quaternary Buffer Valleys*

I am only interested in cut and fill cycles controlled by upstream processes with very little or no tectonic involvement. The best place to examine such valleys is in the Quaternary rock record, where the response of stream systems to tectonic controls is minimized by the fact that tectonic uplift or subsidence may represent a change of only a few 10s of meters given the slow rates of change over the relatively short period of time represented by the Quaternary. A relatively fast uplift would be 5mm/year, as reported for the Monroe uplift of eastern Louisiana and Arkansas (Burnett and Schumm, 1983). Rates less than 1mm per year are more likely for our examples. I will examine buffer valleys in various climatic regimes around the globe ranging from arid deserts to humid tropics.

#### *2.1.2.1. Colorado River*

Our first example of aggradation and incision due to upstream controls a large, continental river in a temperate climate. Howard et al. (2008) examined how paleovalleys<sup>2</sup> of the Colorado River of the American Southwest evolved and inferred the extent of incision and aggradation over the past 5 Ma (Figure 7).

---

<sup>2</sup> Valleys through which a stream flowed but was abandoned due to stream capture, stream blockage due to mass wasting events, or some other natural phenomena.

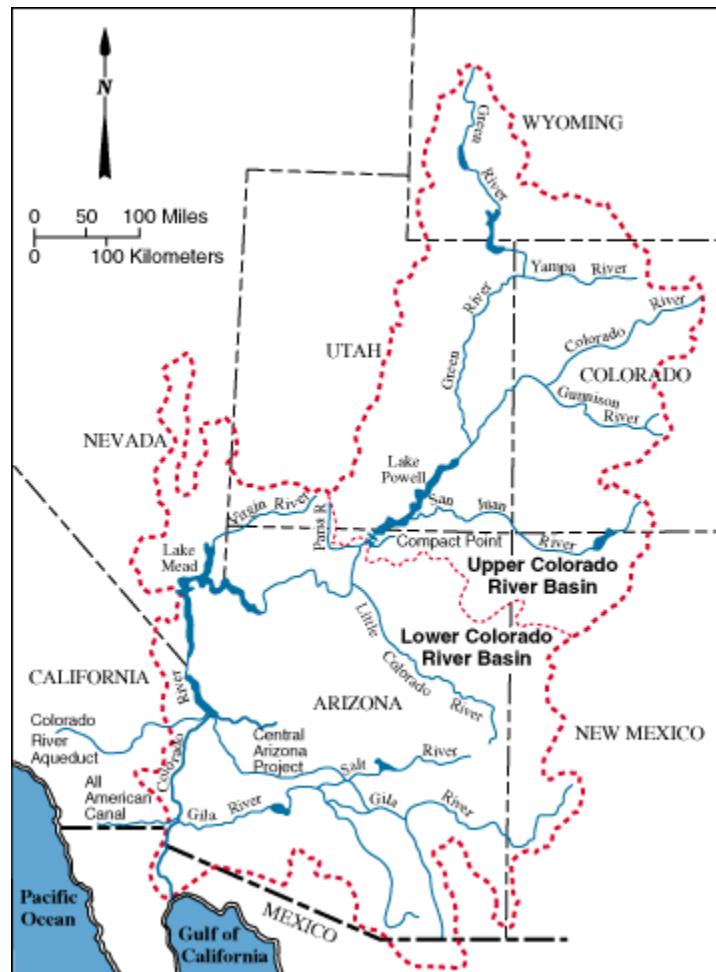


Figure 7: Watershed of the Colorado River (red stippled line), Southwestern United States. Area of interest for this paper is from the Lake Mead area south to the United States/Mexico border.  
 From <http://www.usbr.gov/lc/images/maps/crbsnmap.gif>.

They reported incision/aggradation thicknesses up to 250m in Pliocene fluvial sand and gravel at the Cottonwood, Mohave, and Palo Verde valleys [Figure 7, their figure 1]. Almost certainly there is a tectonic signal captured here, because even at a vertical change of  $1/10^{\text{th}}$  of a millimeter/yr for 1 million years there would be 100 meters of elevation change. However, I assume that 10's of meters of the 250m valley can be attributed to climate controls only.

For the Quaternary Howard et al. (2008) recognize 150m of incision/aggradation, whereas the Holocene produced as much as 40m of deposition in the buffer zone. As above, it is

likely that there is a tectonic signal in the Quaternary. The Holocene aggradation is considered to represent upstream controls only, and therefore the buffer zone is at least 40m in this environment for this continental river.

In the same Geological Society of America Special Paper (number 439), Lundstrom et al. (2008) examined stream aggradation and degradation in the lower Colorado River from Lake Mead to the Yuma, Arizona area in the Southwestern United States (Figure 7). At Yuma, the river is still far enough from the Gulf of California that shifts of the buttress have no effect or is negligible. They noted an approximately 10m thick terrace some 90m above the historic Colorado River (historic referring to the time before the eight dams along the river were built), which shows that the river would have to aggrade at least that amount to deposit the terrace. Using an infrared-stimulated luminescence (IRSL) dating method, which dates the approximate time of most recent subaerial exposure of potassium feldspars, they report that the terrace was formed rapidly in the middle part of the Late Pleistocene. Given the recent age of the terraces, it is reasonable to conclude that the aggradation to that elevation above the river was solely the result of upstream controls and records a buffer zone of approximately 90m within this valley.

#### 2.1.2.2. Upper Thames River, U.K.

Stemerink et al. (2010) examined terraces of the Upper Thames River that formed in the late Pleistocene (Figure 8). They reported nearly 15m of aggradation as measured by the deposition of a terrace above a datum representing the equilibrium elevation profile (Figure 9). The focus of their work was to reconstruct paleodischarges for the Upper Thames river basin using the Fluv2 model (Veldkamp and van Dijke, 1998) and compare their results with field data. Interestingly, their model recreated aggradation of terraces to nearly 15m as was noted in the field.



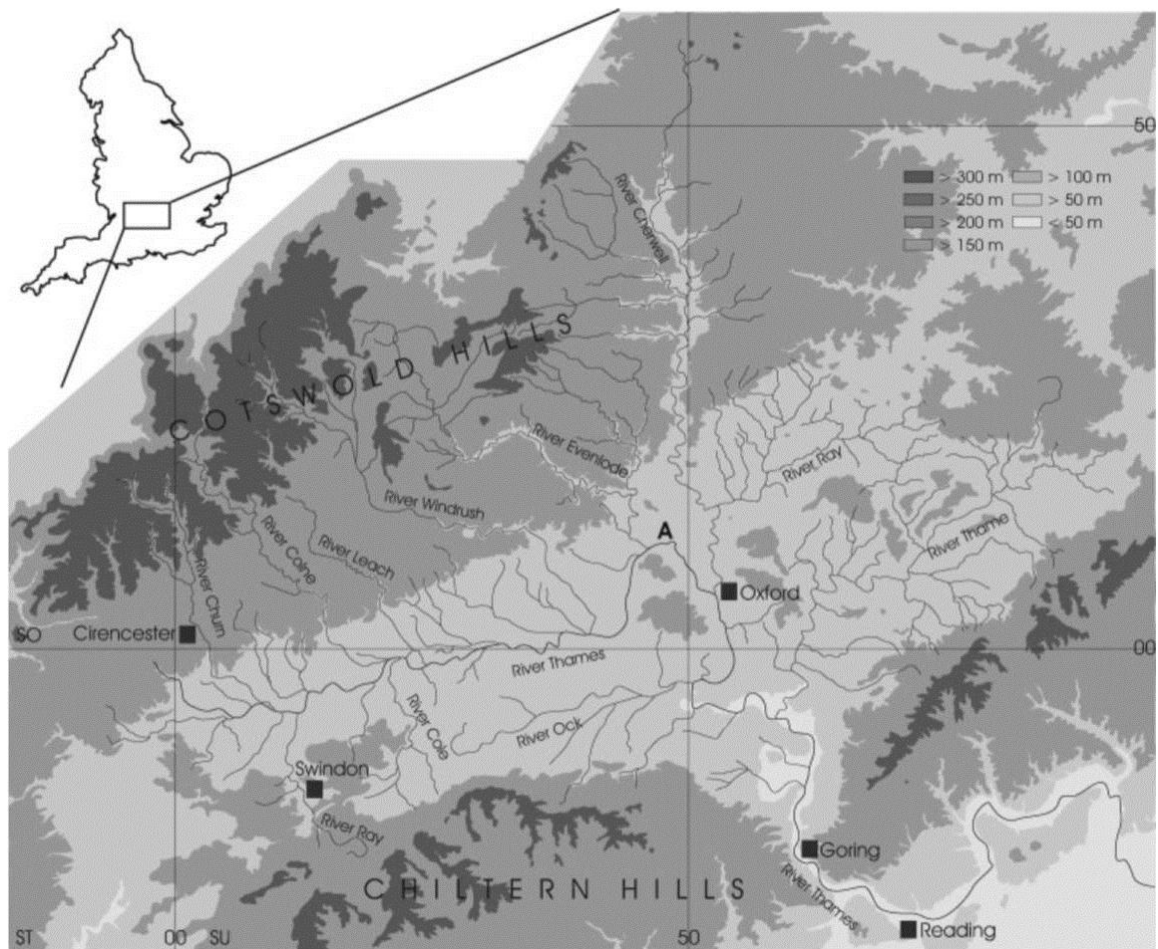


Figure 8: Map of Upper Thames River from Stermerdink et al., 2010, (their Figure 1) showing their study location at "A". The Legend shows ground elevation in meters.

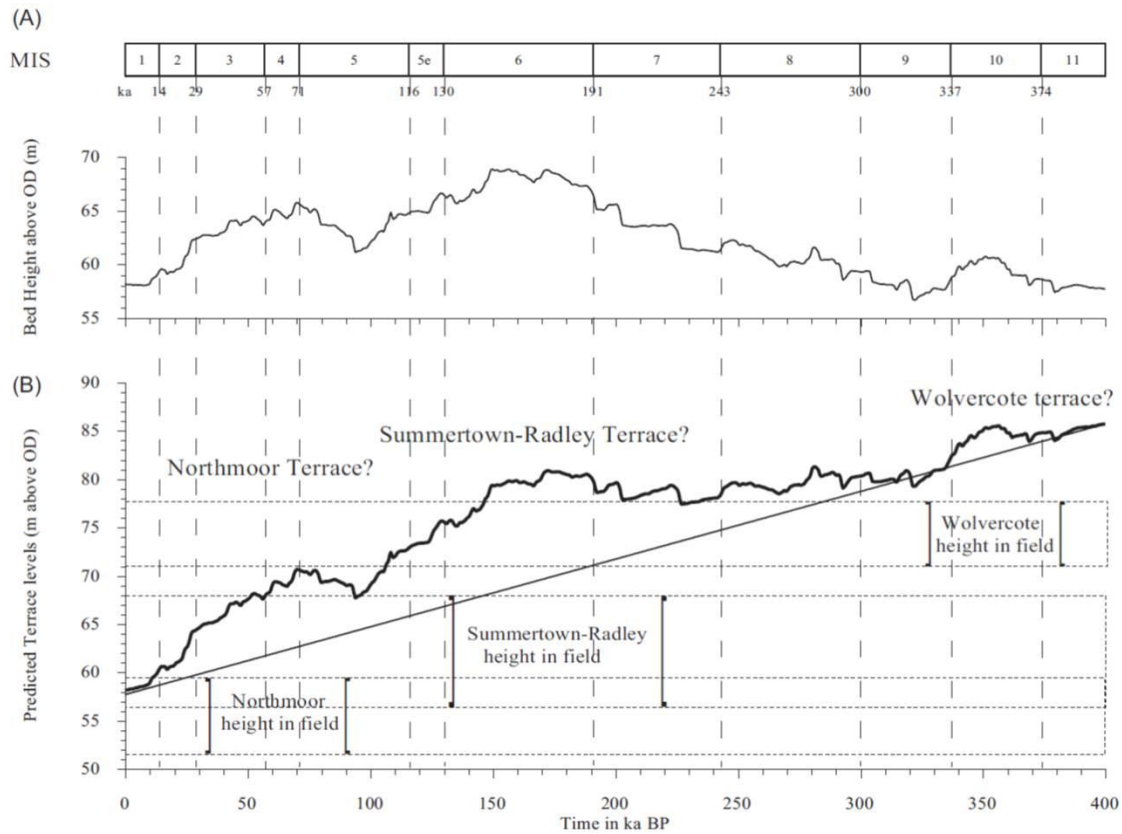


Figure 9: Stermerdink et al. (2010) figure showing Marine Isotope Stages (Emiliani, 1955), modeled elevations of beds using the Fluver2 model (A), and actual heights of beds from field data (B).

Discharge fluctuated in their model as a result of changes in vegetation; change in vegetation is the result of climate change. For example, they argued that during interglacial periods coniferous boreal forests would be well developed and catch 70% of the precipitation. Percent of captured precipitation was used as one set of conditions for the model. An intermediate set of conditions for their model considered a cold but not glacial period where a less well developed forest catches only 50% of the precipitation. Finally, the other end member set of conditions assumes—that during glacial periods the land is covered only by tundra, which would absorb only 20% of the precipitation. Data for percentages and vegetation types were empirically derived by other workers, who are all cited in Stermerdink et al., (2010). This is an interesting approach and one which I adopted in my modeling work described in Chapter Three; however in

my model the climate changes the vegetation, which in turn changes the critical shear stress required to entrain sediment.

#### 2.1.2.3. Gibbler Gulch, Colorado

The Gibbler Gulch area of western Colorado (Figure 10) contains sediment deposited during the mid – late Holocene, approximately 7ky bp Jones et al. (2010). The climate in this region is a semi-arid environment dominated by juniper and pinion pine trees, sagebrush, and various grasses (Jones et al., 2010). Recurrence of major fires that affect the basin is generally every several hundred years (Romme et al., 2009), which is consistent with the minimum of 15 fires that occurred in strata of Gibbler Gulch aggradational cycles (Jones et al., 2010). This example of a buffer valley occurs in a climate similar to those reported earlier for the Colorado River, although this example is in a smaller valley containing a river of less discharge.

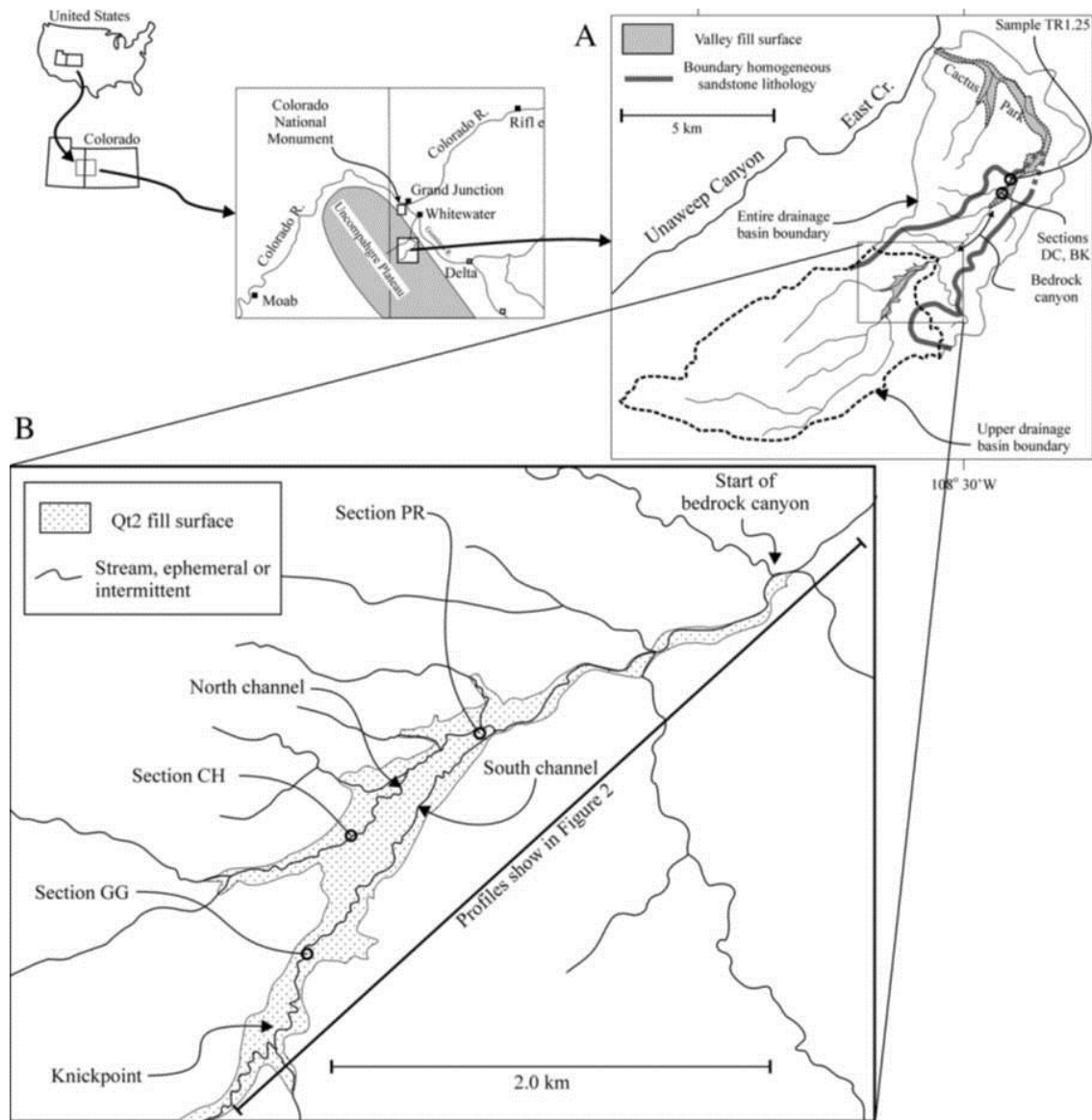


Figure 10: Gibbler Gulch in western Colorado near Moab, Utah where incision / aggradational cycles are present. (a) Map of drainage basin, (b) larger scale map showing extent of the Qt2 terrace.

Two cycles of incision and aggradation are present (Jones et al., 2010). The Qt2 terrace, 14m in thickness (Figure 11), is the thickest of the aggradational cycles. Jones et al. (2010) attributed the cyclicity of sedimentation to be driven primarily by the effects of forest fires. Swanson (1981) speculated that the effects of forest fires may cause aggradation of sediments in

a valley. The conclusions of Swanson (1981) are a plausible explanation because the critical shear stresses required to entrain sediment, particularly on hillslopes, would immediately drop after a widespread fire; thus a great deal of sediment would be entrained and “choke” the streams, i.e.,  $Q_s$  would be much greater than  $Q_w$ , causing aggradation.

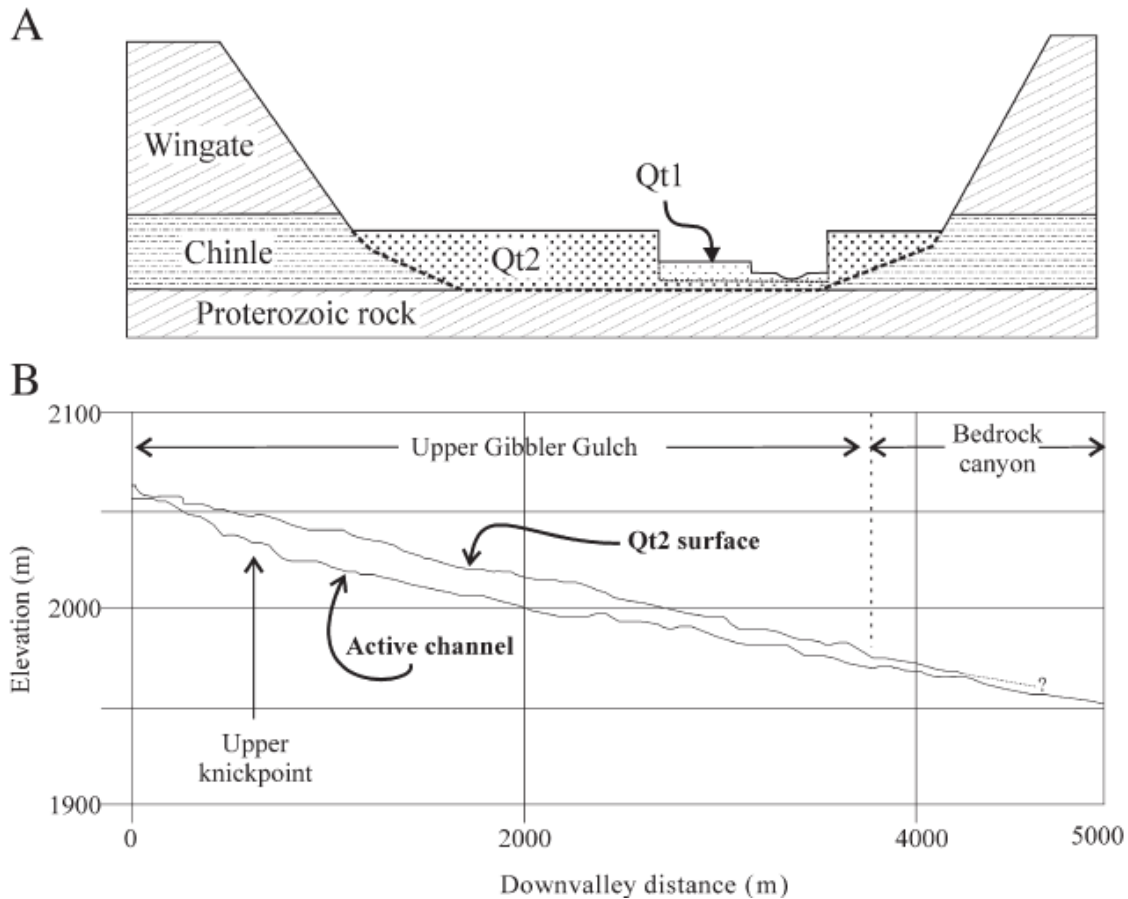


Figure 11: Cross-section and longitudinal profile of the Gibbler Gulch in western Colorado. A) Initial surface beneath Qt2 is a denudation valley, very likely produced by uplift of the Colorado Plateau; aggradation above that surface produces the Qt2 terrace. The Qt2 terrace is subsequently incised, then aggradation occurs to produce the Qt1 terrace, and finally incising to the present day elevation. From Jones et al. (2010)

#### 2.1.2.4. Rio Diamante, Argentina

Baker et al. (2009) studied a reach of the Rio Diamante river in the Patagonia region of Argentina (Figure 12). Here, the river runs from the Andes eastward through an arid rain shadow

environment comprised mostly of desert shrub (D'Antoni, 1983). This climate comprises an end member condition for our study.

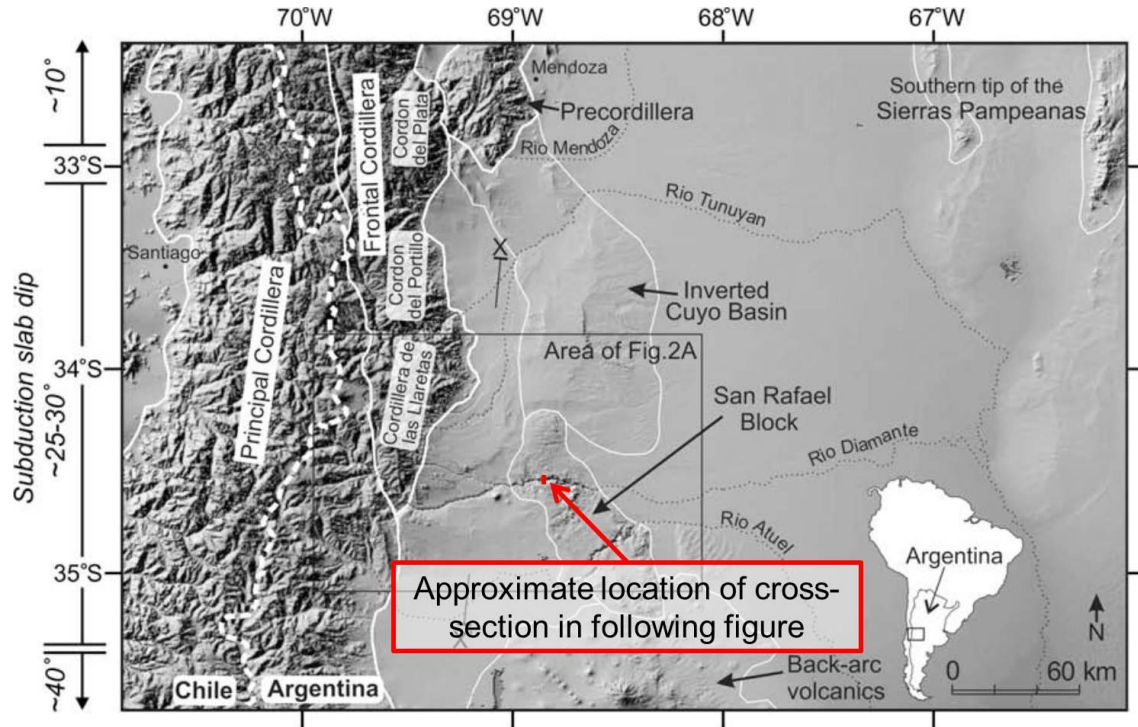


Figure 12: Area studied by Baker, et al., 2010, showing the location of the cross-section in Figure 13. Notice that their study area is in a region of uplift mostly responsible for the deep incision of the Rio Diamante River. Because the location is at a latitude that produces a rain shadow, we expect that only desert vegetation existed there in the recent past. Modified from Baker et al., 2010.

Evidence of the buffer valley exists in the San Rafael Block shown in Figure 12, which is an area of active uplift. One would expect—as in the case of tectonic valleys introduced in Chapter One—that only incision of the river would occur. Though that is the case overall, of interest here is the Qt<sub>2</sub> fill terrace that aggraded on a well-developed strath (Figure 13). Baker et al., 2010, report that this terrace ranges in thickness from 110m upstream to 45m downstream. They speculated that the deposit ranges in age from mid to late Pleistocene, tentatively correlated to a MIS stage 12 glacial advance, which would span a time of a few tens of thousands of years (e.g., Emiliani, 1954; Emiliani, 1955).

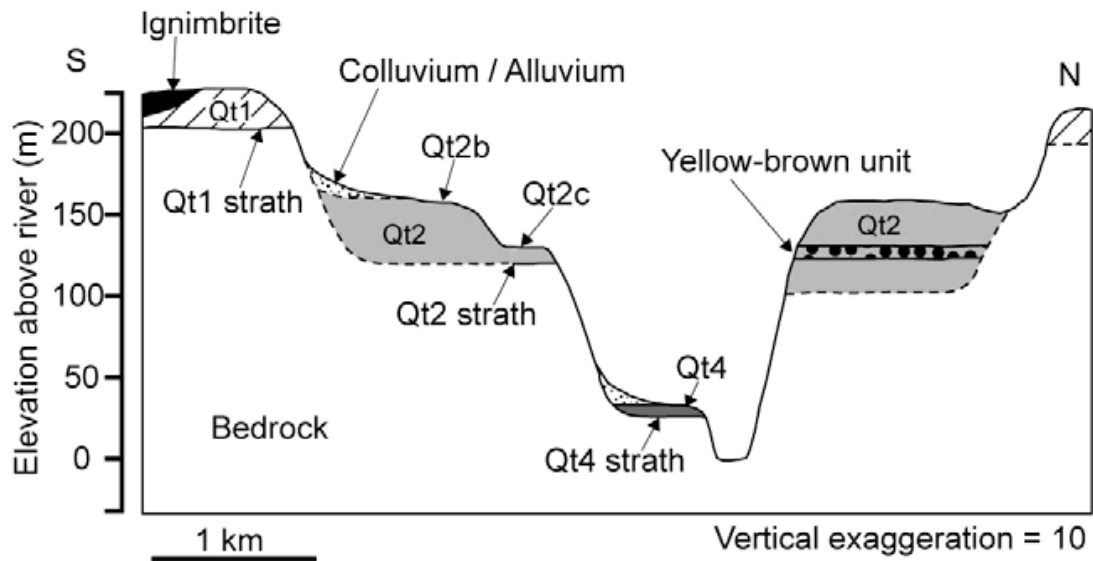


Figure 13: Cross-section of the Rio Diamante River, in the piedmont area of Argentina, showing overall incision with intervals of aggradation. This is shown to illustrate the aggradation of the Qt2 terrace, which is built upon the Qt2 strath terrace. From Baker et al., 2010.

Examination of Figure 13 shows that during an overall incision of the Rio Diamante River, there were periods of aggradation. My interest here is to show that in an overall arid climate, climate change can create a substantial buffer zone, and that buffer aggradation can still occur in the midst of overall incisional trends.

#### 2.1.2.5. Texas Gulf Coast

Incision and aggradation along the gulf coast of Texas has received attention in recent decades (Blum, 1993; Blum and Aslan, 2006; Blum and Price, 1998; Blum and Valastro, 1994; Sylvia and Galloway, 2006). The significance of these studies is that they occur at the distal end of the longitudinal profiles of the rivers they examine (e.g., the Colorado river of Texas, and the Brazos river); we expect that their proximity to the coast would be dominated by the buttress (Figure 14).

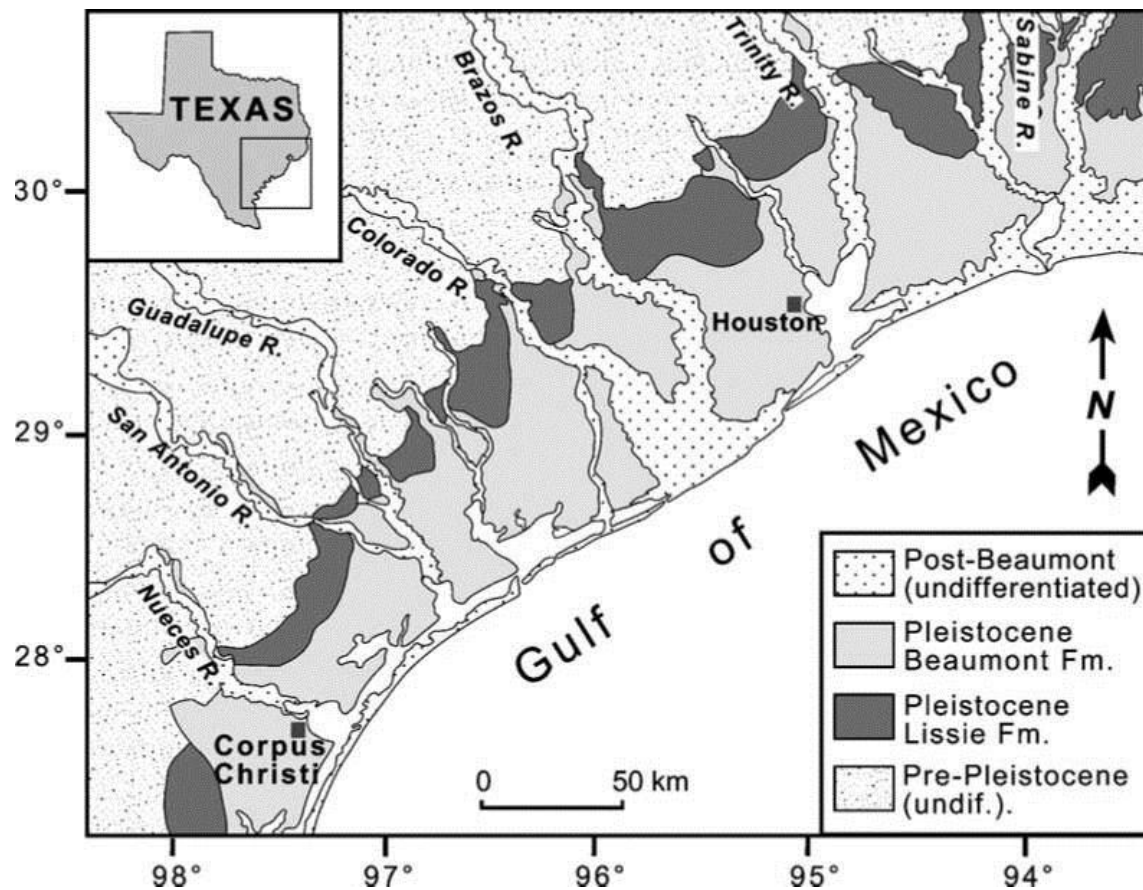


Figure 14: Map of fluvial valleys along the Texas Gulf Coast. From Blum and Aslan, 2006.

Earlier thinking from a sequence stratigraphic perspective, predicted that as the sea regressed fluvial systems would only incise the exposed shelf and aggrade during transgression (e.g., Van Wagoner, 1992; Weimer, 1984). However, the works cited in the previous paragraph show that during regression rivers are still able to aggrade and deposit terraces (Figure 15).



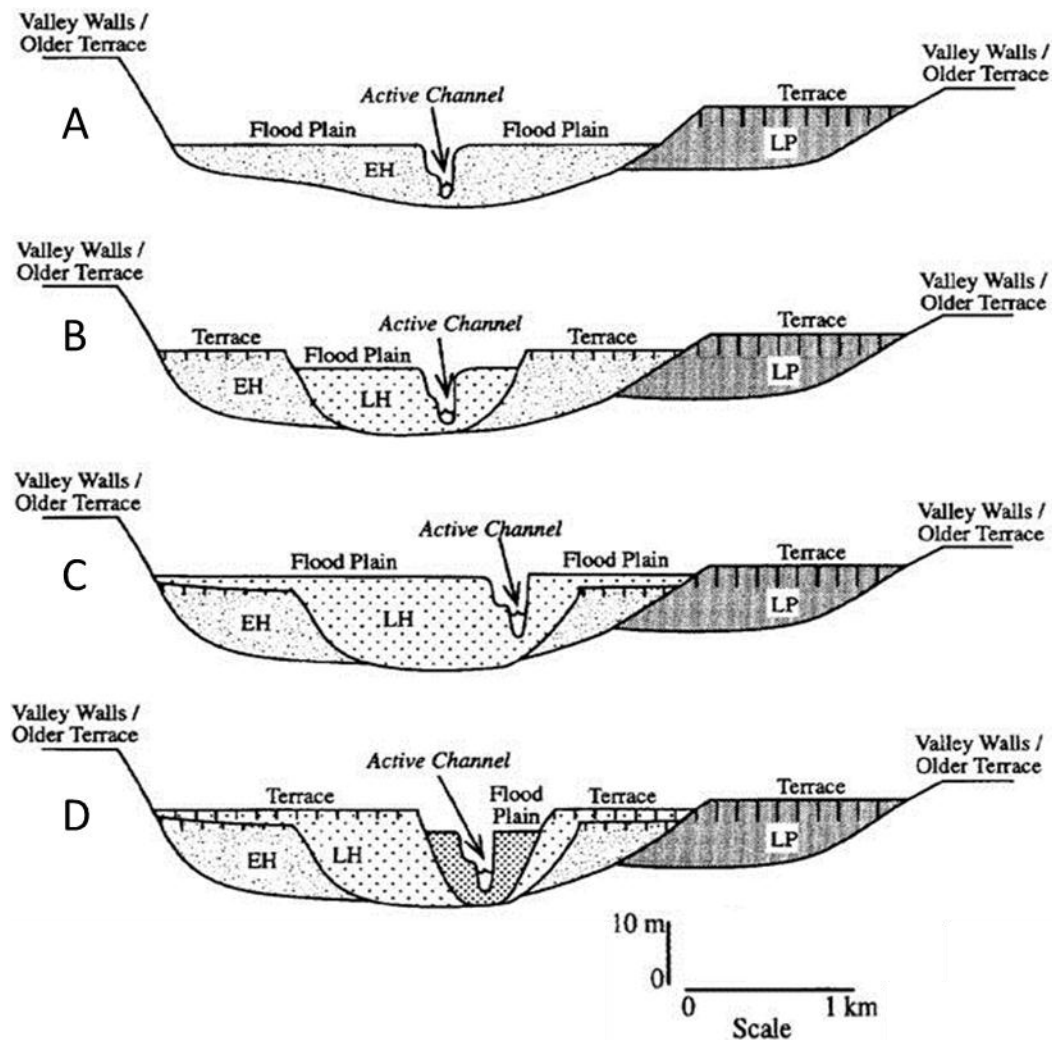


Figure 15: Figure modified from Blum, 1993, showing schematic cross section of Holocene terraces ~ 10m thick in the Colorado River Drainage, Texas gulf coast. (A) Relationship of EH incising into LP; (B) LH incising into EH; (C) LH aggrading over EH; (D) modern river incising into LH.

The terraces measured for the most recently deposited sediment aggrades approximately 10m above the paleo-floodplain. Blum and Aslan (2006) attributed the continuity of major stratigraphic units that extend from the continental interior to the coast as evidence of upstream climate control. Thus, aggradation relatively close to the strand driven by upstream controls

produces a buffer valley confined to a buffer zone. The buffer zone is much thinner due to its proximity to a buttress. Significantly, petroleum reservoir scale sands can be preserved on the shelf during regression (Holbrook and Bhattacharya, *in press*).

### 2.1.3. Discussion

In this chapter, we have shown that:

- Buffer valleys are to be found in a variety of environments and climates;
- Buffer valleys can be as much as 100m in thickness when driven by climate controls only, and it is common to find buffer zones that are several 10s of meters in thickness;
- Buffer valleys are to be found near the buttress, albeit confined to a thin buffer zone.

I have shared only a sampling of buffer valleys to be found in the literature, and this work is certainly not exhaustive. Mack et al. (2006), for example, reported evidence of ~ 100m of incision driven by climate by the Rio Grande River in the Rio Grande Rift. Rittenour et al. (2007) reported incision and aggradation of the Mississippi River in the continental interior that occurred in the last 100kyrs. Hereford (2002) found aggradation related to the Little Ice Age (1400 – 1880 A.D.) on the Colorado Plateau. Workers in England have examined a number of rivers and have noted incision and aggradation driven by climate changes (e.g., Macklin et al., 1992; Rumsby and Macklin, 1994; Taylor et al., 2000). There are certainly other excellent examples of well-developed buffer valleys that were not found in my research. I am confident that more research will identify additional buffer valleys in the modern and recent, and lead to models that can identify buffer valleys preserved in the rock record either in outcrop or in subsurface data-sets such as high-resolution 3D seismic surveys and well-logs.

## CHAPTER 3

### LANDSCAPE EVOLUTION MODELING

#### 3.1 Channel-Hillslope Integrated Landscape Development Model

In this study, we use the physically based, numerical model called the Channel-Hillslope Integrated Landscape Development (CHILD) model to virtually recreate and explore the evolution a buffer valley. We will briefly introduce the CHILD model here, for a more detailed description of CHILD the reader is referred to Tucker et al., (2001).

The CHILD model simulates landscape evolution by running algorithms which compute the movement of water and transport of sediment across an irregular lattice of points that represents the landscape surface in three dimensions (Figure 16). However, CHILD is actually considered a two-dimensional model because the processes are calculated in X and Y dimensions; Z is merely a function of the two spatial dimensions (Gasparini et al., 2008). For example, the continuity of mass, which is conserved and is the difference between the rate of sediment flux in and transport rate out of a cell, can determine the elevation of Z. Local or regional uplift or subsidence also plays a role in the elevation of Z.

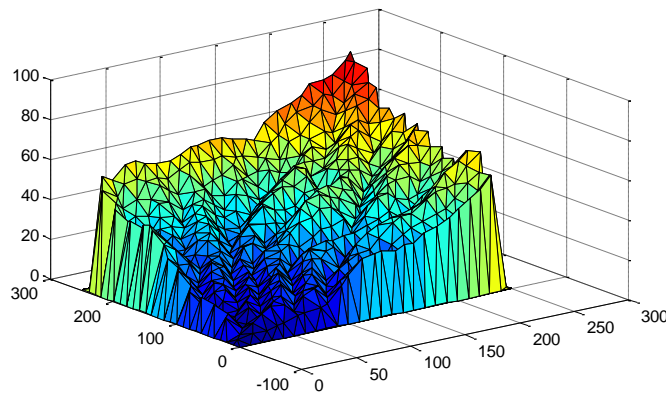


Figure 16: Example of a 3D surface created by CHILD and displayed with MATLAB software. Dimensions are in meters.

The CHILD model is one of several LEM's that exist in the literature. SLOP3D (Ahnert, 1977) SIBERIA (Willgoose et al., 1991), GOLEM (Tucker and Slingerland, 1997); ARMOUR (Willgoose and Sharmeen, 2006); and FLUVER2 (Veldkamp and van Dijke, 1998) are but a few. They share common features. All conserve mass, route water over the landscape and run equations for hydrological, hillslope, and fluvial processes at local to 100's of km<sup>2</sup> spatial scales over short (hours) to geological (10<sup>7</sup>) timescales.

### 3.1.1. *Triangulated Irregular Network (TIN)*

The landscape is represented in the form of a mesh comprised of nodes, triangles and directed edges which all comprise a TIN. Nodes comprise the vertices of each triangle and are located in three dimensions. Data for the landscape (e.g., elevation, discharge, shear stresses) are all associated with a node.

Triangles are assigned to nodes in what is called a "Delaunay triangulation". Delaunay triangulation is the most equable triangle among three nodes; it is a set of points such that a circle passing through each of the nodes will encompass no other points. This type of triangulation gives rise to a Voronoi or Theissen Polygon, which is a polygon formed by connecting the bisectors of the triangles (Figure 17).

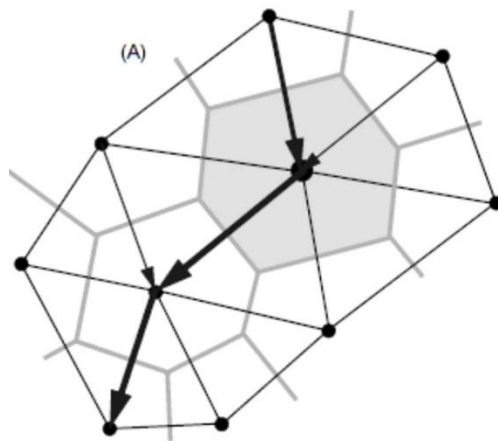


Figure 17: Nodes, Delaunay Triangles (Black lines), Voronoi Polygons (gray lines), and flow lines (arrows) of the TIN. Modified from Tucker et al., 2001.

These polygons provide the framework for the numerical modeling of the LEM; in CHILD the Voronoi Polygon determines the surface area associated with each node and contain a finite volume (Tucker et al., 2001).

CHILD can create three mesh types as an initial starting point for a run (Figure 18). The starting elevation of the mesh can be assigned, as well as an option to slope the surface.

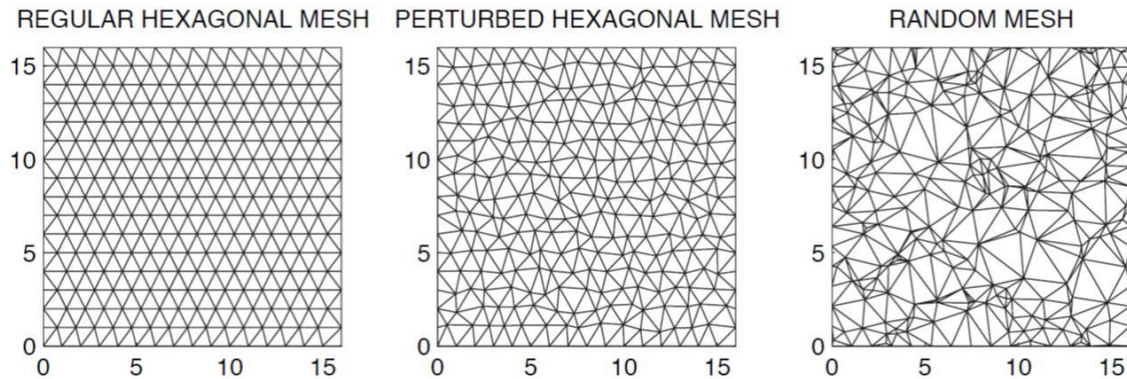


Figure 18: Mesh types used to begin a new run in CHILD. We used the Perturbed Hexagonal Mesh for runs in this work.

Node spacing and grid size are defined by the user, in meters. Large grid sizes with tight nodal spacing results in mesh with many cells. A grid of more than 200k cells took too much computer time, taking days to complete a single run. Though figure 18 shows two-dimensions for each node, CHILD actually will randomly assign noise within defined parameters to the initial surface. For example, if the initial surface is set to an initial elevation of 200 meters, random topography across the TIN can be set at 3 m of relief. This will help the program initiate the movement of water, and ultimately sediment, across the surface.

Outlet points, points across which water and sediment can exit the TIN, are assigned by the user. Several options are available and are shown in Figure 19.

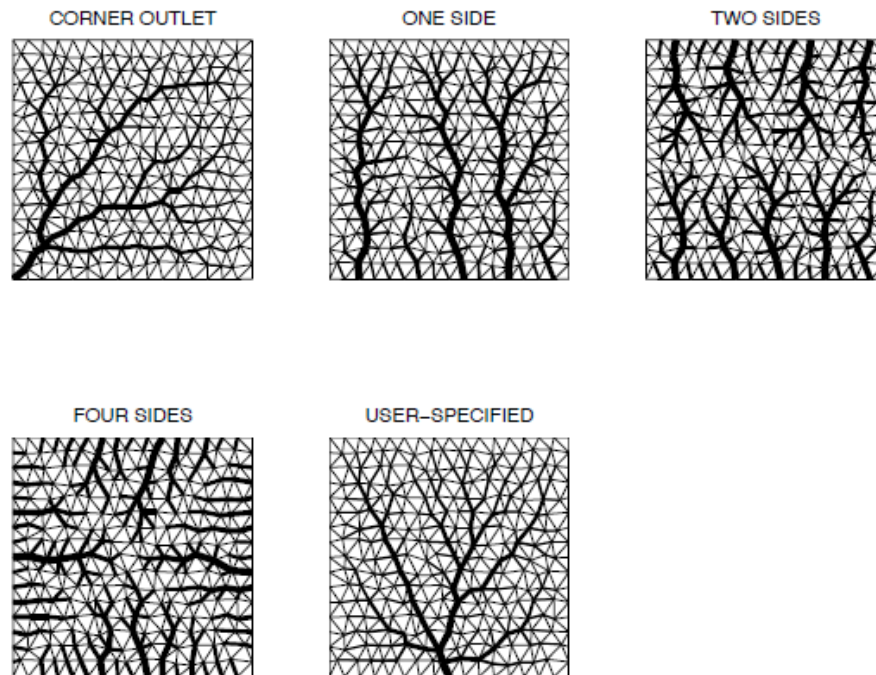


Figure 19: Example of various boundary types that CHILD can implement.

Finally, it is possible to begin a run on an existing mesh, which may be the resultant mesh at the end of an earlier CHILD run, or an exported TIN from ArcInfo, though, a grid from ArcInfo can only have one outlet point.

### 3.1.2. Governing Equations

Essentially, the program modifies the Z value of each node. An increase in elevation represents deposition of sediment and therefore aggradation of the system. A decrease in elevation represents erosion and therefore incision of the stream channel. A background signal of regional uplift or subsidence would also effect the elevation.

CHILD, along with other LEMs, run geomorphic transport functions (GTFs), which themselves have a long history of establishment in the literature. A GTF as defined by Dietrich et al. (2003) is:

“...mathematical statement derived from a physical principle or mechanism, which expresses the mass flux or erosion caused by one or more processes in a manner that: 1) can be parameterized from field measurements, 2) can be tested in physical models, and 3) can be applied over geomorphically significant spatial and temporal scales.”

We will consider GTFs for water and sediment discharge and look at other equations in the CHILD program.

#### 3.1.2.1. Conservation of Mass

The first equation to consider is the continuity of mass. Mass is conserved at each node according to the following equation:

$$\frac{dz}{dt} = \sum_i \frac{Q_{s_i} - Q_{t_i}}{a}$$

where  $Z$  is the node elevation (landscape surface),  $t$  is the time step,  $Q_{s_i}$  is the volumetric sediment influx of the  $i$ -th grain fraction,  $Q_{t_i}$  is the volumetric sediment transport capacity (outflux) of the  $i$ -th grain fraction, and  $a$  is the area (the voronoi cell which is associated with the node) for which erosion is calculated. This work only considered one grain size, 1mm quartz sand, for simplicity. This equation considers bedload only; suspended load is assumed to exit the network and not to interact with the bed. Steady state for the system is achieved when the rate of erosion matches the rate of uplift and occurs when the expression on the right of equation 1.1 is equal to zero.

#### 3.1.2.2. Climate Inputs

Rainfall is considered to fall across the entire landscape. Characteristics of the precipitation event that can be changed in the model are: 1) mean rainfall intensity in m/yr; 2) mean storm duration (yr); and 3) mean time between storms (yr). Volumetric distribution of water from a single storm are gained from an examination of the work of Eagleson (1978), which distributes the above parameters according to the hydrograph shown in Figure 18.

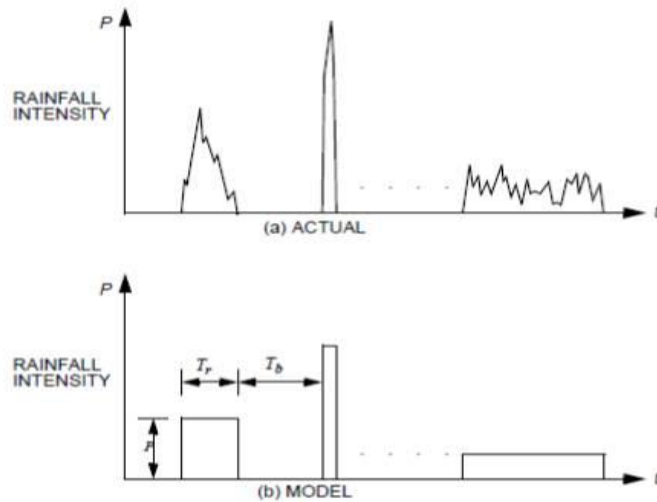


Figure 20: Distribution of rainfall from a single storm event. From Tucker et al., 2001, modified after Eagleson, 1978.

CHILD will randomly pick intensity, duration, and frequency from among the hydrograph above if the user chooses. A constant climate input is also available, in which case the rainfall essentially represents an effective rainfall. For this work, we chose the latter, similar to Tucker and Slingerland (1997).

Climate change varies greatly through relatively short periods of geologic time; in my model I assume that climate is constant and therefore rainfall through any given year is the same over the interval of the model run; that is, for a model run over a million year time frame, the amount and distribution of rainfall is the same as any other year for that iteration. Though this approach is unrealistic compared to what actually happens in nature, it is generally accepted that a representative climate can be modeled over the intervals of time that we examine.

To examine the effects of changing climate on a landscape, CHILD allows an iteration to run from the stopping point of the previous run. For example, a run of 20 kyr at a certain climate setting (intensity, duration, and return frequency of storms) can be followed by another 20 kyr run with different settings. “Climate change” can therefore be happen fairly abruptly depending on how inputs are defined.



One generally considers an “abrupt” event to be something like a bolide impact, for example. However, to an earth scientist an abrupt event can be on the order of  $10^3 - 10^4$  years. It is recognized that climate changes can be on the order of  $10^3$  years (e.g., Crowley and North, 1988; Zachos et al., 2001). The abruptness of climate change is of tremendous social interest and a great deal of effort is currently focused on understanding how quickly and to what magnitudes climate may change in the future. For example, the Younger Dryas stadial (approximately 12,800 - 11,500 yrs before 1950) is readily recognizable in Greenland ice cores. It is generally accepted that the climate change at the end of the Younger Dryas is on the order of decades (e.g., Dansgaard et al., 1989; Taylor et al., 1997). Alley (2000) studied the Younger Dryas cold interval in a Greenland ice core and stated “...even the possibility of a 1-yr end of the Younger Dryas is provocative...”. Changing climate parameters over seemingly short geologic time intervals thus is considered justifiable.

The effects of climate on fluvial strata have been a focus of research for a considerable time. Vandenberghe (1995, 2003) and Vandenberghe and Maddy (2001) offers nice reviews of the evolution of these concepts that span more than a century. I am in agreement with the fore-mentioned studies that the distributions of peak storm intensities affect the landscape the most. This includes the low frequency, high amplitude events that occur beyond seasonal distributions.

#### 3.1.2.3. Surface Runoff

Volume of the rainfall is a starting point, so to speak, of the model run. The volume of water on the landscape is calculated as:

$$(Q = PA)$$

where  $Q$  is volume in cubic meters,  $P$  is precipitation in meter's per year, and  $A$  is square meters.

It is possible to set infiltration rates into the sediment, which would leave less water from precipitation to run across the land. In this work we chose not to use the infiltration option and therefore all precipitation was available for runoff.

Channel width has been shown to have a power-law relation to fluvial discharge in alluvial channels (e.g. Leopold and Maddock, 1953; Yalin, 1992) where downstream channels widen as the 0.5 power of discharge. Schumm (2005) warned that this relationship is limited in its predictive power, stating that any particular reach of a stream is not dominated solely by discharge with regards to channel morphology. We, however, make the assumption that the relationship holds for the purposes of this model.

Computation of channel width is dependent on discharge and is based on the work of Leopold and Maddock (1953), which derived a relationship between discharge and channel width

$$W_b = k_w Q_b^{wb},$$

$$W = W_b (Q/Q_b)^{ws}$$

Where  $W_b$  is bankfull width,  $k_w$  is bankfull width per unit scaled discharge,  $Q$  is total discharge,  $Q_b$  is bankfull discharge,  $wb$  is a downstream scaling exponent, and  $ws$  is at-a-station scaling exponent.

Once channel width is calculated, discharge per unit width of channel, designated with a lower case  $q$ , is calculated:

$$q = Q / W$$

where  $Q$  is discharge and  $W$  is channel width as introduced above. Once  $q$  is calculated, shear stress on the channel bed exerted by the stream is calculated by the formula:

$$\tau = k_t * q^{mb} * S^{nb}$$

where  $S$  is slope, and  $k_t$ ,  $mb$ , and  $nb$  are parameters. All units are SI units and therefore  $\tau$  is in pascals.

#### 3.1.2.4. Hillslope Processes

Hillslope processes are important to consider because they can transfer a significant sediment volume to a channel. These can be soil creep, rain splash, mass wasting events, and even sheet flow across the hillslope. In CHILD the processes are those of soil creep, which can

be either linear or non-linear. Linear hillslope processes describe volume of sediment discharge per unit width ( $q_c$ ) by the equation:

$$q_c = K_d S$$

where  $K_d$  is the diffusion coefficient, and  $S$  is slope. Non-linear hillslope processes consider a critical slope angle and sediment discharge per unit width is defined by the equation:

$$q_c = (K_d S) / 1 - (S/S_c)^2$$

where  $S_c$  is the critical slope angle. In CHILD the slope angles are given in degrees; here, we see that as a hillslope approaches the critical slope angle, that is, where  $S \approx S_c$ , the denominator approaches zero and thus the critical slope angle is asymptotic. Non-linear hillslope diffusion was used with the critical angle set at  $38^\circ$  (0.38, or a 78% slope), which is a reasonable upper-limit value for wet, coarse sand.

The coefficient of diffusivity,  $K$  in the previous equation, is the parameter  $KD$  in CHILD. Though generally accepted as an acceptable analog for the diffusion of hillslopes, Tucker and Bradley (2010) state that the analogy doesn't hold true for high gradients. A threshold parameter can be set related the angle of repose, or critical slope angle, which is set in percent. Roering et al.(2002) stated the hillslope diffusivity is approximately equal to  $0.01 \text{ m}^2 / \text{yr}$ , which is the value used in my model runs.

### 3.1.2.5. Bed Load Transport Equations

In the CHILD User's Guide (Tucker, 2009), Tucker introduces the various formulas available that the program uses which are dependent on settings determined by the user. We chose the "TRANSPORT\_LAW=0" option for calculating bed-load transport of sediment in channels. The formula introduced in the Users Guide for this particular transport law is:

$$\tau_0 = K_t \left( \frac{Q}{W} \right)^{M_f} S^{N_f}$$

where  $Q$  is water discharge,  $W$  is channel width,  $S$  is slope, and  $K_t$ ,  $M_f$ , and  $N_f$  are parameters. Also, Tucker states that the parameters can be adjusted to "...represent any power-weighted

combination of slope and unit discharge.” For example, stream power would be represented by setting MF = NF = 1 and KT = unit weight of water (1000kg/m<sup>3</sup>).

#### 3.1.2.5.1. Meyer-Peter and Müller:

One of the fundamental bed-load transport equations is that of Meyer-Peter and Müller, or often referred to as the MPM equation (Meyer-Peter and Muller, 1948)

$$q_s = 8(\tau - \tau_{cr})^{3/2}$$

where  $q_s$  is sediment discharge per unit width of channel,  $\tau$  is bed shear stress,  $\tau_{cr}$  is the critical shear required to entrain the sediment. This equation is for a specific set of circumstances however, and a more general form of the equation is:

$$q_s = k(\tau - \tau_{cr})^n$$

where k is a parameter set by the user (Dietrich et al., 2003); . It is interesting to note the popular scientist Albert Einstein (1950) also investigated the bed load transport of sediment in channels, and another popular formula for sediment transport is the “Einstein-Brown” equation, which includes a parameter of probability for the likelihood that a grain of a certain size will be entrained. In CHILD, we chose a transport limited system, and used TRANSPORT\_LAW = 0, where transport capacity is determined by the following formula:

$$Q_c = K_f W(\tau_0 - \tau_c)^{P_f}$$

Where  $K_f$  is a transport efficiency factor, the value of which is placed in the input file by the parameter KF. To use the MPM, several parameters in CHILD are set as: MF=NF=2/3 and PF=3/2, which Tucker (personal communication) advised are the settings for the MPM formula when using Transport\_Law 0.

Bed load transport equations have a long history of empirical derivation. Martin (2003), tested several popular bed load equations and found that, for his study of the Vedder River in British Columbia, the equations were within an order of magnitude of measured volumes. Similarly, Barry et al. (2008), found that several of the popular equations were within several

orders of magnitude of empirically derived volumes. Figure 21 is a graph showing the results of their work (their Figure 8).

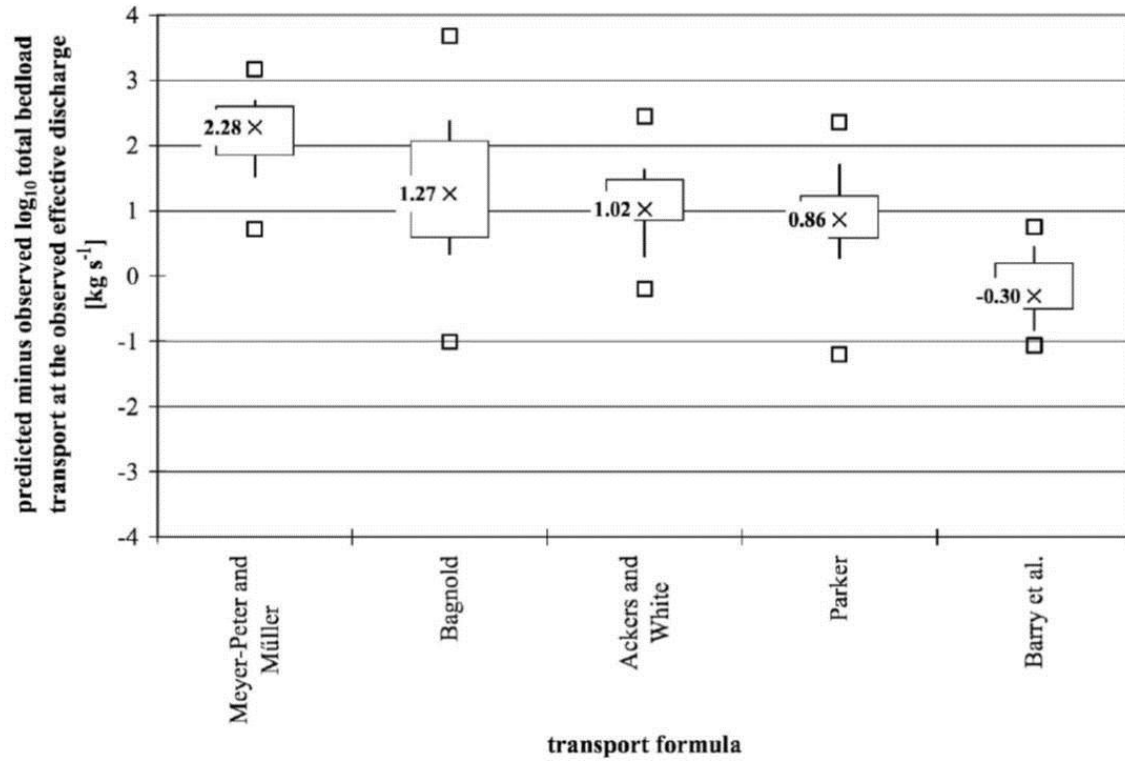


Figure 21: Variation among common bed-load transport equations.

Critical shear stress for the entrainment of sediment is the more important value, which is the stress at which a particle will be entrained. Tucker et al. (2006), gives an introduction to critical shear stresses and display the range of values for different conditions, studied by various workers, in their Table 1. Lick et al. (2004) conducted a nice study investigating shear stresses required to entrain quartz grains, and produced the graph shown in Figure 22.

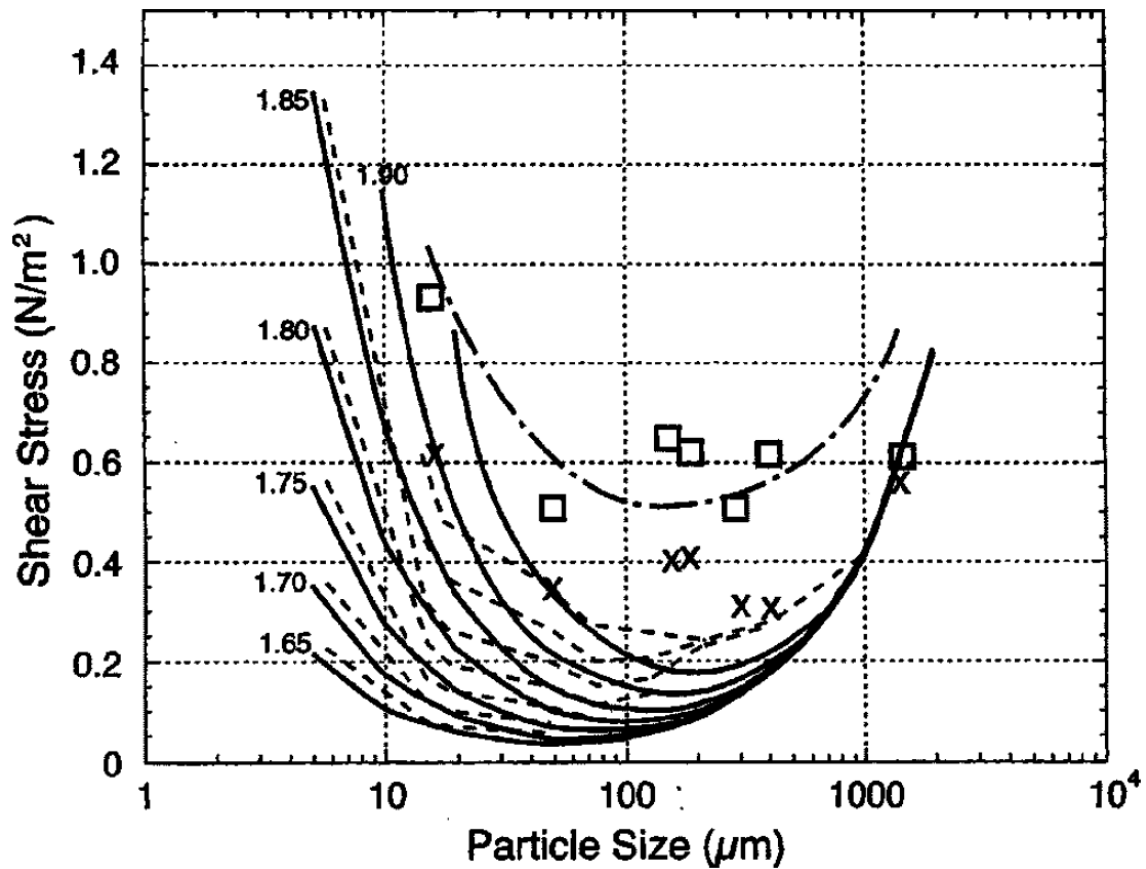


Figure 22: Graph from Lick et al. (2004), showing critical shear stress for various quartz grain sizes. Their Figure 6. Boxes are data points for a mixture of sand and 2% bentonite; x's are quartz grains only. Notice that 1000 micrometers (1 mm), critical shear stress is set at 0.4 newton's per square meter.

The value of  $0.73 \text{ N/m}^2$  (equal to 0.73 Pascals) was used as the “taucr” (tau critical) value in the CHILD input file. Essentially, adjusting this value determines the erodability of the channel bed. However, there is discrepancy amongst empirically derived data for values of critical shear. In Figure 23, Miller et al. (1977) show a value of  $70 \text{ dynes/cm}^2$  for 1 mm sand, which is equal to seven Pascals of shear stress.

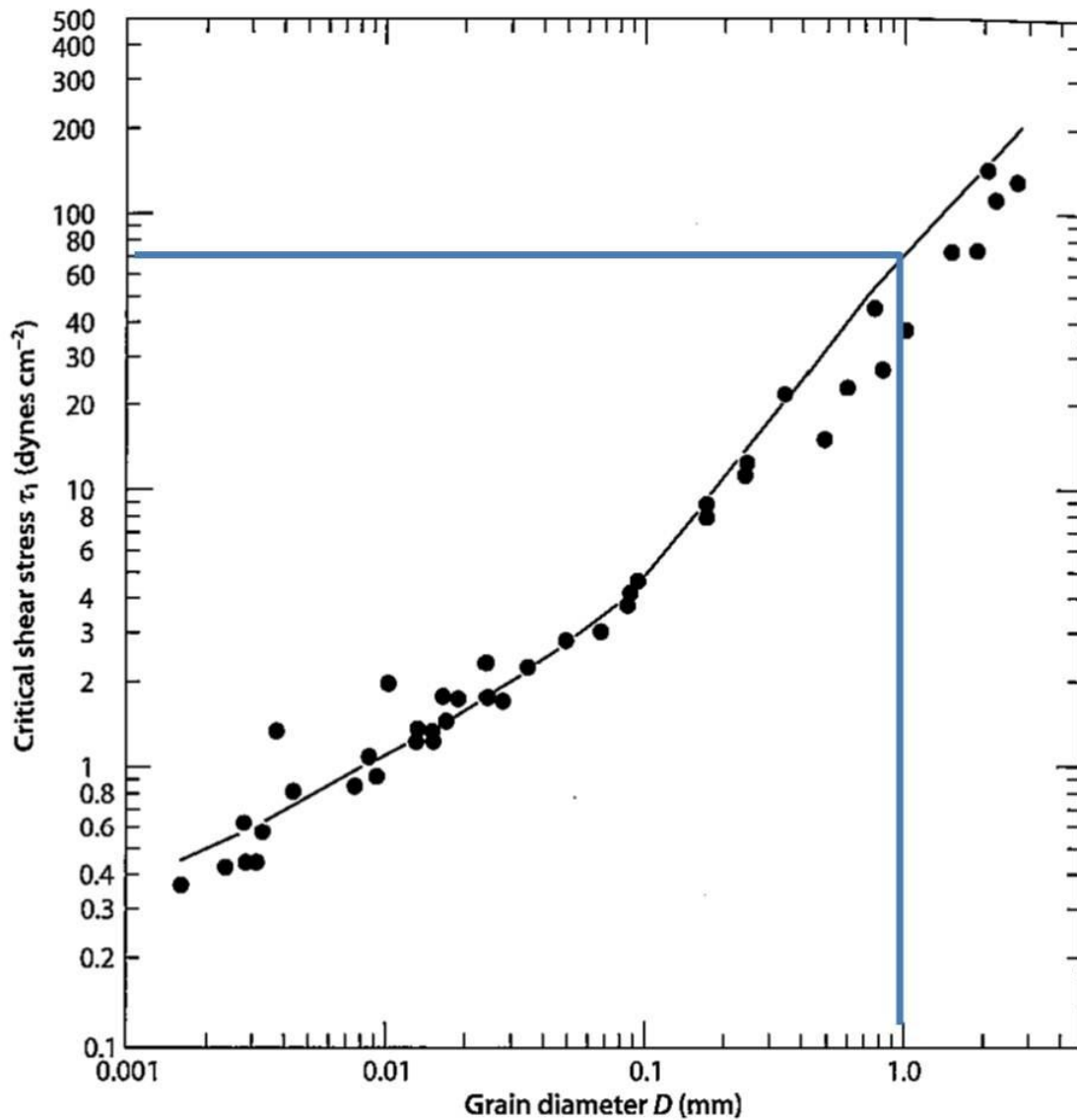


Figure 23: Modified after Miller et al. (1977), showing a critical shear stress value of 70 dynes per  $\text{cm}^2$  for a 1 mm sand grain. When converted, 70 dynes per  $\text{cm}^2$  is equal to seven Pascals.

Similarly, the Bureau of Reclamation conducted studies to obtain critical shear stress values and report what they termed “critical tractive force” to range from about  $170 \text{ g/m}^2$  up to  $450 \text{ g/m}^2$ , which correspond to a range of 1.66 pa to 4.41 pa (Figure 24).

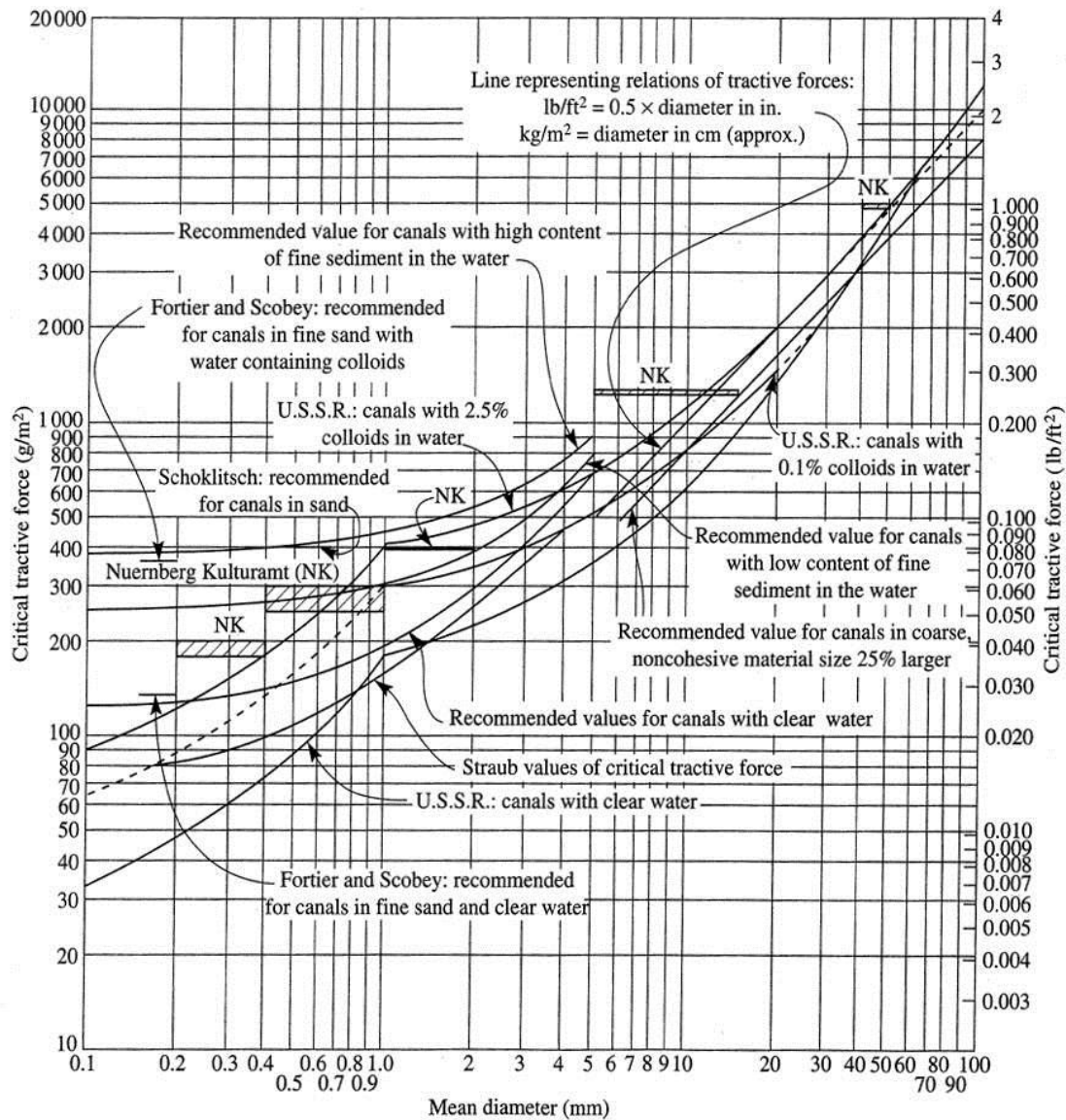


Figure 24: Graph produced by the U.S. Bureau of Reclamation showing critical tractive force required to entrain a sand grain; notice that for a 1mm grain the force ranges from 170 – 450  $\text{g/m}^2$ , which converts to 1.66 to 4.41 pascals.



### 3.1.2.6. Dynamic Vegetation

Vegetation on the landscape is simulated as 1) percent coverage at every node, which is reduced after a storm, 2) regrowth of vegetation during the inter-storm interval, and 3) the critical shear stress in both uncovered and covered portions of the grid.

Erosion of vegetation is computed according the following equation:

$$dV/dt = -Kvd V ( \tau - \tau_{uc} )$$

where  $V$  represents the proportional cover (0 to 1),  $\tau$  is shear stress exerted by the stream,  $\tau_{uc}$  is critical shear stress of the vegetation as set by the user, and  $Kvd$  is a vegetation erodibility coefficient.

Regrowth of vegetation during the inter-storm interval is calculated as:

$$dV/dt = (1/Tv) ( 1 - V )$$

where  $Tv$  is the timescale of vegetation regrowth. In my runs I set  $Kvd$  and  $Tv = 1$ , only changed critical shear values for vegetation.

Critical shear stress is calculated at each node following a storm according to the following equation:

$$Tc = Tcb + V Tcv$$

where  $Tcb$  is critical shear stress when no vegetation cover is present and  $Tcv$  is critical shear stress under 100% vegetation cover.

The role of vegetation in changing critical shear stress required for particle entrainment has been studied (e.g., Fischenich and Abt, 1995; Reid, 1989). These types of investigations are important for stream restoration projects. We use the values reported in a stream restoration study by Fischenich (2001), the values of which are shown in Figure 20.

<u>Vegetation</u>	Class A turf	3.7
	Class B turf	2.1
	Class C turf	1.0
	Long native grasses	1.2 – 1.7
	Short native and bunch grass	0.7 - 0.95
	Reed plantings	0.1-0.6
	Hardwood tree plantings	0.41-2.5

Figure 25: Shear stresses which different types of vegetation are able to withstand in lbs / sq ft. Modified from Fischenich, 2001.

We consider a range for the development of hardwood tree plantings which extends from 0.41 lbs / sq ft to 2.5 lbs / sq ft. When converted to Pascal's, the range becomes 19.6 to 120. This range covers the other vegetation types reported in the study, except for Class A turf.

#### 3.1.2.7. Slope Area Relationship

A linear log-log, channel slope to catchment area relationship has long been recognized in fluvial systems (e.g., Flint, 1974; Hack, 1957). Mathematically this relationship is described according to the formula:

$$A^{\alpha}S = constant$$

Where  $A$  is contributing area,  $\alpha$  is an exponent, commonly between 0.4 and 0.7 (Tarboton et al., 1989), and  $S$  is slope.

Equilibrium—e.g., when uplift is perfectly matched by erosion—of a landscape in the CHILD model occurs when the data on the log-log chart plot along a constant regression line (Figure 26).

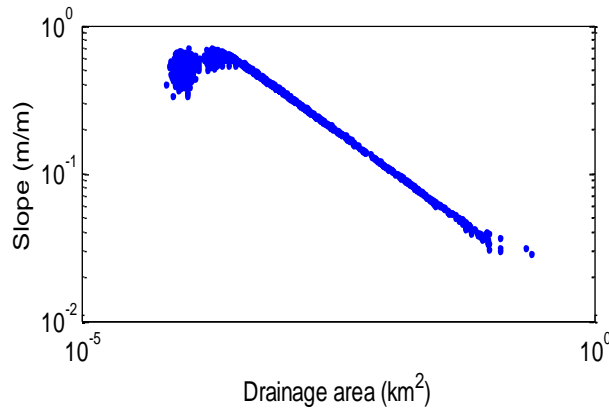
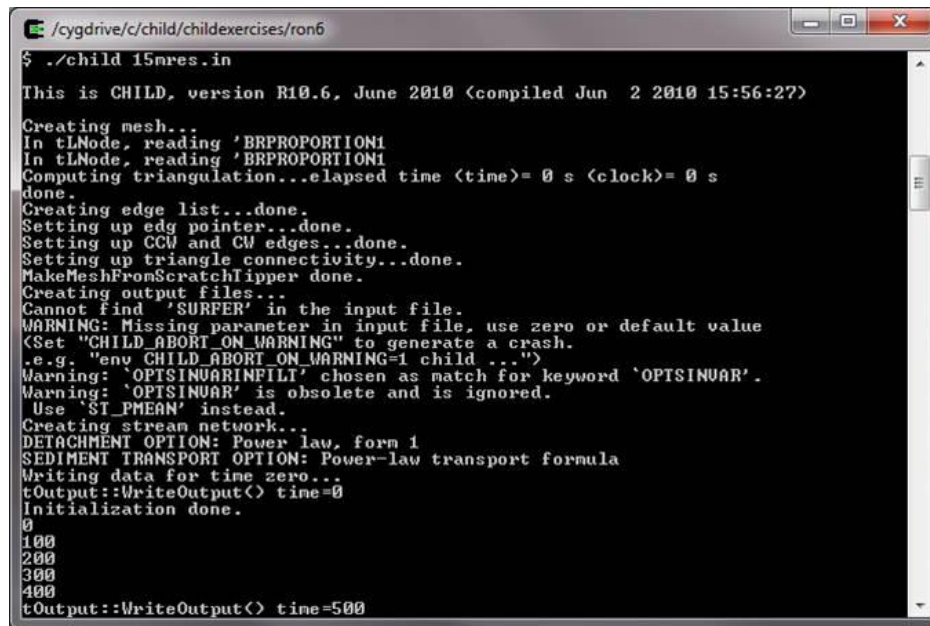


Figure 26: Display of channel slope vs. catchment area on log-log plot showing a constant regression. It is normal for there to be variation of slope for small drainage areas when landscapes are at equilibrium.

### 3.1.3. Running CHILD

A “run” of the program entails setting the values of various parameters (length of the run in years, size of the landscape, rainfall intensity, critical bed shear for entrainment of sediment, etc.) in an input file, which the program accesses when a run is initiated. Outputs from the program consist of a number of ASCII character text files which record the results of each run. To display results of a run the output files can be accessed and displayed in MatLab<sup>®</sup> per the User’s Guide (Tucker, 2009). Similarly, any program that can display x,y,z, data should easily display the outputs. Files representing the modified landscape at various times of a run are exported at designated intervals. For example, a 15,000 year run with 500 year output intervals would create 30, time-lapse ‘landscapes’ so the user can examine how the run modified the landscape through the entire run. In this work, we imported the x,y,z data into an Oil and Gas industry standard software for subsurface evaluation called Petrel<sup>®</sup>, which is a better program to display the 3D landscape.

CHILD was developed in the C++ computer language and can be run with computers running either Linux, Windows, or MacOS operating systems. As such, the program is run by typing commands in a prompt window such as the one shown below (Figure 27).



```
/cygdrive/c/child/childexercises/ron6
$ ./child 15mres.in
This is CHILD, version R10.6, June 2010 <compiled Jun  2 2010 15:56:27>

Creating mesh...
In tLNode, reading 'BRPROPORTION1
In tLNode, reading 'BRPROPORTION1
Computing triangulation...elapsed time <time>= 0 s <clock>= 0 s
done.
Creating edge list...done.
Setting up edge pointer...done.
Setting up CCW and CW edges...done.
Setting up triangle connectivity...done.
MakeMeshFromScratchTipper done.
Creating output files...
Cannot find 'SURFER' in the input file.
WARNING: Missing parameter in input file, use zero or default value
<Set "CHILD_ABORT_ON_WARNING" to generate a crash.
.e.g. "env CHILD_ABORT_ON_WARNING=1 child ...">
Warning: 'OPTSINUARINFILT' chosen as match for keyword 'OPTSINUAR'.
Warning: 'OPTSINUAR' is obsolete and is ignored.
Use 'ST_PMEAN' instead.
Creating stream network...
DETACHMENT OPTION: Power law, form 1
SEDIMENT TRANSPORT OPTION: Power-law transport formula
Writing data for time zero...
tOutput::WriteOutput() time=0
Initialization done.
0
100
200
300
400
tOutput::WriteOutput() time=500
```

Figure 27: Example of the computer interface initiating a run of the CHILD model.



Figure 28: Flow chart showing how CHILD iterates through a run. Modified after Tucker et al., 2001.

The user modifies parameters in an “input” file, such as the original grid size, the climate inputs, and values for vegetation. Input files used in this study are included in the appendices.

### 3.1.3.1. Simplicity of Mass Transport Laws

Any model of the evolution of a landscape is inherently simple in the sense that the way in which it simulates natural processes are very simplified; it is extraordinarily difficult to account

for every variable that effects the redistribution of sediment, from clay sized particles to boulders to monoliths, and the probability that each separate variable may occur. Even more difficult is to model the effects of rarer natural phenomena (bolide impacts, a jokulhlaup event, the breaking of a large glacial ice-dam, or an extreme weather event, to name just a few). We recognize that models are heuristic (i.e., experience guides the process) in nature (sensu, Oreskes et al., 1994) and have a limited ability to recreate natural phenomena in the “virtual world”. However, Maddy et al. (2001), while reviewing the LEM work of Tebbens and Veldkamp (2001), state that “Encouragingly, the results demonstrate that the models perform well enough to allow the testing of hypotheses of long-term fluvial system dynamics.” We agree with their statement.

### 3.2. Methods

In this section the specifics of running the CHILD program are introduced. Primarily I will show the input parameters that I adjusted to create a buffer zone and then display the results of program runs.

Figure 28 represents a landscape created by CHILD run for  $2.0 \times 10^6$  years. This landscape is vegetated, with critical shear stress required for entrainment set at 100 Pascals. Climate was set at 20m/yr intensity, with 2 year storms that recur every 8 years. Though this is unrealistic, I consider heuristically that in any given year, storms occur 20% of the time with the reported intensity. Snyder et al. (2000) report that Honeydew, California (located near the coast some 200 miles north of San Francisco, CA, about 50 miles south of Eureka, CA) has storm intensities of 25.3 m/yr. Tucker (2009) reports that the intensity of Atlanta, GA is 16.4 m/yr. In separate studies, Collins et al. (2004) and Gasparini (2008) used precipitation intensities of 14 m/yr and 1 m/yr, respectively. The point is that the range of intensities I have chosen, 10 m/ yr – 20 m/yr, are within the realm of reason for this investigation.

Similarly, per the reports of vegetation in the Fischenich (2001) study, a range of critical shear values for vegetation ranging from 20 – 100 pascals is also considered to be within the

realm of reason for this study.

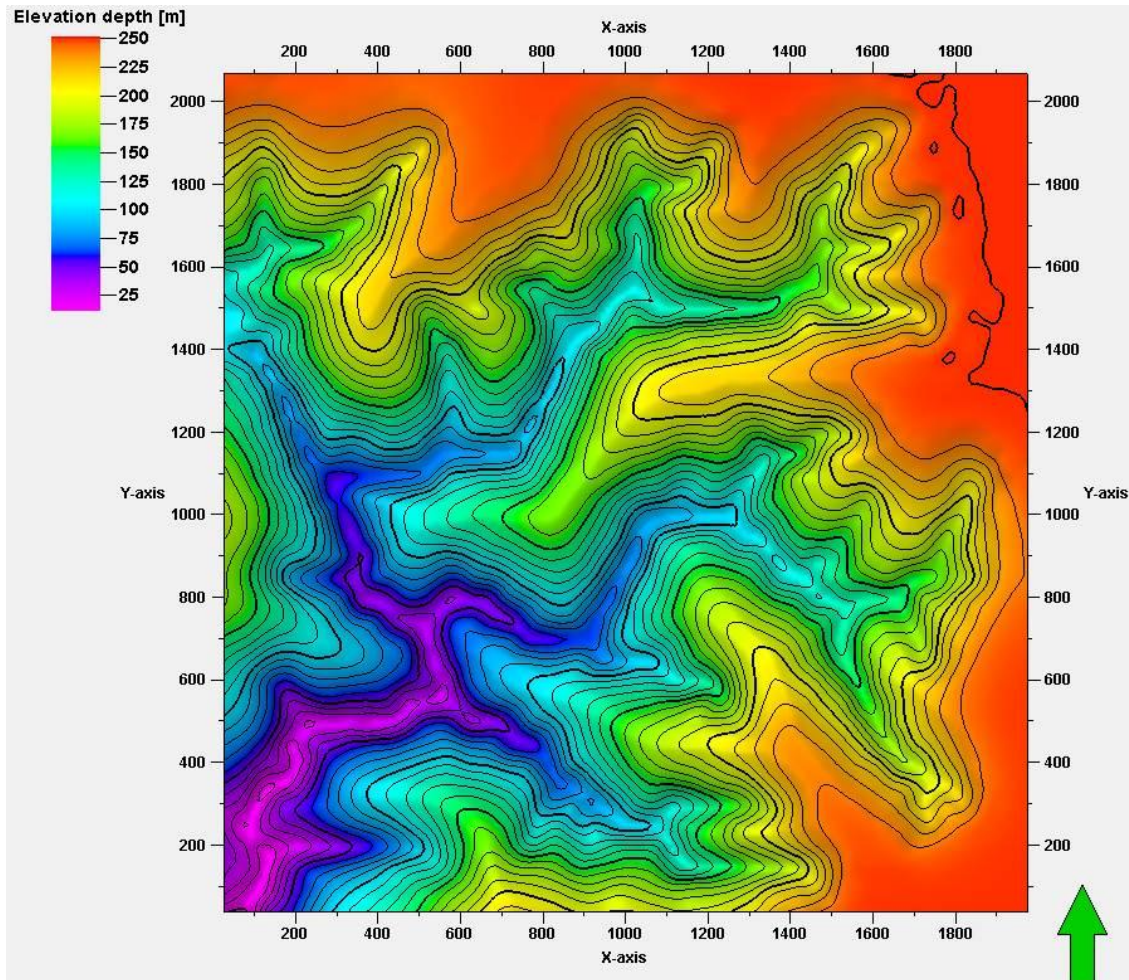


Figure 29: Original surface topography for which changes in vegetation shear stresses and climate parameters were changed to initiate aggradation.

Figure 29 was displayed in Petrel, a 3D oil and gas industry standard software program used to examine subsurface data. Its strength in displaying these data was why it was chosen. A statistical analysis of the surface can be made using Petrel. Figure 30 is the same original surface displayed above, though this time showing slope angles.



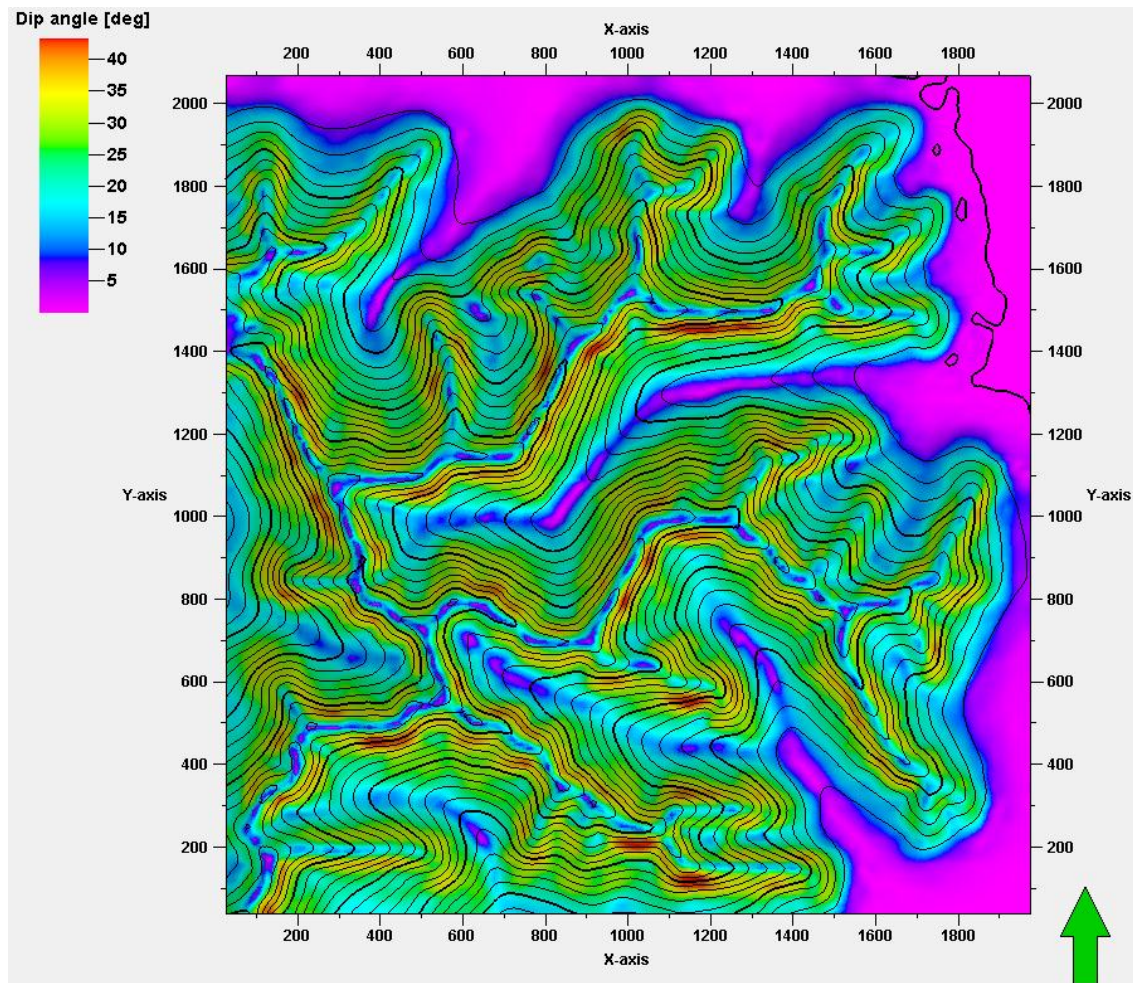


Figure 30: Display of original surface showing slope angles of the drainage basin.

This display shows the hillslopes better, as well as the channels in the valleys. A histogram of the data is shown in Figure 31.



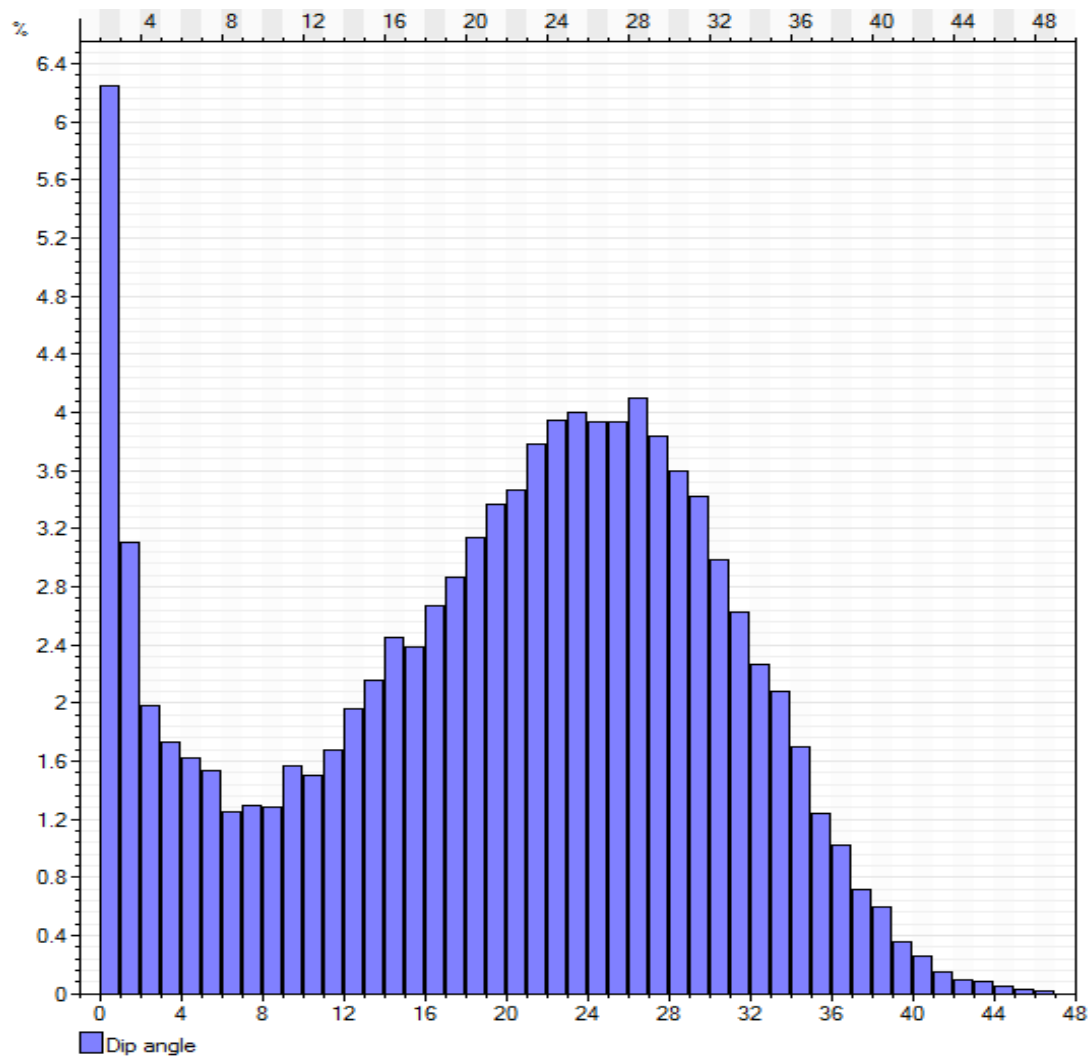


Figure 31: Histogram showing distribution of Dip angles for original surface; max = 46.73 degrees; mean = 19.53 degrees; standard deviation = 10.55. Percent of total data points (Y axis) and angle in degrees (X axis).

The mean slope angle is about 20°, which would represent a fairly mature and denuded environment, particularly for a more humid environment where one would see a greater percentage of the steeper slopes.

A modern comparison for this drainage basin was found in an area south of Albuquerque, NM, between the peaks of North and South Black Mountain (Figures 32, 33).

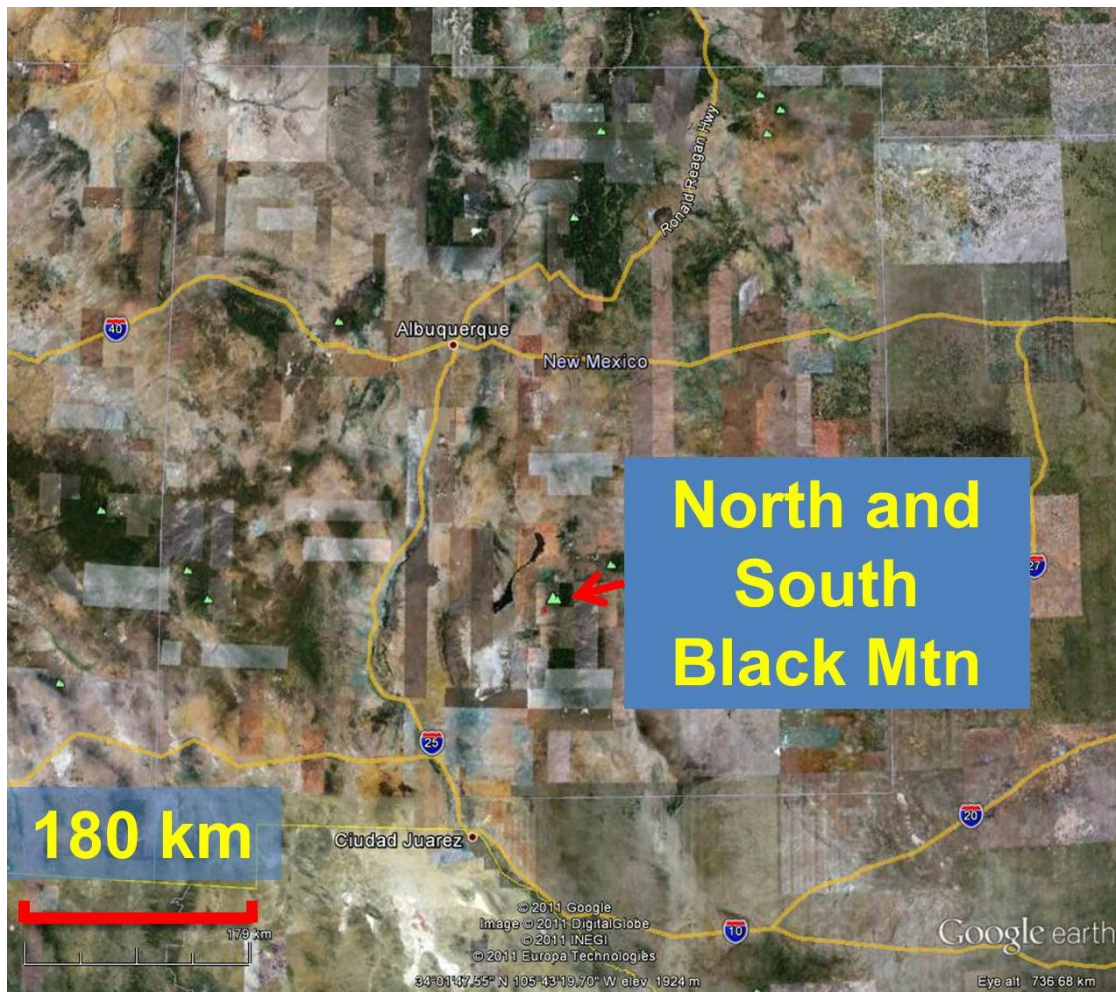


Figure 32: Satellite image from GoogleEarth showing the location of the Black Mountains in New Mexico, United States.

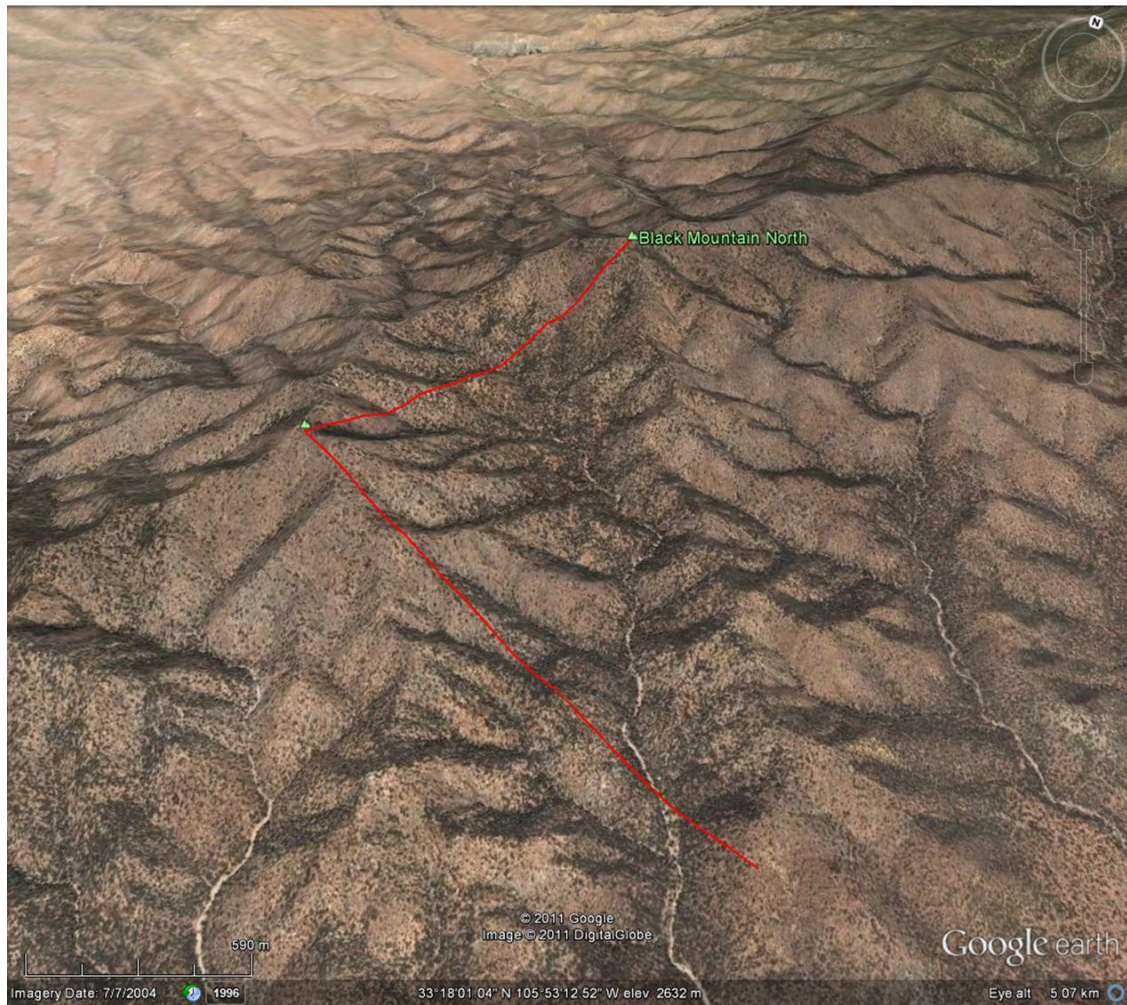


Figure 33: GoogleEarth image of a drainage basin considered comparable to the one created by CHILD in this study located near the Black Mountains of New Mexico, United States.

Publicly available digital elevation model data for the drainage basin was imported into Petrel (Figure 34).



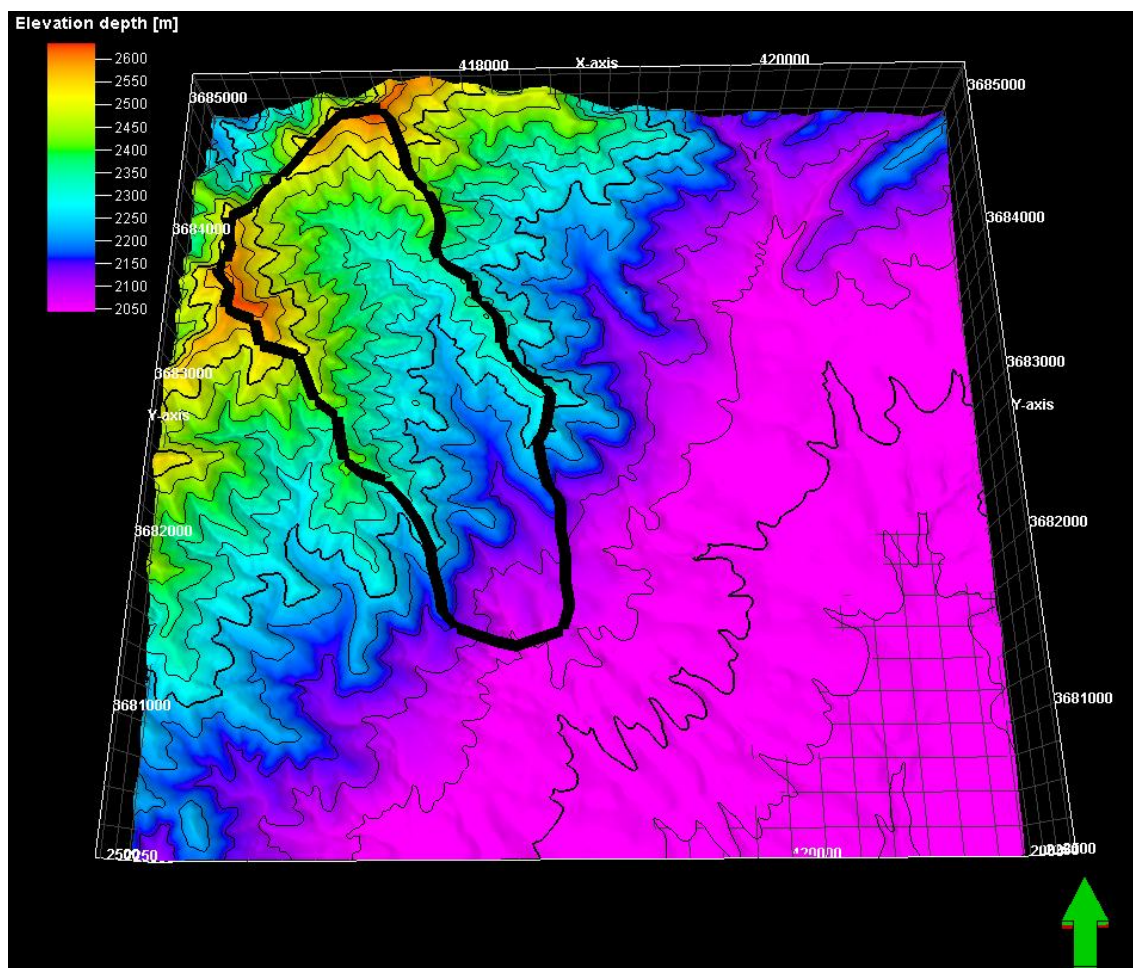


Figure 34: DEM data from the USGS of North and South Black Mountains, NM. Black polygon shows area that was initially clipped and used for statistical analysis.

The clipped polygon was flipped so that it more closely matches the theoretical basin (Figure 35).

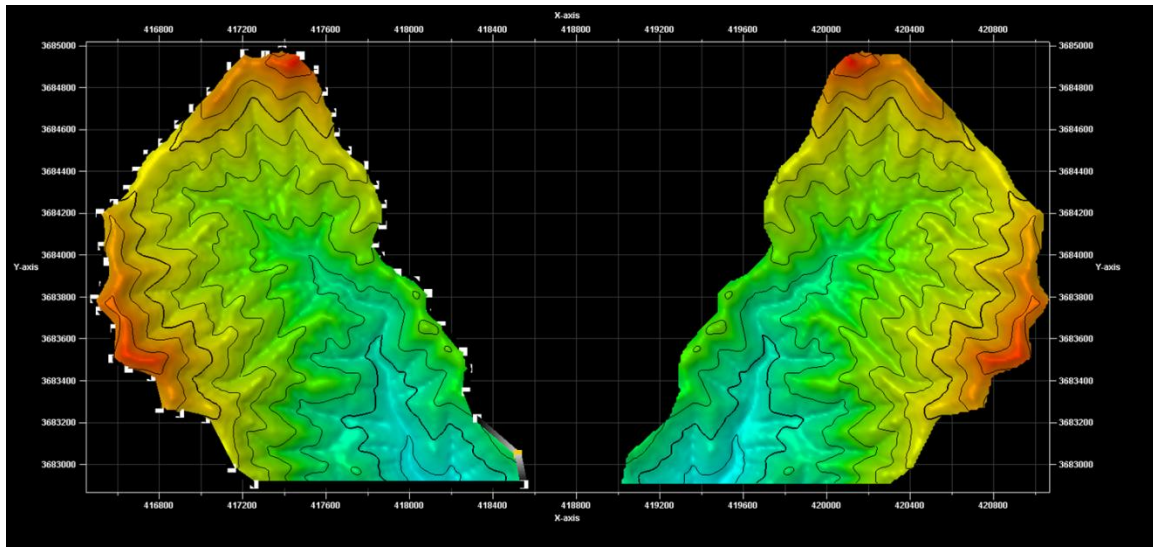


Figure 35: Flipped drainage basin on the western flanks of the Black Mountains, NM.

The flipped drainage basin was superimposed on the original surface (Figure 36). Though data for storm intensities, storm durations, and critical shear stresses to remove vegetation are not available, this is considered to be a comparable basin in size, drainage density, and slope angles. The purpose of this comparison is to illustrate that the drainages generated by CHILD geometrically resemble drainages that naturally form on modern landscapes

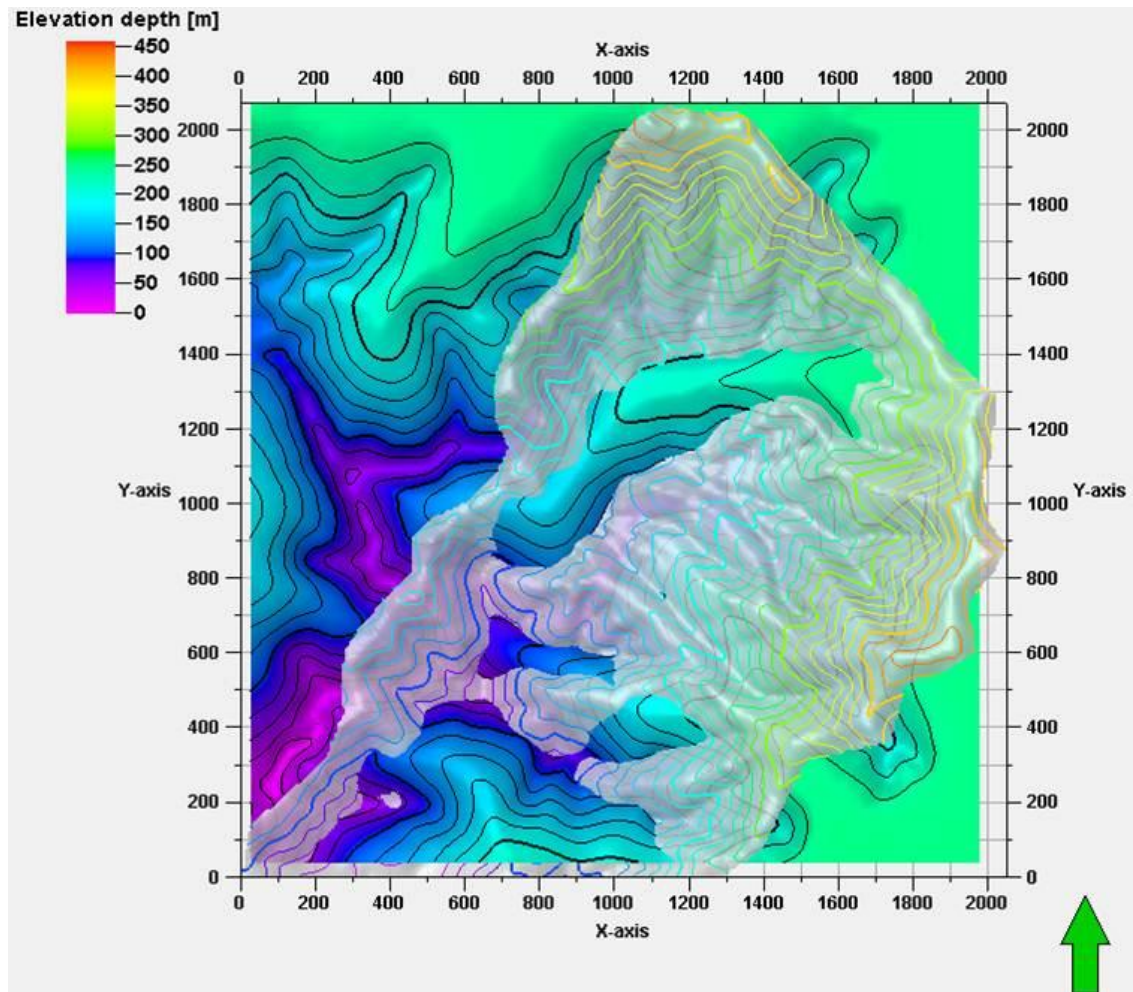


Figure 36: Comparable basin from New Mexico (clear). Though the drainage basin is slightly steeper with a greater range of elevations, we consider it to be a comparable basin in drainage density and hillslope angles.

Finally, a statistical analysis between the two is shown in Figure 37.

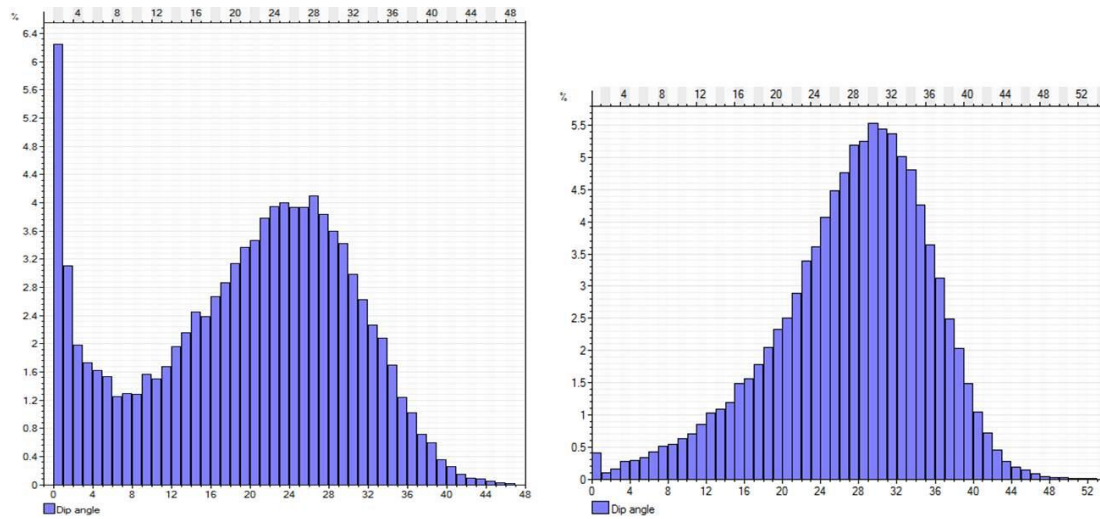


Figure 37: Histograms showing distributions of hillslope dip angles for surfaces in Figure 35.  
 Right Histogram: max = 46.73 degrees; mean = 19.53 degrees; standard deviation = 10.55.  
 Left Histogram: max = 52.13 degrees; mean = 27.21 degrees; standard deviation = 8.13.  
 Percent of total data points (Y axis) and angle in degrees (X axis)

Though the New Mexico landscape is steeper over a broader range of elevations it is a comparable landscape. Variations between the simulated and natural basin likely reflect the greater complexity of the natural system. For example, it is comprised of multiple, coarse grain sizes with a resistant vegetative cover.

### 3.2.1. Aggradation of Sediment in Valleys

Aggradation in the valleys was achieved by changing parameters of climate and vegetation simultaneously. Essentially, decreases in precipitation intensities and frequencies, as well as lowering shear stresses for vegetation cover, liberated sediment from the headlands of first order valleys which was stored in the bottoms of higher order valleys. The figures that follow will graphically show the process.

The initial surface, as described earlier, had a storm lasting 20% of the iteration time, with 20 m/yr precipitation intensity and vegetation shear stress set at 100 Pascals. This was run to

bring the initial 2 square kilometer grid into equilibrium. For the aggradational phase, the settings were set according to Table One.

Table 1: Parameters used in the CHILD model to simulate stream aggradation due to changes of upstream controls only.

Storm duration (% of iteration)	Precipitation Intensity m / yr	Vegetation Shear Stress Pascals	# of years
20	20	100	2.00E+06
15	18	80	10
10	16	60	10
10	14	40	20
10	12	20	60

The parameters above were chosen after many trial and error iterations. Basically, once the initial landscape was created, parameter settings were run with the numbers above over hundreds of years. The landscape would initially aggrade, then begin to incise. When aggradation approached its high point, the parameters were changed again. Indeed, for the purposes of this study, merely changing the settings in the first step would have been sufficient to answer my question, which was to find the controls on aggradation of a landscape.

Figure 38 shows the modified landscape after 10 years of evolution. The new climate was set so that storm intensities and durations decreased; critical shear stress to remove vegetation was also decreased. Examined closely one sees the increase in elevation in the valleys and increased erosion at the headlands.



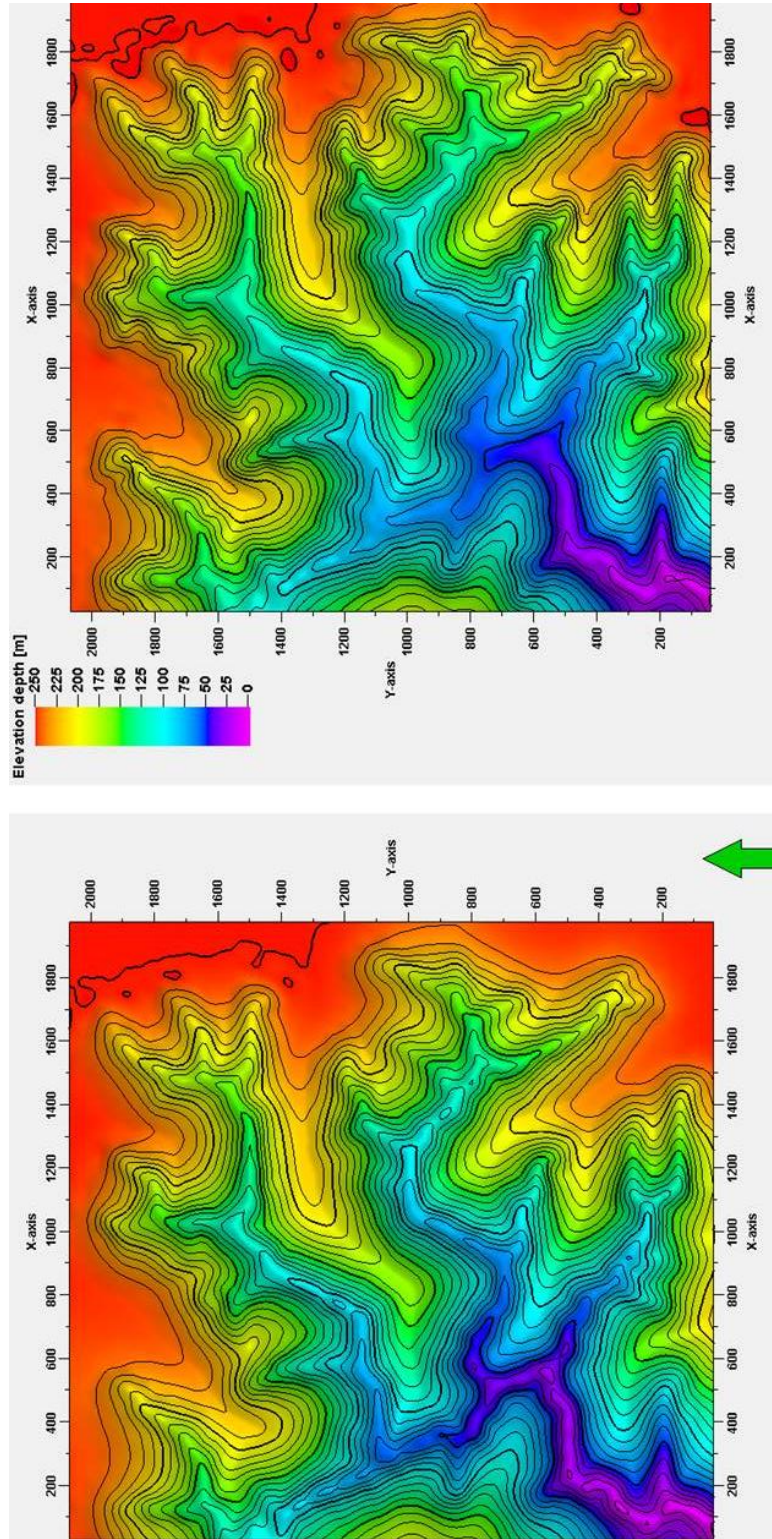


Figure 38: Comparison of original surface and the modified landscape after 10 years of climate and vegetation change. Notice that erosion occurs at the headlands of first-order valleys whilst deposition occurs in the higher-order valley bottoms.

An isopach between the two surfaces is shown in Figure 39. Negative thickness are areas where the modified landscape after 10 years of model run are below the original surface; the landscape overall is slightly denuded, with areas of rapid erosion. Areas of positive thickness are those shown where the modified surface is above the original, and is the result of deposition of sediment.

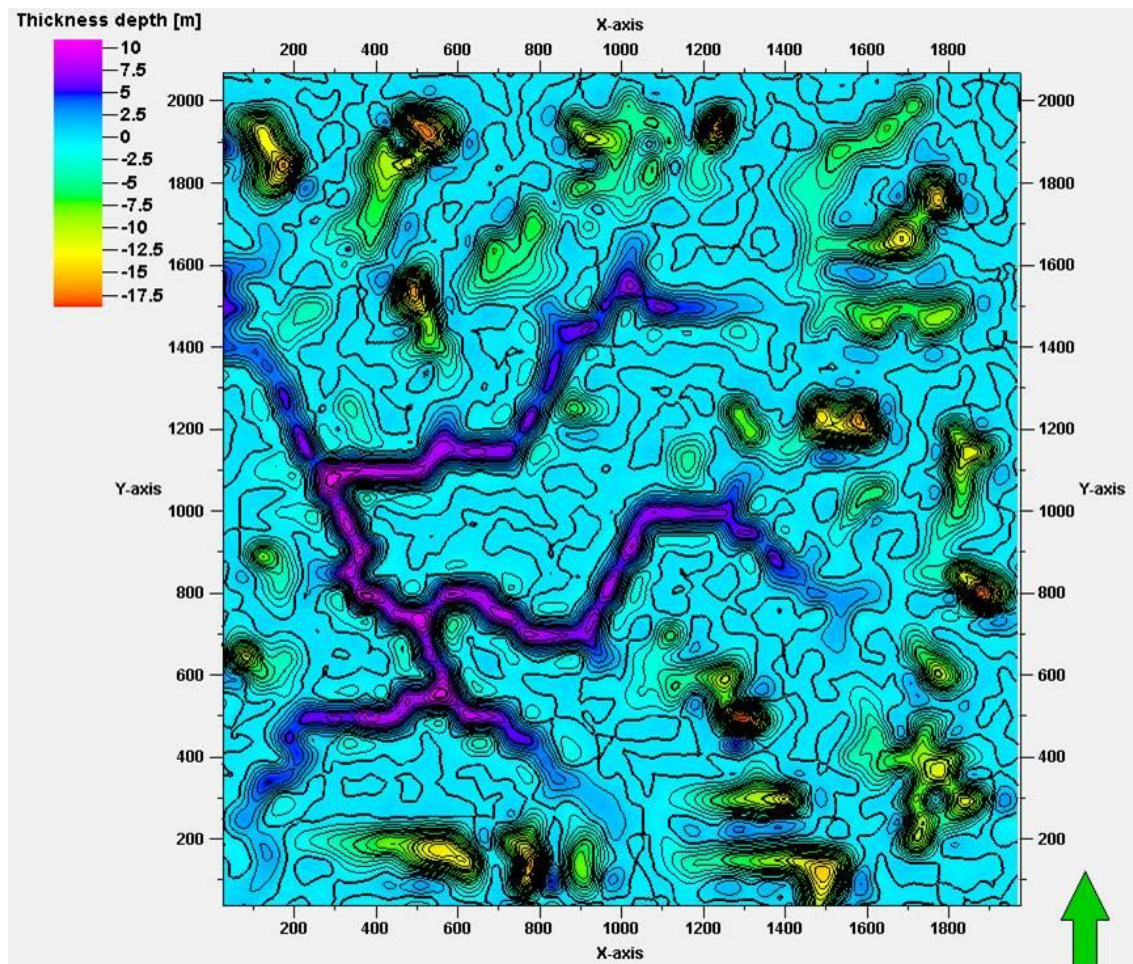


Figure 39: Isopach between the original surface and a 10 year surface which represents 10 years of model run at new climate and vegetation parameters.



Deposition of sediment in higher order valleys is easily seen on the isopach map of Figure 39. The distribution of highly eroded areas, those which have high negative thicknesses, is curious. Figure 40 is a modified version of Figure 39, only this time the contour lines of the original landscape, each colored according to its z-value, are superimposed on the isopach map. The solid portion of the original surface was made to be completely transparent.

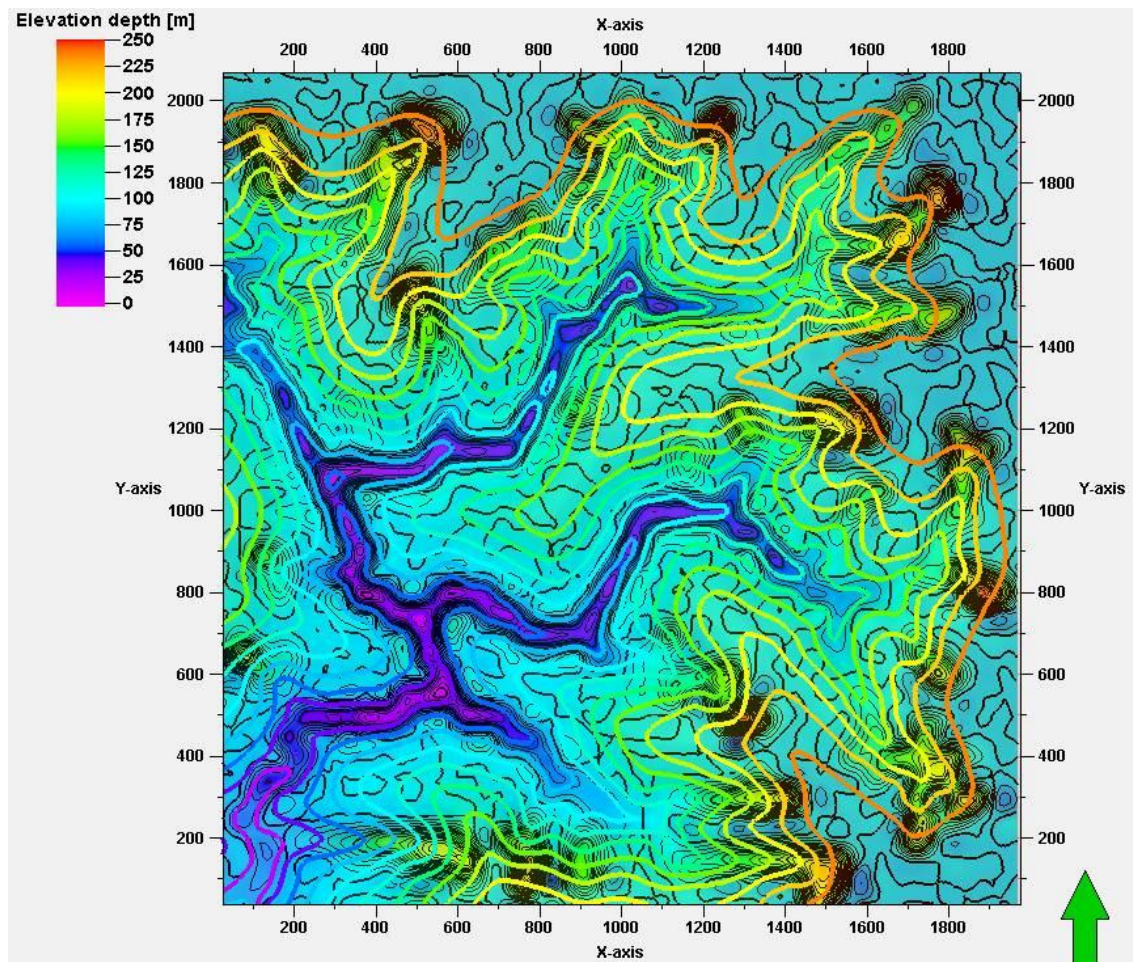


Figure 40: Isopach map between Original surface and 10 year surface of aggradation. Bold contours from the original surface colored according to z-values are superimposed. This display shows the distribution of the eroded areas, which represent areas where the change in vegetation was most susceptible to erosion.

Headward erosion in the first-order valleys was noted over the climate and vegetation changes shown in Table One. Rather than showing surfaces and isopachs for each time interval, the final surface is shown in Figure 41.

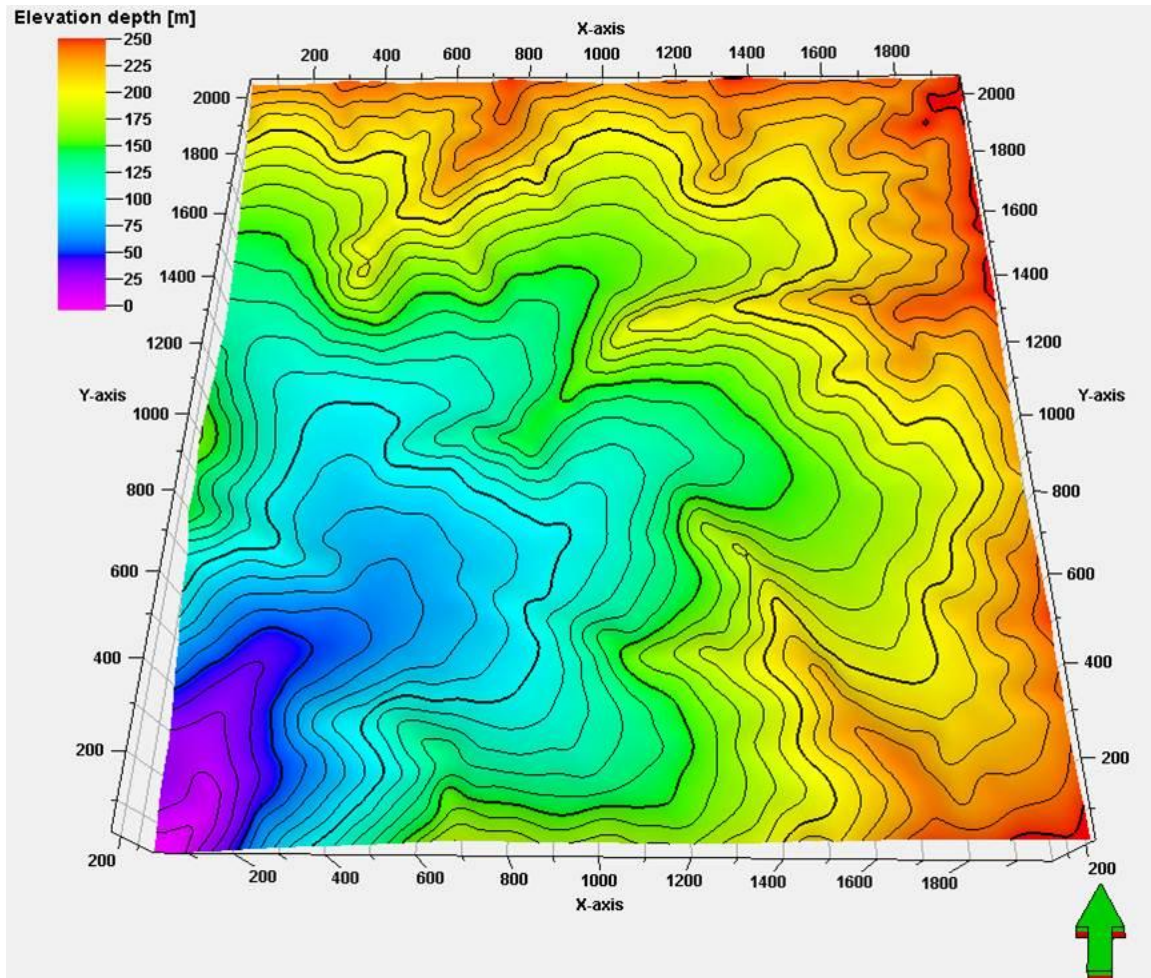


Figure 41: 3D view from above and south of the resultant surface after 100 years of aggradation.

Statistical analysis of the surface was done similar to the original surface and comparable real world surface above. The results are shown in figures 42 and 43.



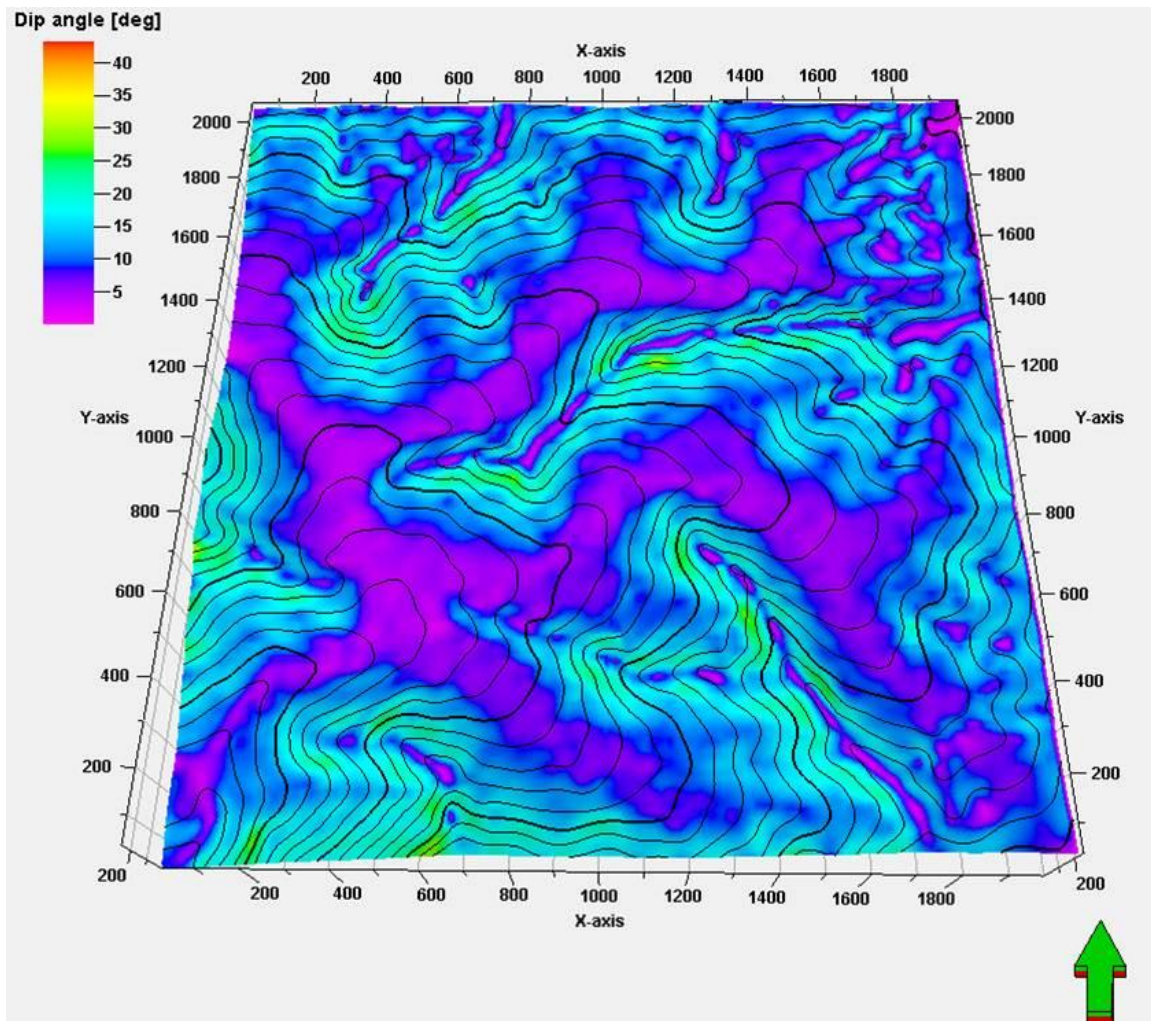


Figure 42: Hillslope dip angles for the final surface of aggradation. Notice that the landscape overall is denuded, with low hillslope dip angles and relatively flat valley floors.

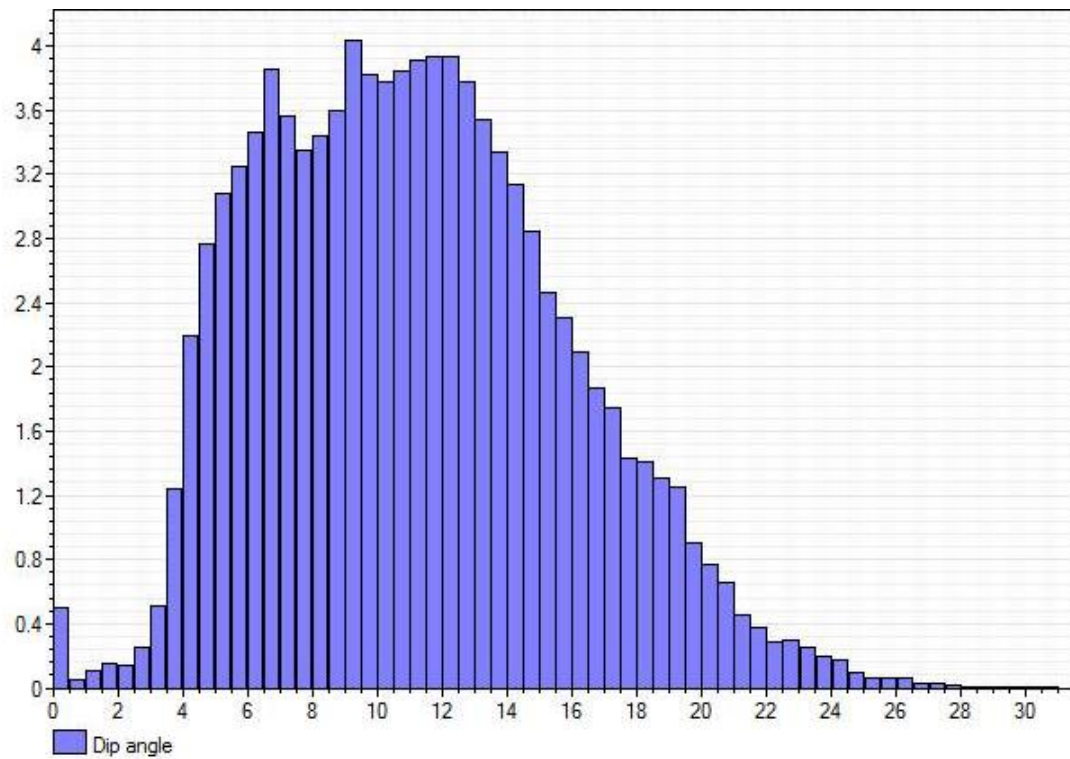


Figure 43: Histogram showing distribution of hillslope angles for the final surface of aggradation. Percent of total data points (Y - axis) and dip angle in degrees (X - axis).

These results are compared to the original surface in figures 44 and 45.

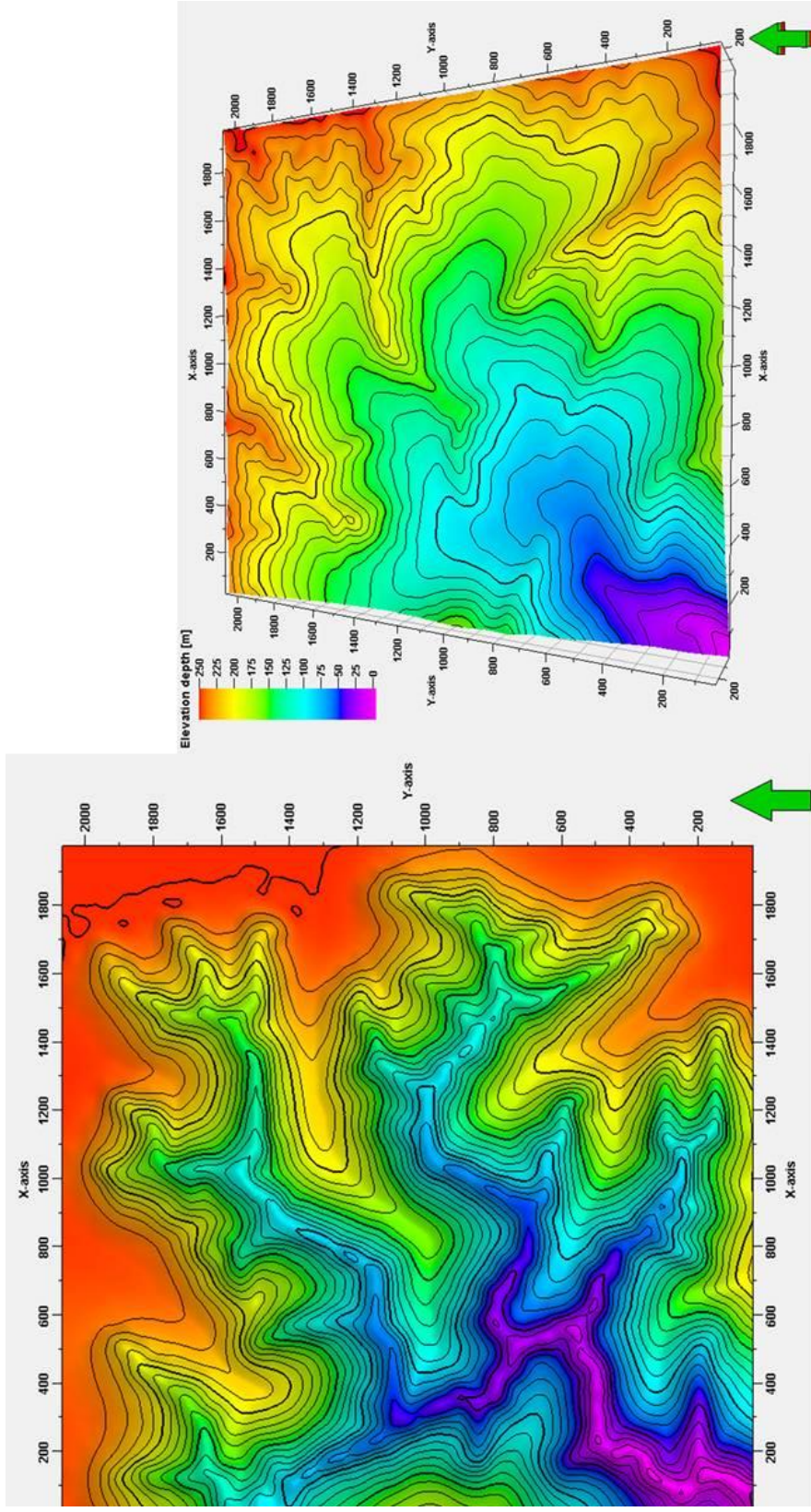


Figure 44: Original surface and final surface of aggradation.

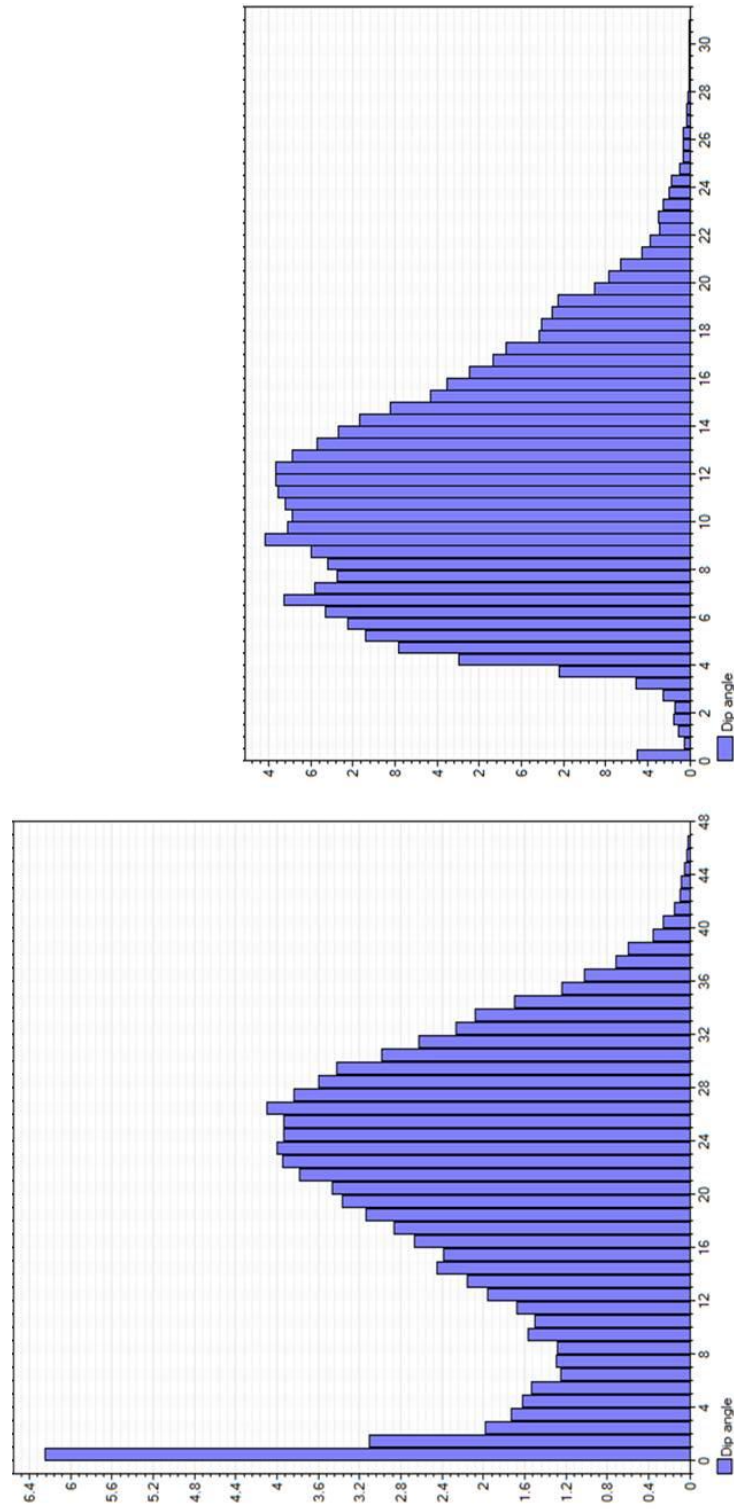


Figure 45: Histograms showing the distribution of hillslope dip angles for the original surface (left) and final surface of aggradation (right). Original Surface: max = 46.73 degrees; mean = 19.53 degrees; standard deviation = 10.55. Final Surface: max = 30.72 degrees; mean = 11.16 degrees; standard deviation = 4.67



Figure 45 above is somewhat misleading. The mean dip angle for the original surface is shown to be approximately 19 degrees. The data are skewed however by the large flat areas at the edge of the landscape where the streams never reached. Those flat areas, shown on the histogram as the bars to the left, comprise a disproportionately large area of the landscape and therefore pull the analysis of the data set to the left. Visual examination of the distribution of the data shows that the mean value should actually be about 24° - 25°.

Cross sections were made showing the evolution of the landscape. Figure 46 shows the location of the first cross section, which was run from the outlet point of the drainage basin, along the axis of the major valleys, to the furthestmost first-order valley head.

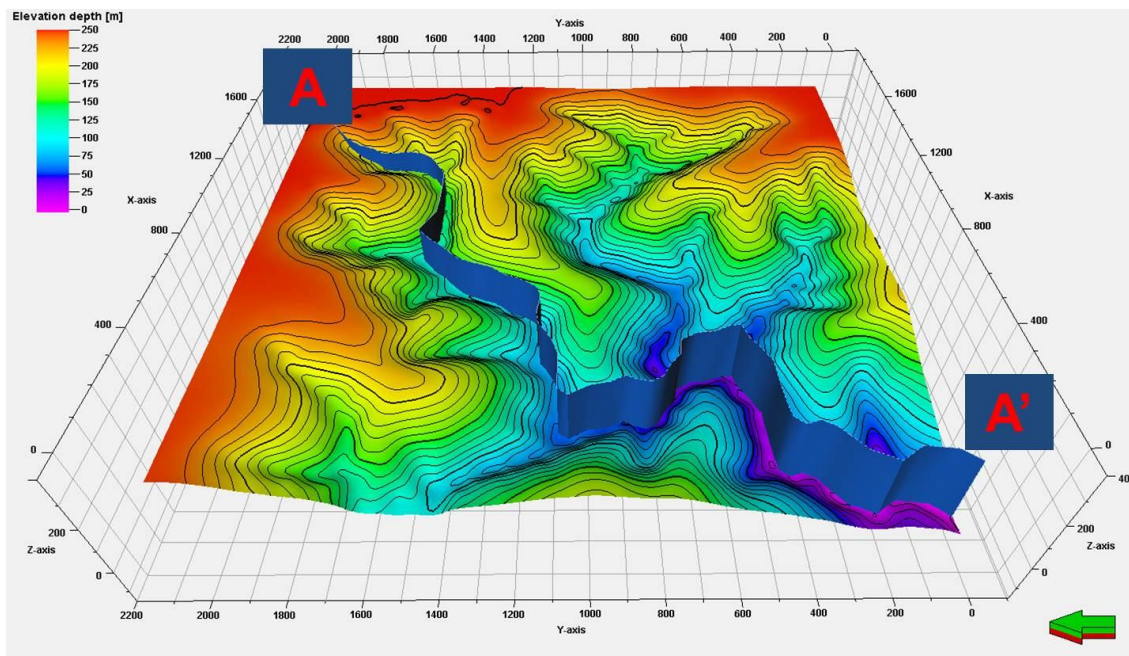


Figure 46: Location of cross section A - A' which is run from the furthestmost first-order valley through the higher-order valleys to the outlet point of the drainage basin.

Figure 47 shows the elevations for each ten year time step of landscape evolution.

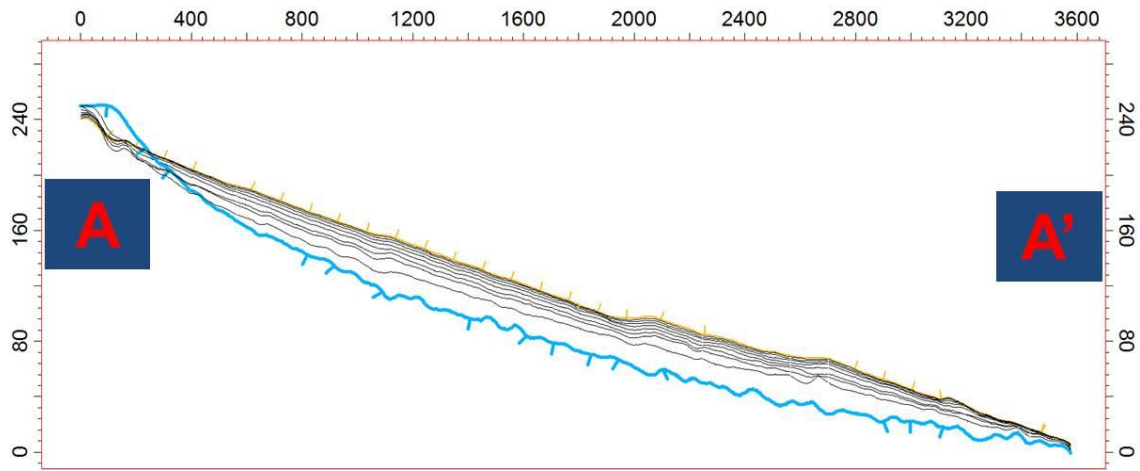


Figure 47: Cross section of a buffer zone, showing the original surface (cyan) at the bottom, 10 year time steps (black), and the highest surface (light brown) at the top. 2X vertical exaggeration.

A north – south, cross section near the center of the landscape was made as well, the location of which is shown below (Figure 48). Figure 49 is similar to Figure 47, with the original surface shown in cyan, 10 year time steps shown in black, and the final surface of aggradation at 100 years shown in light brown.

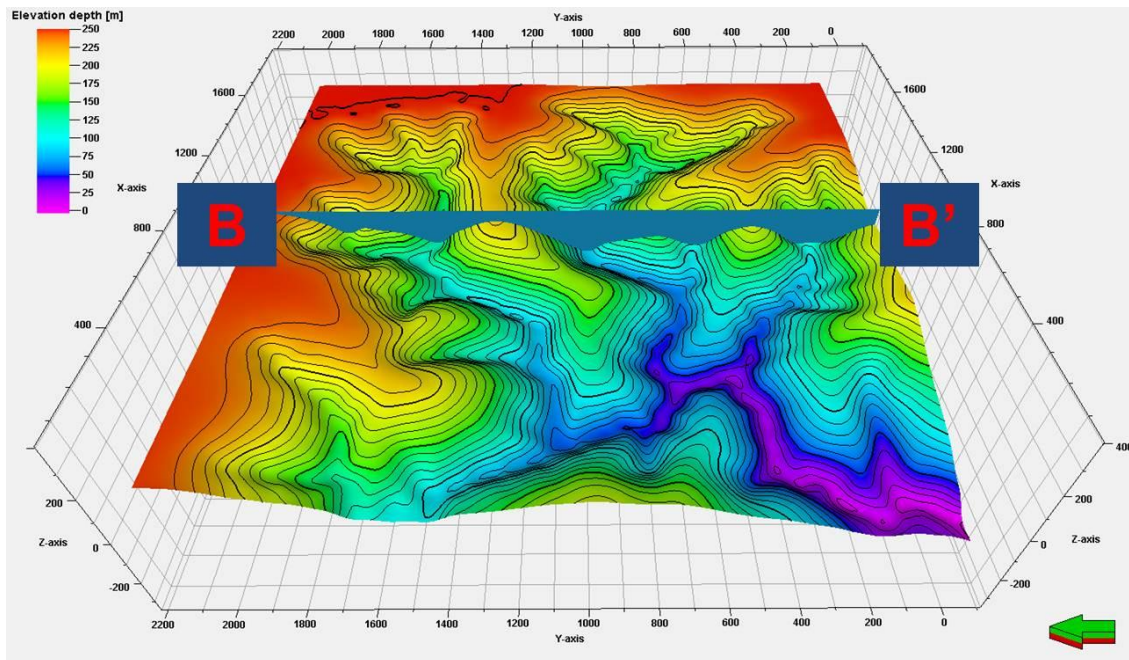


Figure 48: View from above and west showing the location of a North - South cross section near the center of the drainage basin.

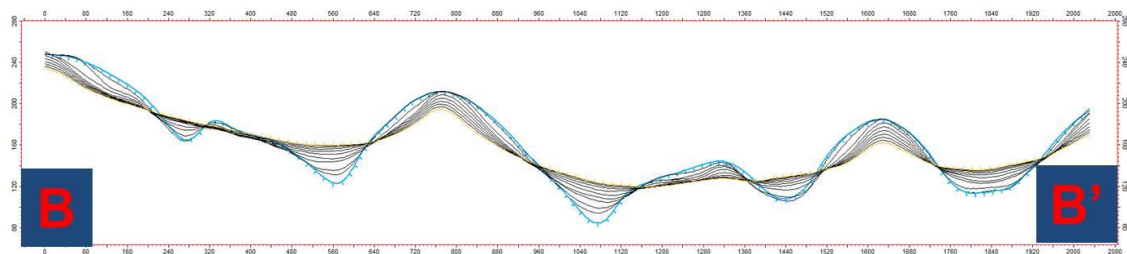


Figure 49: North to South cross section of the landscape. Cyan line represents the original surface, light brown line represents the upper-most surface of aggradation, and black lines are 10 years steps of time.

Finally, to examine the buffer zone, an isopach was created between the highest surface of aggradation and the original surface. Unlike the previous isopach maps where the negative thickness was shown, the isopach of figure 50 shows only the thickness due to deposition in the valleys.

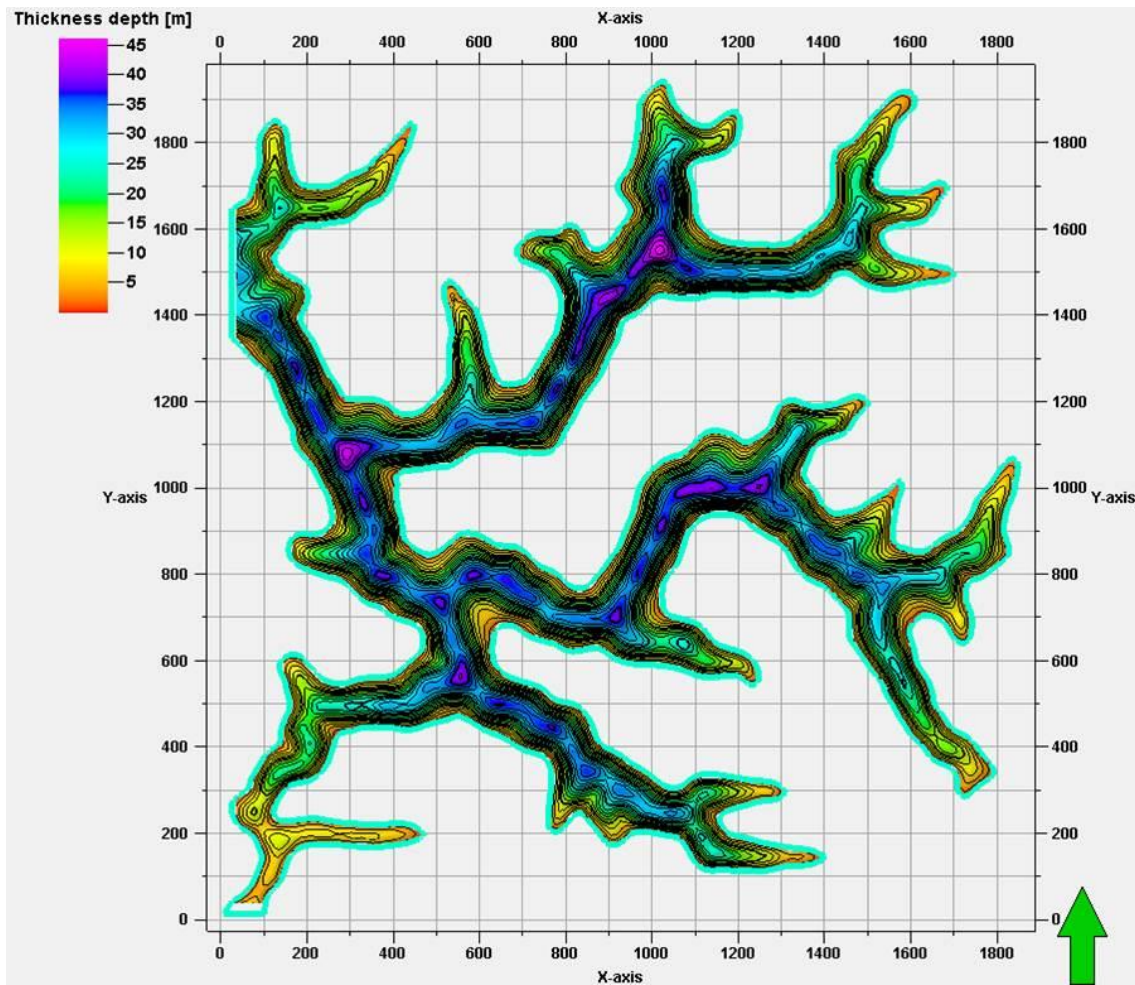


Figure 50: Isopach showing aggradation due to deposition in the valleys after 100 years of climate change. Cyan polygon outline is the position of zero thickness; outside of this polygon the surface would show negative thickness, representing erosion and denudation of the landscape.

Figure 50 shows only the thickness of accumulation of sediment in the valleys, which represents the extents of the buffer valley for this cycle. We did attempt to reincise and aggrade the system again, but, the model incised the system in exactly the same valley configuration. We then attempted to change the outlet of basin, but, was unable to do that either. Migration of the valleys laterally during aggradation and incision within a buffer zone would create a regional composite scour (RCS) surface (*sensu*, Holbrook and Bhattacharya, in press) which defines the

base of the buffer preservation space, and the composite upper aggradational surfaces would define the top of the buffer preservation space. Unfortunately, we were unable to do this.

Finally, a log – log plot of channel slope to drainage area was plotted in Matlab to examine the landscape at each of the climate and vegetation changes shown in Table One (Figure 51).

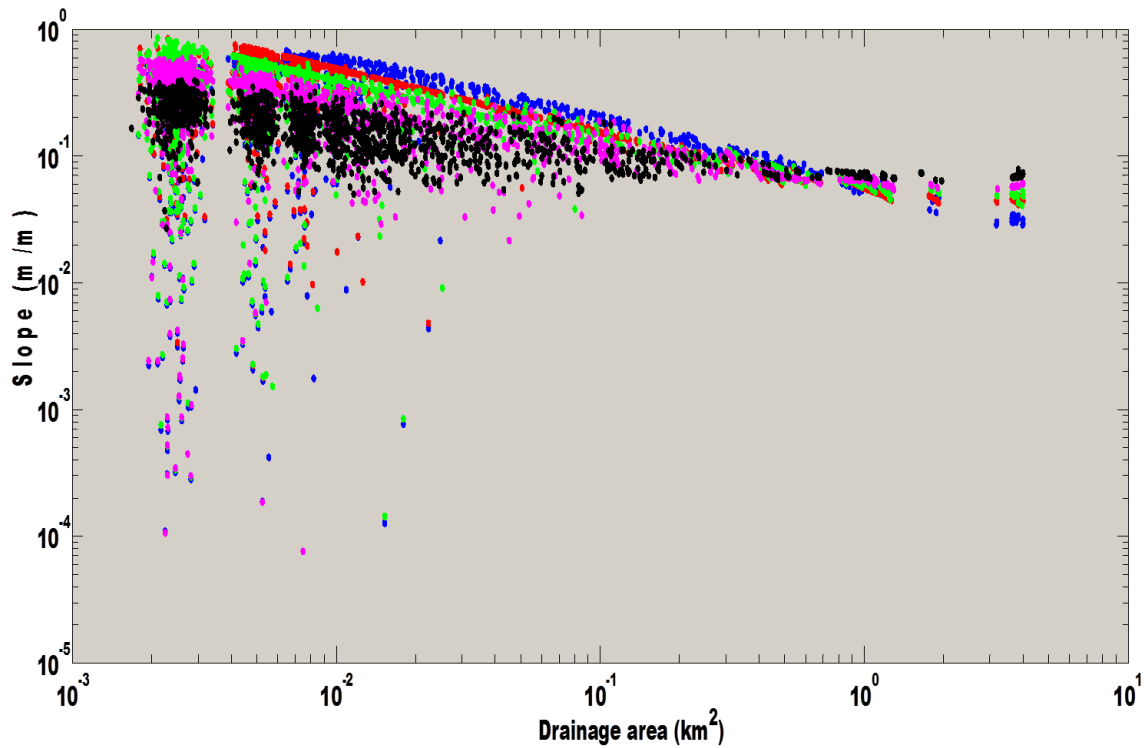


Figure 51: Log - log plot for the landscape at each time when the climate and vegetation parameters were changed. Original landscape (Blue); 10 years aggradation (Red); 20 years aggradation (Green); 40 years aggradation (Magenta); 100 years aggradation (Black).



### 3.3. Discussion

This study is an examination of process, and therefore we are interested to determine if the processes we see in the model are realistic. Because the model is simplified as much as possible to answer my question, I do accept some unrealistic aspects of the model. The parameters above yielded a lot of aggradation in a relatively short period of time. I recognize that all the potential controls on rates of change of the system are not accounted for. Thus, though the rates of change are likely unrealistic, the processes of change are realistic.

Climate change, as mentioned in section 3.1.1.2., can change abruptly. In a personal communication with Dr. Anthony Burgess, botanist in the Environmental Sciences department of Texas Christian University, I learned it is both reasonable to expect the vegetative cover to change rather abruptly in response to a change in climate as well as to repopulate the landscape fairly quickly once removed. I recognize that the step wise change of climate, along with a step wise change in vegetation cover, is rather abrupt in the model, but certainly not beyond the realm of reason. I do feel that the accelerated rate of climate change, changes of vegetation critical shear stresses, and the regrowth of vegetation, are all reasonable to investigate the controls on aggradation.

This investigation considers the substrate to be comprised of 1mm quartz sand. The critical shear stress required for entrainment of an unvegetated surface was set at 0.73 Pascals. Recall, per Figures 22 – 24, that there is a range of values of shear stress required to entrain a 1mm quartz grain. Vegetation cover in the model was set to change from hardwood tree saplings to sparse grass cover. Thus, once a threshold is reached for the removal of vegetation, we expect that the streams would dominate the system and transport sediment at their level of competency. In nature, we would not expect such conditions to be as abrupt as is modeled here.

Evidence for abrupt erosion in the model occurs in the very first 10 years of model run, where erosion seems to advance quickly in the first-order valley headlands. The shear stresses exerted by the streams are at their highest, and subside because the hillslopes are shallowing in

their dip angles. The model depicts a drastic case, but, the process created is realistic, in that a change in vegetation due to a change in climate is a means for the liberation of vegetation-bounded sediment and therefore erosion.

Erosion focused at the headlands of first-order valleys also makes sense. Recall that precipitation falls evenly across the landscape. In the headlands, discharge is focused and therefore local shear stresses exerted by water would be higher. Also, these are areas of steepest slope, which also plays a role in local shear stress exerted by running water.

The sediment, once liberated from the headlands from the first-order valleys is deposited in the valley bottoms. The deposition represents aggradation due to changes on the system, induced by climate, but specifically changes in the critical shear stress related to removal of vegetation. It is the vegetative feedback of the system that is key to aggradation in the valley bottoms.

Aggradation of sediment in the valleys resulted in a low relief landscape, something similar to bajada flanking low lying hills. Davis (1902) would have called such a landscape a mature landscape. What we recognize is that this is a transient landscape responding to mechanisms that are driving it towards a new equilibrium. Thus, it may or may not be a mature landscape, for reincision, valley widening, etc., can all happen fairly quickly on geologic time scales.

The plot of Figure 51 shows that for aggradation to occur, the channel slope to catchment area must change in such a way that the regression line of equilibrium on the plot shallows. The shallowing regression line represents a shallow stream depositional dip angle for both small catchments and larger drainages—the streams overall have shallowed in dip to aggraded the system.

The simplicity of models to recreate natural phenomenon is only part of the explanation as to why this is true. Computers in future, perhaps, will be sufficiently complex to capture and account for the many variables affecting the evolution of a landscape from minute to geologic

temporal and spatial scales. However, the fundamental governing equations of those models are themselves evolving, and the vagaries that exist around regression lines, say, for depth to width relationships in a downstream direction, will perhaps be more tightly constrained. Similarly, low frequency, high amplitude, random events that create rapid changes, e.g., the 10,000 year flood event, will have to be considered. It is my conclusion that the results presented here for size and amplitude of the buffer zone is correct in a gross sense, though I recognize, as stated above, that the evolution of technology concurrent with an evolution of the science may further refine these results.



CHAPTER 4

RIVER SCOUR

4.1 Scour Types

River scour at confluences and sharp bends is well recognized in fluvial systems (e.g., Best, 1988; Best and Ashworth, 1997; Feldman et al., 1995; Mosley, 1976; Plint, 2002; Salter, 1993). Though not a primary aim of this research, the evolution of river scour at sharp channel-bends and confluences was modeled. Scour is also known to occur at lateral constrictions in the stream (i.e., where shear stresses required for erosion laterally are relatively high). Various types of scour are shown in Figure 52.

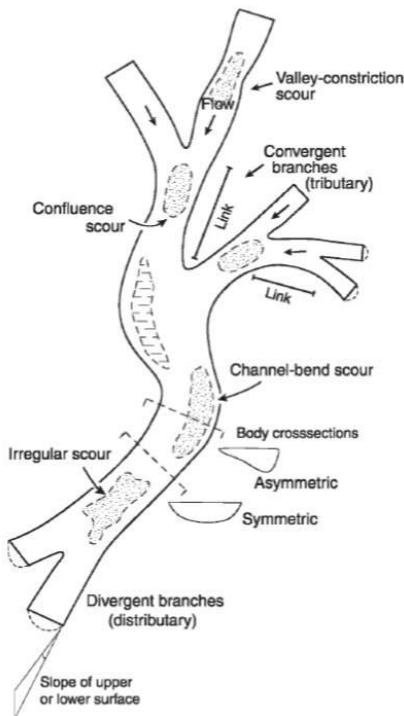


Figure 52: Types of channel scour recognized in river systems. From Gibling (2006).

Channel scour at channel confluences and at sharp bends is an important area of investigation for various fields of study. Civil engineers are interested in the presence of channel scour as a variable of consideration in design criteria for infrastructure such as pipelines and bridges; also, when managing flood scenarios and computing flood routing and discharges through a channel network the presence of scour may play an appreciable role. Geomorphologists are interested in an examination of how streams evolve, particularly with respect to how sediment is transported and what sorts of bed-forms are produced. Open channel flows for agricultural irrigation canals have also been investigated (Vargha, 1948), which is another area of interest for the formation of scour during flooding.

Fluvial stratigraphers are interested in the types of surfaces that are preserved in the rock record and what can be gleaned about the fluvial system when examining those surfaces in outcrop. Growing interest exists for the identification criteria of fluvial scours at the outcrop. Similarly, surfaces resolved in well-log data or present in cores taken from water or oil and gas wells may owe their origin to scour and therefore an atypically thick section of channel deposits may exist locally around the well-bore that is not laterally extensive—an important fact to consider when inferring changes of base-level or climate of the system. Finally, economic geologists have interest in scours as possible locations of placer deposits of heavy metals (i.e., gold) or base-metal sulfide minerals (Mosley and Schumm, 1977).

#### *4.1.1. Characteristic Fluid Flow at Confluences*

Fluid flow characteristics at channel confluences are complex and need to be understood in a three-dimensional sense. Investigations of flow characteristics at channel junctions have typically been in a laboratory, which can be dated back to Taylor (1944). He experimented with open channel flows of the same width and depth that met at angles of 45° and 135°. Trilita et al. (2010) stated that the experimental results were in agreement with calculated results for the 45° junction, but not for the 135°. Other notable studies are those of Chow (1959) and Lin and Soong

(1979). In a series of papers, Best (1987; 1988) created a confluence flume to examine the intricacies of flow dynamics in sediment-free, rectangular channels, then latter examined how earlier findings effect sediment discharge and bed morphology. Figures 53 and 54 show some of the characteristics of flow in two dimensions. The studies mentioned above, with the exception of Best (1988), were more interested in what is happening with the fluids rather than the effects on stream beds

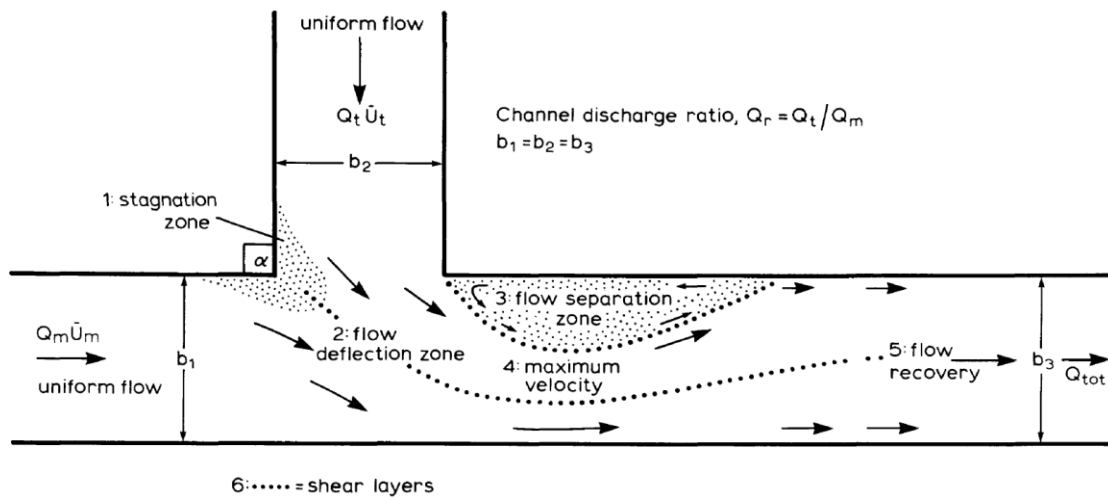


Figure 53: Flow dynamics at channel junctions. Notice the presence of zones of stagnation, flow separation, and maximum velocity. This work was originally examined by Taylor (1944) and expounded upon in subsequent years. From Best (1987).

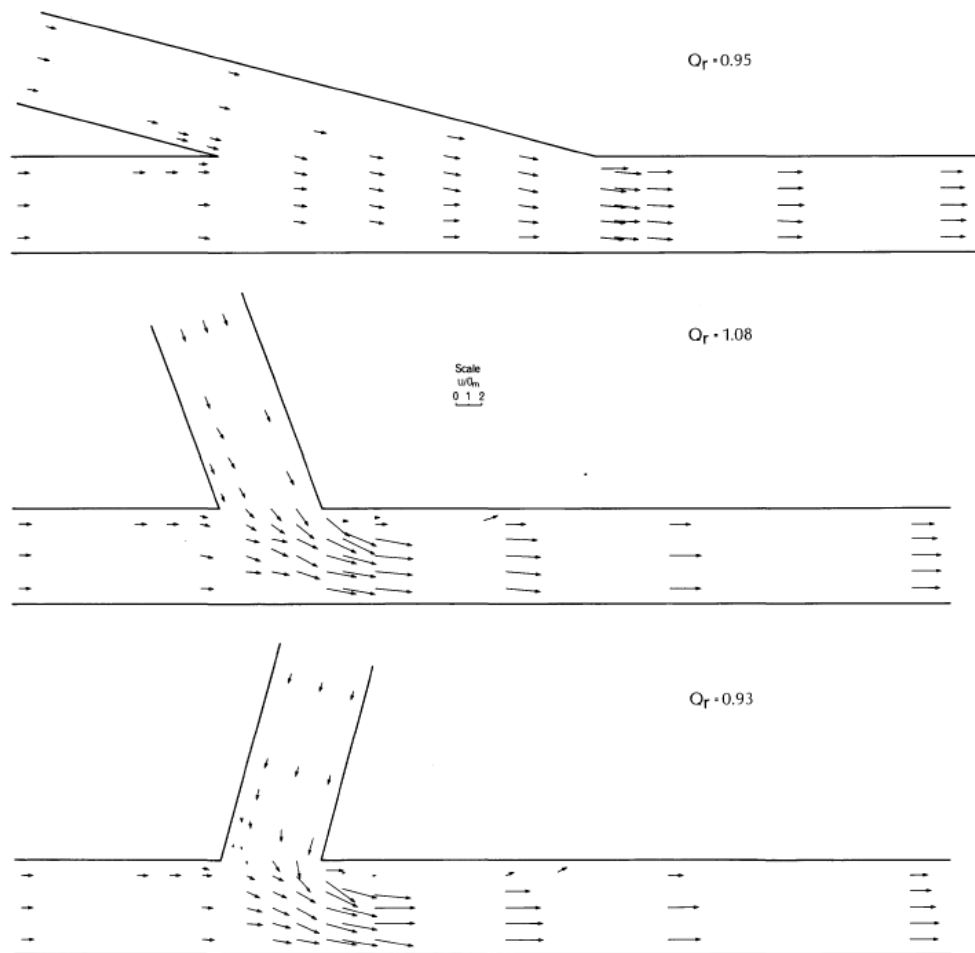


Figure 54: Velocity vectors of stream flow at channel junctions. From Best, 1987.

#### 4.1.2. Flume Studies and Field Investigations of Channel Scour

Much of the work that specifically examined channel scours were carried out in the controlled environment of flume studies (e.g., Mosley, 1976). Field experiments of natural rivers (e.g., Rhoads and Sukhodolov, 2001; Riley and Rhoads, *in press*; Roy and Bergeron, 1990), do exist in the literature. Probably the most notable of field investigations is the work Best and Asworth (1997) on the Brahmaputra river that culminated in a paper in the high-impact factor journal called *Nature*. Their work followed the evolution of changes in a braided stream system

using bathymetric surveys spanning several years of data collection, the end of studying showing an area of ~15m of channel erosion (Figure 55).

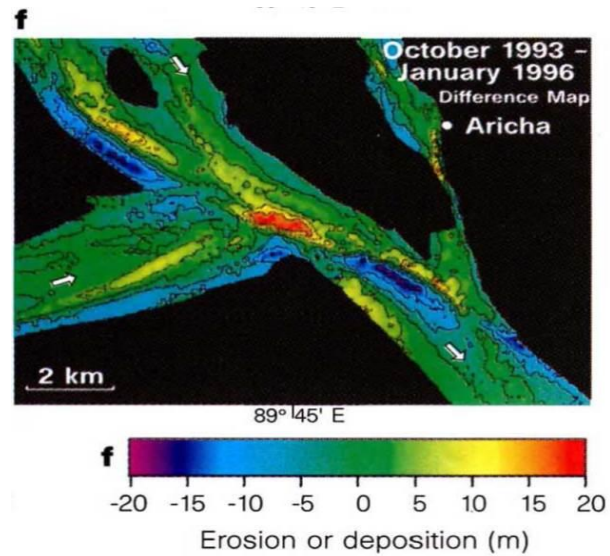


Figure 55: Channel scour in a modern braided stream. (Best and Ashworth, 1997)

Mosley (1976) is a key flume experiment investigating scour. His work pointed to the importance of what he termed “helical flow cells” in the origin of scour at confluences (Figure 56).

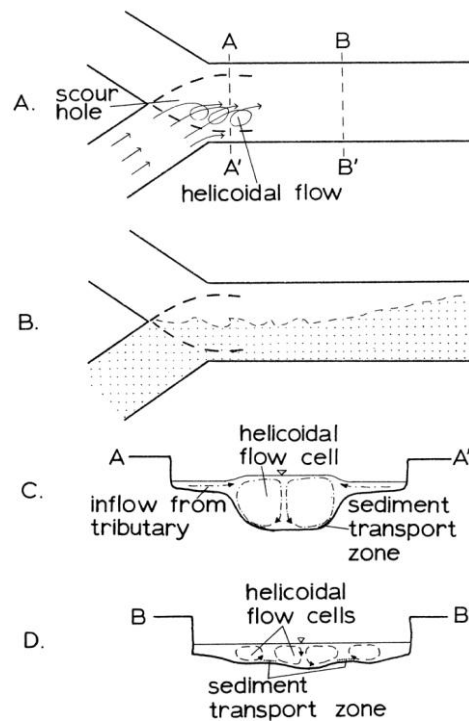


Figure 56: Diagrams showing fluid flow dynamics at a stream channel junction (a) location of scour hole in relation to streams, and locations of cross sections A-A', and B-B'; (b) mixing of stream channel waters view from above; (c) cross section A-A' showing fluid flow dynamics (d) cross section B-B' showing fluid flow dynamics. From Mosely, (1976)

The helicoidal cells form from an increase in water discharge locally at the confluence of two tributaries of equal depth. Paola (1997), in his letter included in *Nature* introducing the work of Best and Ashworth (1997), similarly wrote about the importance of helicoidal flow which locally forms an area of downwelling surface waters (Figure 57).

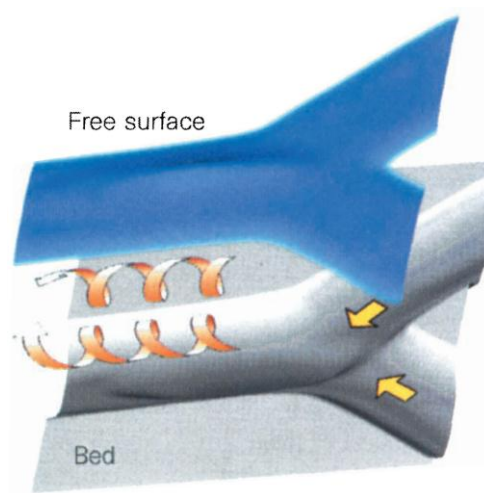


Figure 57: Depiction of helicoidal flow as shown by Paola (1987).

The role of helical vortex's, particularly where the two tributaries that contribute to the confluence are of equal depth (e.g., Paola, 1997), is fairly well understood. Where flow is of unequal depth, the helicoidal flow may not originate.

Biron et al. (1993) and Serres et al. (1999) worked field locations where the confluence of the contributing tributary channels were of unequal depth. They found that when the above condition is true, channel scour may not form, an important fact to consider when examining confluence scour.

Other field studies of note are the work of Salter (1993), and Ashmore and Parker (1983). Salter (1993) looked at modern rivers in an attempt to examine models of scour and overall fluvial incision. Of interest to this work was his observation that the preservation potential of fluvial scours is very high. Ashmore and Parker (1983) examined flume studies in conjunction with field data. They stated that scour depths can be as much as six time the channel depth, which is higher than the value reported by—perhaps the more famous study—of five times the channel depth reported by Best and Ashworth (1997).

## 4.2 Methods

The CHILD model recreated fluvial scour in the original surface (Figure 29, Figure 58).

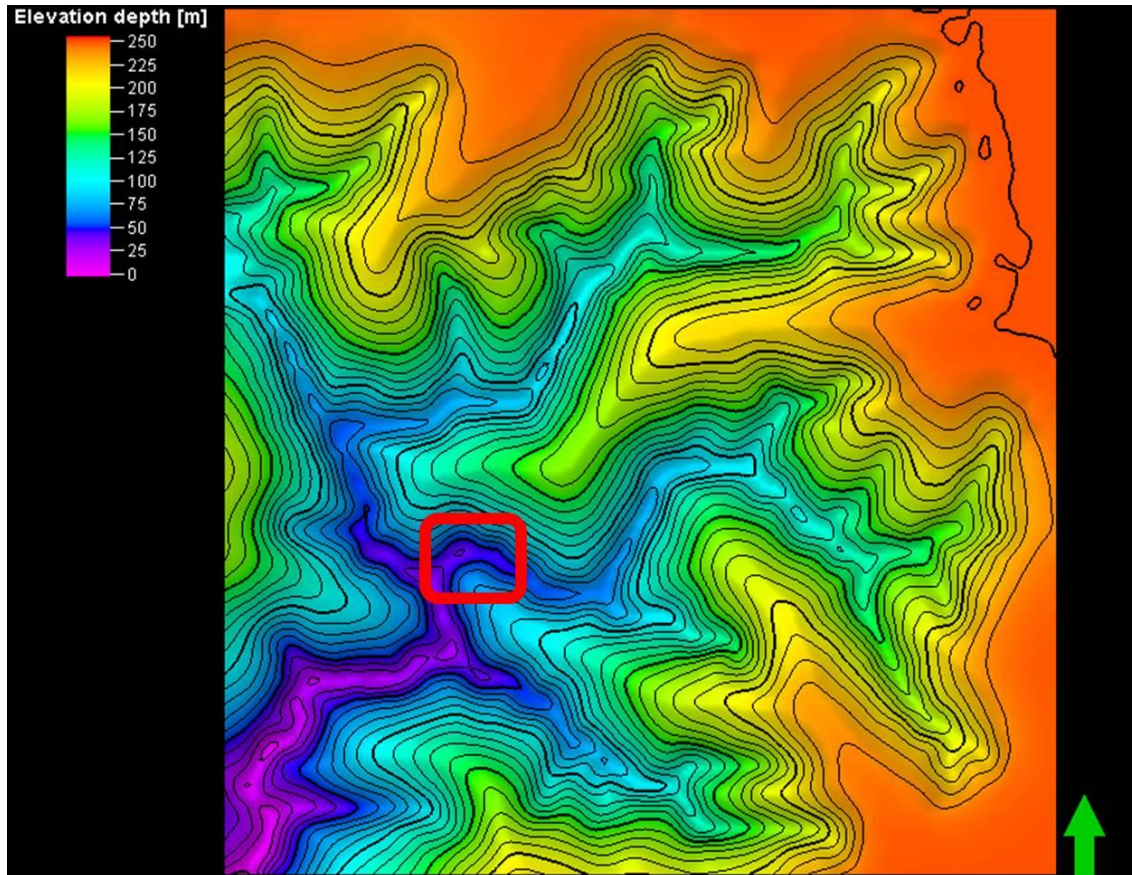


Figure 58: Original landscape used in this study with a red outline showing the location of both channel-bend scour and confluence scour examined in the following figures.

The presence of scour on surfaces created by the model was an unexpected outcome, though, one worthy of discussion. They, in effect, add credence to the model because the model captures a naturally occurring phenomenon. Particularly, it is well recognized that the numerical model is—though complicated overall—is simplistic when trying to capture all the variables at play in a natural system.



The primary change that occurs at channel-bends and at stream confluences in the system is the increase in water discharge. To examine exactly what the model was doing to create local scour, data output files were examined and displayed in the Petrel software used in earlier chapters to display results of CHILD runs. Water discharge was examined by displaying the values in cubic meters per minute for the basin (Figure 59).

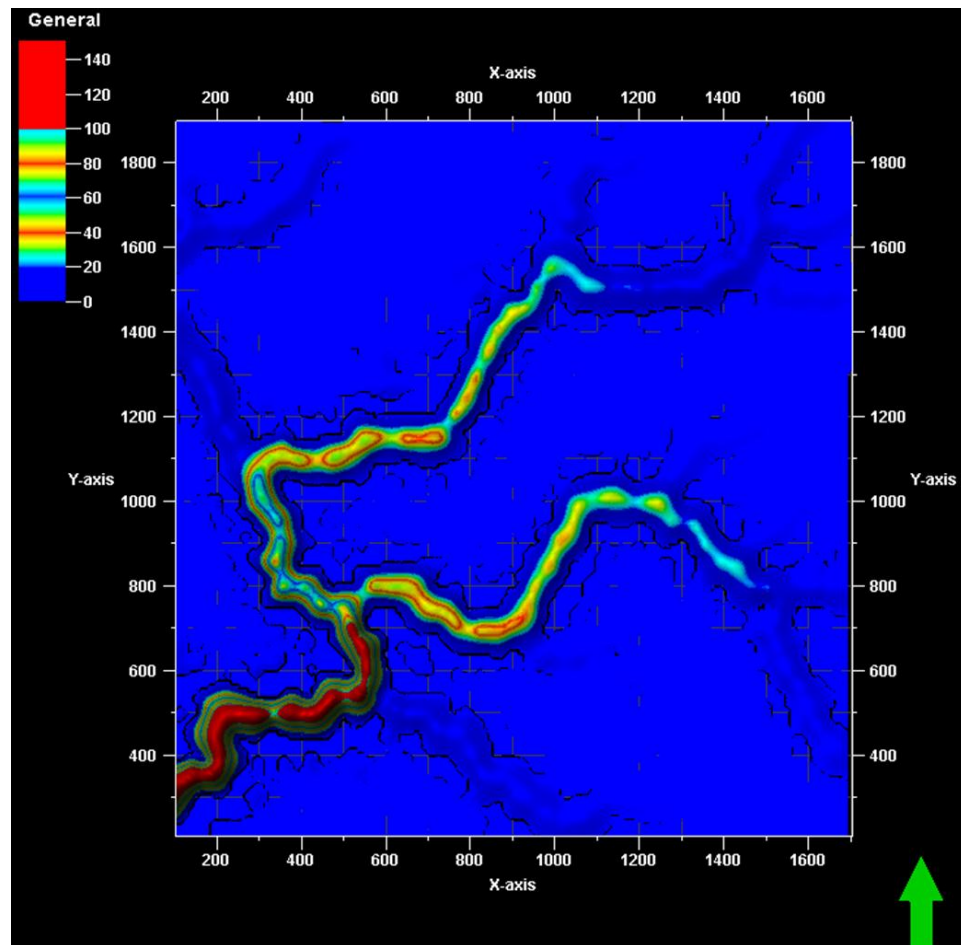


Figure 59: Water discharge across the basin in cubic meters per minute; color bar adjusted to show slight increases at channel-bends and at confluences.

A closer examination of those data was also done in Petrel by displaying values of sediment and water discharge next to the actual nodes comprising the surface. Figure 60 is a

close-up of the area delineated on Figure 58. What we see is an increase in discharge at the channel-bend, as well as at the confluence of two higher-order streams in the basin.

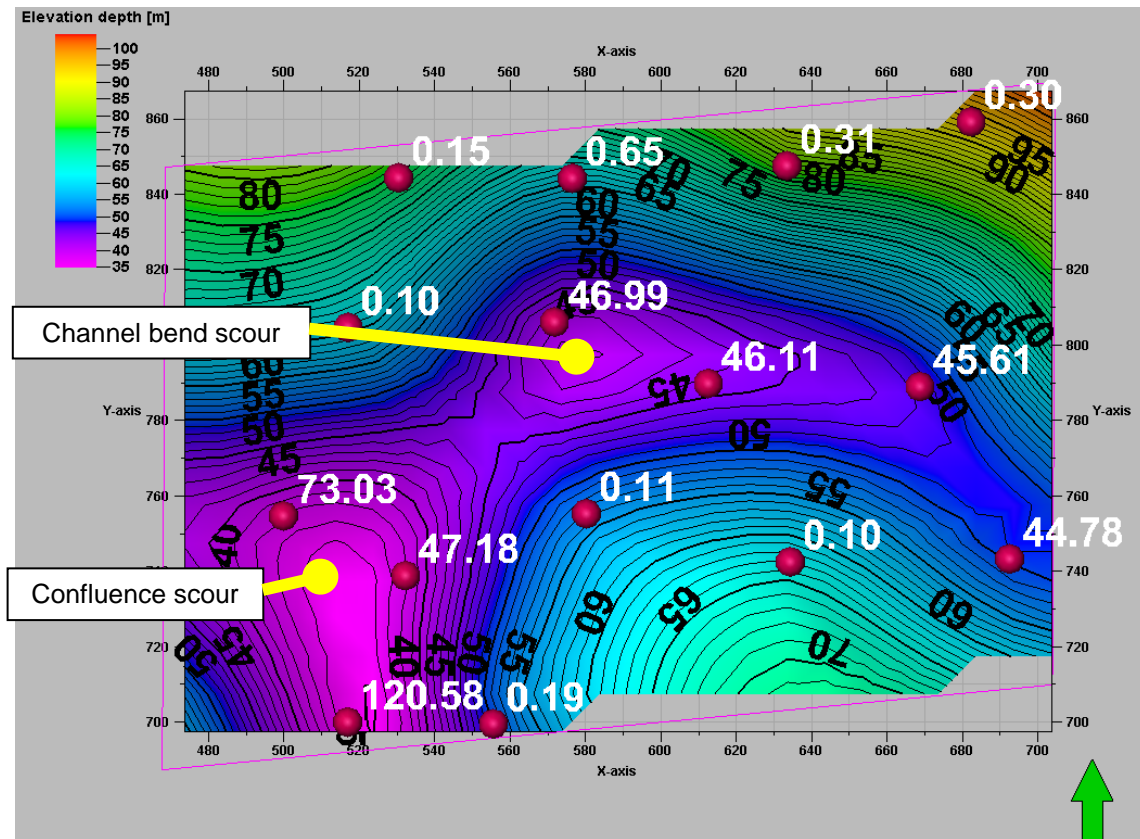


Figure 60: Water discharge in cubic meters per minute shown in white; contours of elevation shown in black. Notice that a slight increase in discharge exists at the bend in the channel to 46.99.

Increase in water discharge at the channel-bend does not necessarily correspond to an increase in bed shear stress, as is shown in Figure 61.

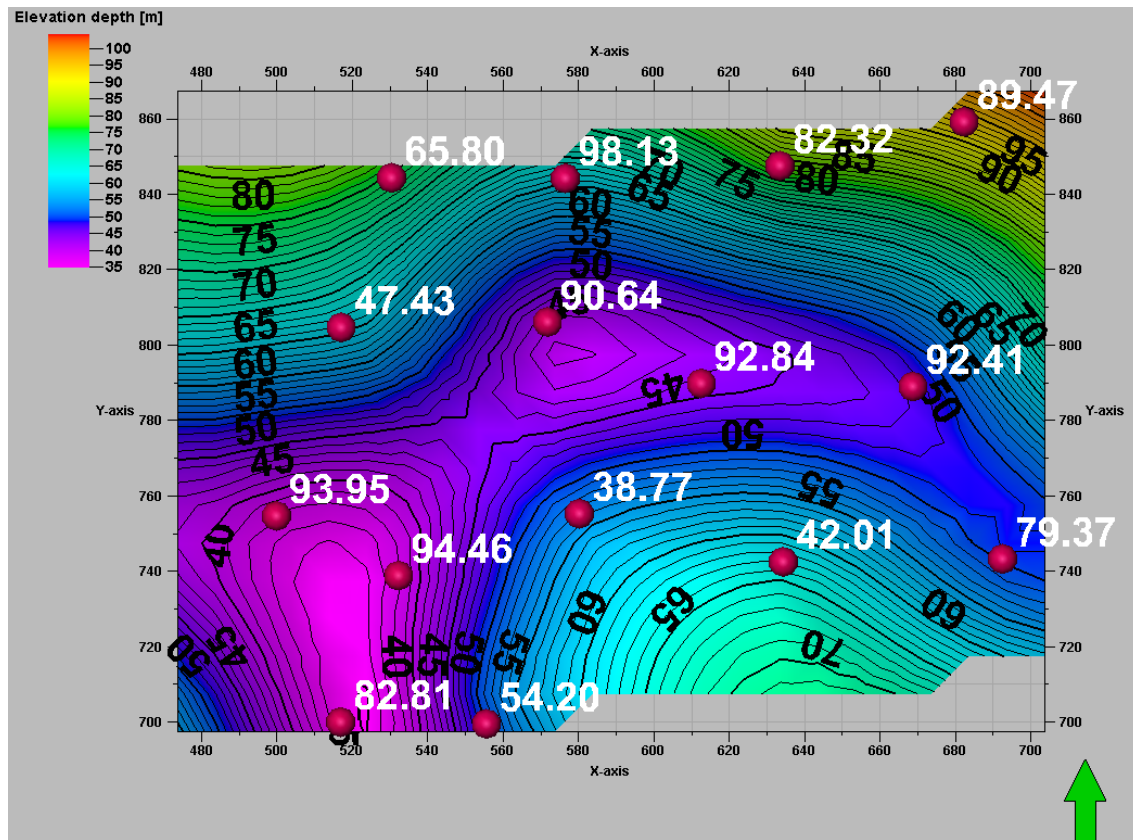


Figure 61: Shear stresses in pascals shown in white at nodes comprising the surface. Elevations shown in black. Notice that at the channel-bend where an increase in water discharge exists, an increase in bed shear stress does not necessarily exist (the value of 90.64 at the bend, down from 92.84 just upstream).

Fluvial scours are the result of purely autocyclic processes. What the CHILD model has recreated, teased out through the high resolution surfaces produced by Petrel from CHILD outputs, is fluvial scour at confluences and channel-bends in response to an increase in water discharge. A substantial increase in bed shear stresses, or even a slight increase, isn't necessary. Though CHILD does not model the flow of fluids and therefore the presence of back to back helicoidal vortices, it does accommodate increased discharge in the stream system by locally scouring the stream bed.

## CHAPTER 5

### 5.1. Conclusions

The primary goal of this research was to ascertain the controls on the aggradation in fluvial valleys. This research has found the following:

- The role of vegetation is key to aggradation; it is not so much climate change, but rather the change in vegetation as a result of climate change that liberates sediment from the headlands of first-order valleys and deposits sediment in the higher order valleys that triggers the aggradation phase of aggradation/incision cycles..
- Buffer Zones are at a minimum thickness at the drainage divides, thicken as they approach the medial areas of the drainage basin, and thin as the buttress is approached.
- Rates of aggradation occur most quickly for equilibrium landscapes with slopes at angle of repose, and slow as the hillslope angles of the drainage basin shallow.
- The upper buffer limit of preservation is approached slowly due to the fact that the drivers of aggradation are weakening. As the landscape shallows in overall hillslope dip angles, the shear stresses generated by the streams decreases overall, leading to slower rates of aggradation.
- Aggradation occurs when depositional dip angles of streams for both small and large catchments shallow.
- Though one expects that a drop in critical shear stress to erode vegetation would lead to rapid incision, the opposite is true. Drop in critical shear stress allows

- sediment to be liberated from steep valley-heads and choke the alluvial valleys within the buffer zone.

## REFERENCES

- Ahnert, F., 1977, Some Comments on Quantitative Formulation of Geomorphological Processes in a Theoretical-Model: *Earth Surface Processes and Landforms*, v. 2, p. 191-201.
- Alley, R. B., 2000, The Younger Dryas cold interval as viewed from central Greenland: *Quaternary Science Reviews*, v. 19, p. 213-226.
- Ashmore, P., and G. Parker, 1983, Confluence scour in coarse braided streams: *Water Resources Research*, v. 19, p. 392-402.
- Baker, S. E., J. C. Gosse, E. V. McDonald, E. B. Evenson, and O. Martínez, 2009, Quaternary history of the piedmont reach of Río Diamante, Argentina: *Journal of South American Earth Sciences*, v. 28, p. 54-73.
- Barry, J. J., J. M. Buffington, P. Goodwin, M. Asce, J. G. King, and W. W. Emmett, 2008, Performance of bed-load transport equations relative to geomorphic significance: Predicting effective discharge and its transport rate: *Journal of Hydraulic Engineering-Asce*, v. 134, p. 601-615.
- Best, J. L., 1987, Flow dynamics at river channel confluences; implications for sediment transport and bed morphology: *Special Publication - Society of Economic Paleontologists and Mineralogists*, v. 39, p. 27-35.
- Best, J. L., 1988, Sediment Transport and Bed Morphology at River Channel Confluences: *Sedimentology*, v. 35, p. 481-498.
- Best, J. L., and P. J. Ashworth, 1997, Scour in large braided rivers, and the recognition of sequence stratigraphic boundaries: *Nature*, v. 387, p. 275-277.
- Biron, P., A. Roy, J. L. Best, and C. J. Boyer, 1993, Bed morphology and sedimentology at the confluence of unequal depth channels: *Geomorphology*, v. 8, p. 115-129.
- Blum, M. D., 1993, Genesis and architecture of incised valley fill sequences; a late Quaternary example from the Colorado River, Gulf Coastal Plain of Texas: *AAPG Memoir*, v. 58, p. 259-283.
- Blum, M. D., and A. Aslan, 2006, Signatures of climate vs. sea-level change within incised valley-fill successions: Quaternary examples from the Texas Gulf Coast: *Sedimentary Geology*, v. 190, p. 177-211.
- Blum, M. D., and D. M. Price, 1998, Quaternary alluvial plain construction in response to glacio-eustatic and climatic controls, Texas Gulf Coastal Plain: *Special Publication - Society for Sedimentary Geology*, v. 59, p. 31-48.
- Blum, M. D., and S. Valastro, 1994, Late Quaternary Sedimentation, Lower Colorado River, Gulf Coastal-Plain of Texas: *Geological Society of America Bulletin*, v. 106, p. 1002-1016.
- Bolton, W. R., L. Hinzman, and K. Yoshikawa, 2004, Water balance dynamics of three small catchments in a Sub-Arctic boreal forest: *Northern Research Basins Water Balance*, v. 290, p. 213-223.
- Bull, W. B., 1990, Stream-terrace genesis; implications for soil development: *Geomorphology*, v. 3, p. 351-367.
- Burnett, A. W., and S. A. Schumm, 1983, Alluvial-River Response to Neotectonic Deformation in Louisiana and Mississippi: *Science*, v. 222, p. 49-50.
- Catuneanu, O., V. Abreub, J. P. Bhattacharya, M. D. Blum, R. W. Dalrymple, P. G. Eriksson, C. R. Fielding, W. L. Fisher, W. E. Galloway, M. R. Gibling, K. A. Giles, J. M. Holbrook, R. Jordan, C. G. S. C. Kendall, B. Macurda, O. J. Martinsen, A. D. Miall, J. E. Neal, D. Nummedal, L. Pomar, H. W. Posamentier, B. R. Pratt, J. F. Sarg, K. W. Shanley, R. J.

- Steel, A. Strasser, M. E. Tucker, and C. Winker, 2009, Towards the standardization of sequence stratigraphy: *Earth-Science Reviews*, v. 92, p. 1-33.
- Chow, V., 1959, *Open-Channel Hydraulics*: New York, McGraw-Hill, 690 p.
- Collins, D. B. G., R. L. Bras, and G. E. Tucker, 2004, Modeling the effects of vegetation-erosion coupling on landscape evolution: *Journal of Geophysical Research-Earth Surface*, v. 109.
- Cross, T. A., and M. A. Lessenger, 1998, Sediment volume partitioning: rationale for stratigraphic model evaluation and high-resolution stratigraphic correlation: *Sequence Stratigraphy - Concepts and Applications*, p. 171-195.
- Crowley, T. J., and G. R. North, 1988, Abrupt Climate Change and Extinction Events in Earth History: *Science*, v. 240, p. 996-1002.
- D'Antoni, H. L., 1983, Pollen Analysis of Gruta del Indio, Quaternary of South America and Antarctic Peninsula, p. 83 - 104.
- Dansgaard, W., J. W. C. White, and S. J. Johnsen, 1989, The Abrupt Termination of the Younger Dryas Climate Event: *Nature*, v. 339, p. 532-534.
- Davis, W. M., 1902, Baselevel, Grade and Peneplain: *The Journal of Geology*, v. 10, p. 77-111.
- De Serres, B., A. G. Roy, P. M. Biron, and J. L. Best, 1999, Three-dimensional structure of flow at a confluence of river channels with discordant beds: *Geomorphology*, v. 26, p. 313-335.
- Dietrich, W. E., D. G. Bellugi, L. S. Sklar, J. D. Stock, A. M. Heimsath, and J. J. Roering, 2003, Geomorphic transport laws for predicting landscape form and dynamics: *Geophysical Monograph*, v. 135, p. 103-132.
- Eagleson, P. S., 1978, *Climate, Soil, and Vegetation .1. Introduction to Water-Balance Dynamics*: Water Resources Research, v. 14, p. 705-712.
- Einstein, H. A., 1950, The bed-load function for sediment transportation in open channel flows: Technical Bulletin 1026, Washington, D.C., U.S. Department of Agriculture, p. 78.
- Emiliani, C., 1954, Temperatures of Pacific Bottom Waters and Polar Superficial Waters during the Tertiary: *Science (New York, N.Y.)*, v. 119, p. 853-5.
- Emiliani, C., 1955, Pleistocene temperatures: *Journal of Geology*, v. 63, p. 538-578.
- Feldman, H. R., M. R. Gibling, A. W. Archer, W. G. Wightman, and W. P. Lanier, 1995, Stratigraphic Architecture of the Tonganoxie Paleovalley Fill (Lower Virgilian) in Northeastern Kansas: *AAPG Bulletin*, v. 79, p. 1019-1043.
- Fischenich, C., 2001, Stability Thresholds for Stream Restoration Materials, ERDC Technical Note No. EMRRP-SR-29, Vicksburg, MS, U.S. Army Engineer Research and Development Center, p. 10.
- Fischenich, J. C., and S. R. Abt, 1995, Estimating flow resistance in vegetated channels: Proceedings of the 1995 First international conference on Water resources engineering: New York, NY, American Society of Civil Engineers, 805-809 p.
- Flint, J. J., 1974, Stream Gradient as a Function of Order, Magnitude, and discharge: *Water Resources Research*, v. 10, p. 969-973.
- Freund, R., I. Zak, and Garfunke.Z, 1968, Age and Rate of Sinistral Movement along Dead Sea Rift: *Nature*, v. 220, p. 253-&.
- Gasparini, N. M., R. L. Bras, and G. E. Tucker, 2008, Numerical Predictions of the Sensitivity of Grain Size and Channel Slope to an Increase in Precipitation, *in* S. P. Rice, A. G. Roy, and B. L. Rhoads, eds., *River Confluences, Tributaries and the Fluvial Network*: Chichester, England, Wiley, p. 367 - 394.
- Gibling, M. R., 2006, Width and thickness of fluvial channel bodies and valley fills in the geological record: A literature compilation and classification: *Journal of Sedimentary Research*, v. 76, p. 731-770.
- Gilbert, G. K., 1877, Geological investigations in the Henry Mountains of Utah: *The American Naturalist*, v. 11, p. 447.

- Hack, J. T., 1957, Studies of longitudinal stream profiles in Virginia and Maryland: U. S. Geological Survey Professional Paper 294-B.
- Hajek, E. A., P. L. Heller, and B. A. Sheets, 2010, Significance of channel-belt clustering in alluvial basins: *Geology*, v. 38, p. 535-538.
- Hayes, A. G., O. Aharonson, J. I. Lunine, R. L. Kirk, H. A. Zebker, L. C. Wye, R. D. Lorenz, E. P. Turtle, P. Paillou, G. Mitri, S. D. Wall, E. R. Stofan, K. L. Mitchell, C. Elachi, and R. T. Cassini, 2011, Transient surface liquid in Titan's polar regions from Cassini: *Icarus*, v. 211, p. 655-671.
- Heller, P. L., H. Jones, C. Paola, and Anonymous, 2004, Autocyclic avulsion clusters in alluvial basins; example from the Maastrichtian/Paleocene of Wyoming: Abstracts with Programs - Geological Society of America, v. 36, p. 462.
- Hereford, R., 2002, Valley-fill alluviation during the Little Ice Age (ca. AD 1400-1880), Paria River basin and southern Colorado Plateau, United States: *Geological Society of America Bulletin*, v. 114, p. 1550-1563.
- Hofmann, M. H., A. Wroblewski, and R. Boyd, 2011, Mechanisms Controlling the Clustering of Fluvial Channels and the Compensational Stacking of Cluster Belts: *Journal of Sedimentary Research*, v. 81, p. 670-685.
- Holbrook, J., 2001, Origin, genetic interrelationships, and stratigraphy over the continuum of fluvial channel-form bounding surfaces: an illustration from middle Cretaceous strata, southeastern Colorado: *Sedimentary Geology*, v. 144, p. 179-222.
- Holbrook, J., R. W. Scott, and F. E. Oboh-Ikuenobe, 2006, Base-level buffers and buttresses: A model for upstream versus downstream control on fluvial geometry and architecture within sequences: *Journal of Sedimentary Research*, v. 76, p. 162-174.
- Holbrook, J. M., 1996, Complex fluvial response to low gradients at maximum regression: A genetic link between smooth sequence-boundary morphology and architecture of overlying sheet sandstone: *Journal of Sedimentary Research*, v. 66, p. 713-722.
- Holbrook, J. M., and R. W. Dunbar, 1992, Depositional History of Lower Cretaceous Strata in Northeastern New-Mexico - Implications for Regional Tectonics and Depositional Sequences: *Geological Society of America Bulletin*, v. 104, p. 802-813.
- Howard, K. A., S. C. Lundstrom, D. V. Malmon, and S. J. Hook, 2008, Age, distribution, and formation of late Cenozoic paleovalleys of the lower Colorado River and their relation to river aggradation and degradation, in M. C. Reheis, R. Hershler, and D. M. Miller, eds., *Late Cenozoic Drainage History of the Southwestern Great Basin and Lower Colorado River Region: Geologic and Biotic Perspectives: Geological Society of America Special Papers*, v. 439, p. 391-410.
- Jones, L. S., M. Rosenburg, M. d. M. Figueroa, K. McKee, B. Haravitch, and J. Hunter, 2010, Holocene valley-floor deposition and incision in a small drainage basin in western Colorado, USA: *Quaternary Research*, v. 74, p. 199-206.
- Klinger, Y., J. P. Avouac, N. Abou Karaki, L. Dorbath, D. Bourles, and J. L. Reyss, 2000, Slip rate on the Dead Sea transform fault in northern Araba valley (Jordan): *Geophysical Journal International*, v. 142, p. 755-768.
- Ladekarl, U. L., K. R. Rasmussen, S. Christensen, K. H. Jensen, and B. Hansen, 2005, Groundwater recharge and evapotranspiration for two natural ecosystems covered with oak and heather: *Journal of Hydrology*, v. 300, p. 76-99.
- Lambeck, K., and J. Chappell, 2001, Sea level change through the last glacial cycle: *Science*, v. 292, p. 679-686.
- Lane, E. W., 1955, The Importance of Fluvial Morphology in Hydraulic Engineering: *Proceedings of the American Society of Civil Engineers*, v. 81.
- Leopold, L. B., and T. Maddock, 1953, The hydraulic geometry of stream channels and physiographic implications: U. S. Geological Survey Professional Paper 252.



- Levander, A., B. Schmandt, M. S. Miller, K. Liu, K. E. Karlstrom, R. S. Crow, C. T. A. Lee, and E. D. Humphreys, 2011, Continuing Colorado plateau uplift by delamination-style convective lithospheric downwelling: *Nature*, v. 472, p. 461-465.
- Lick, W., L. J. Jin, and J. Gailani, 2004, Initiation of movement of quartz particles: *Journal of Hydraulic Engineering-Asce*, v. 130, p. 755-761.
- Lin, J. D., and H. K. Soong, 1979, Junction losses in open channel flows: *Water Resources Research*, v. 15, p. 414-418.
- Lundstrom, S. C., S. A. Mahan, J. B. Paces, M. R. Hudson, P. K. House, and D. V. Malm, 2008, Late Pleistocene aggradation and degradation of the lower Colorado River: Perspectives from the Cottonwood area and other reconnaissance below Boulder Canyon: Late Cenozoic Drainage History of the Southwestern Great Basin and Lower Colorado River Region: *Geologic and Biotic Perspectives*, v. 439, p. 411-432.
- MacDonald, L., and I. Larsen, 2009, Effects of Forest Fires and Post-fire Rehabilitation, *Fire Effects on Soils and Restoration Strategies*, Science Publishers, p. 423-452.
- Mack, G. H., W. R. Seager, M. R. Leeder, M. Perez-Arlucea, and S. L. Salyards, 2006, Pliocene and Quaternary history of the Rio Grande, the axial river of the southern Rio Grande rift, New Mexico, USA: *Earth-Science Reviews*, v. 79, p. 141-162.
- Mackin, J. H., 1937, Erosional history of the Big Horn Basin, Wyoming: *Geological Society of America Bulletin*, v. 48, p. 813-893.
- Mackin, J. H., 1948, Concept of the graded river: *Geological Society of America Bulletin*, v. 59, p. 463-511.
- Macklin, M. G., B. T. Rumsby, and T. Heap, 1992, Flood Alluviation and Entrenchment - Holocene Valley-Floor Development and Transformation in the British Uplands: *Geological Society of America Bulletin*, v. 104, p. 631-643.
- Maddy, D., M. G. Macklin, and J. C. Woodward, 2001, Fluvial archives of environmental change: *River Basin Sediment Systems: Archives of Environmental Change*, p. 3-18.
- Malin, M. C., and K. S. Edgett, 2000, Evidence for recent groundwater seepage and surface runoff on Mars: *Science*, v. 288, p. 2330-2335.
- Martin, Y., 2003, Evaluation of bed load transport formulae using field evidence from the Vedder River, British Columbia: *Geomorphology*, v. 53, p. 75-95.
- Meyer-Peter, E., and R. Muller, 1948, Formulas for Bed-Load Transport: *Proceedings of the 2nd Meeting of the International Association for Hydraulic Structures Research*, p. 39 - 64.
- Miller, M. C., I. N. McCave, and P. D. Komar, 1977, Threshold of Sediment Motion Under Unidirectional Currents: *Sedimentology*, v. 24, p. 507-527.
- Mosley, M. P., 1976, Experimental-Study of Channel Confluences: *Journal of Geology*, v. 84, p. 535-562.
- Mosley, M. P., and S. A. Schumm, 1977, Stream Junctions - Probably Location for Bedrock Placers: *Economic Geology*, v. 72, p. 691-694.
- Oreskes, N., K. Shraderfrechette, and K. Belitz, 1994, Verification, Validation, and Confirmation of Numerical-Models in the Earth-Sciences: *Science*, v. 263, p. 641-646.
- Paola, C., 1997, *Geomorphology - When streams collide*: *Nature*, v. 387, p. 232-233.
- Pazzaglia, F. J., in press, *Fluvial Terraces*, in E. Wohl, ed., *Treatise on Geomorphology*, v. 9: San Diego, CA, Academic Press.
- Phillips, J. D., 2009, The job of the river: *Earth Surface Processes and Landforms*, v. 35, p. 305-313.
- Plint, A. G., 2002, Paleovalley systems in the Upper Cretaceous Dunvegan Formation, Alberta and British Columbia: *Bulletin of Canadian Petroleum Geology*, v. 50, p. 277-296.
- Powell, J. W., 1875, *Exploration of the Colorado River of the West and its tributaries*, v. Washington, DC, Publisher unknown.
- Reid, L. M., 1989, *Channel Formation by Surface Runoff in Grassland Catchments*, University of Washington, Seattle, Washington, 135 p.

- Rhoads, B. L., and A. N. Sukhodolov, 2001, Field investigation of three-dimensional flow structure at stream confluences; 1, Thermal mixing and time-averaged velocities: *Water Resources Research*, v. 37, p. 2393-2410.
- Riley, J. D., and B. L. Rhoads, *in press*, Flow structure and channel morphology at a natural confluent meander bend: *Geomorphology*.
- Rittenour, T. M., M. D. Blum, and R. J. Goble, 2007, Fluvial evolution of the lower Mississippi River valley during the last 100 k.y. glacial cycle: Response to glaciation and sea-level change: *Geological Society of America Bulletin*, v. 119, p. 586-608.
- Roering, J. J., J. W. Kirchner, and W. E. Dietrich, 2002, Hillslope evolution by nonlinear, slope-dependent transport: Steady state morphology and equilibrium adjustment timescales (vol 106, pg 16499, 2001): *Journal of Geophysical Research-Solid Earth*, v. 107.
- Romme, W. H., C. D. Allen, J. D. Balley, W. L. Baker, B. T. Bestelmeyer, P. M. Brown, K. S. Eisenhart, M. L. Floyd, D. W. Huffman, B. F. Jacobs, R. F. Miller, E. H. Muldavin, T. W. Swetnam, R. J. Tausch, and P. J. Weisberg, 2009, Historical and Modern Disturbance Regimes, Stand Structures, and Landscape Dynamics in Pinon-Juniper Vegetation of the Western United States: *Rangeland Ecology & Management*, v. 62, p. 203-222.
- Roy, A., and N. Bergeron, 1990, Flow and particle paths at a natural river confluence with coarse bed material: *Geomorphology*, v. 3, p. 99-112.
- Rumsby, B. T., and M. G. Macklin, 1994, Channel and Floodplain Response to Recent Abrupt Climate-Change - The Tyne Basin, Northern England: *Earth Surface Processes and Landforms*, v. 19, p. 499-515.
- Salter, T., 1993, Fluvial scour and incision; models for their influence on the development of realistic reservoir geometries: *Geological Society Special Publications*, v. 73, p. 33-51.
- Schumm, S. A., 2005, River variability and complexity. [electronic resource], Cambridge, Cambridge Univ Press, p. p.
- Schumm, S. A., and Anonymous, 1993, River response to baselevel change; implications for sequence stratigraphy: *Journal of Geology*, v. 101, p. 279-294.
- Shulits, S., 1972, Rational Equation of River Bed Profile: *River morphology*, Dowden, Hutchinson & Ross; Reprint, 201-210 p.
- Snyder, N. P., K. X. Whipple, G. E. Tucker, and D. J. Merritts, 2000, Landscape response to tectonic forcing: Digital elevation model analysis of stream profiles in the Mendocino triple junction region, northern California: *Geological Society of America Bulletin*, v. 112, p. 1250-1263.
- Stemerdink, C., D. Maddy, D. R. Bridgland, and A. Veldkamp, 2010, The construction of a palaeodischarge time series for use in a study of fluvial system development of the Middle to Late Pleistocene Upper Thames: *Journal of Quaternary Science*, v. 25, p. 447-460.
- Strong, N., and C. Paola, 2008, Valleys that never were: time surfaces versus stratigraphic surfaces: *Journal of Sedimentary Research*, v. 78, p. 579-593.
- Swanson, F. J., 1981, Fire and geomorphic processes: General Technical Report WO, p. 401-420.
- Sylvia, D. A., and W. E. Galloway, 2006, Morphology and stratigraphy of the late Quaternary lower Brazos valley: Implications for paleo-climate, discharge and sediment delivery: *Sedimentary Geology*, v. 190, p. 159-175.
- Talling, P. J., 2000, Self-organization of river networks to threshold states: *Water Resources Research*, v. 36, p. 1119-1128.
- Tarboton, D. G., R. L. Bras, and I. Rodrigueziturbe, 1989, Scaling and Elevation in River Networks: *Water Resources Research*, v. 25, p. 2037-2051.
- Taylor, E. H., 1944, Flow Characteristics at Open Channel Junctions: *Transactions of the American Society of Civil Engineers*, v. 109, p. 19.
- Taylor, K. C., P. A. Mayewski, R. B. Alley, E. J. Brook, A. J. Gow, P. M. Grootes, D. A. Meese, E. S. Saltzman, J. P. Severinghaus, M. S. Twickler, J. W. C. White, S. Whitlow, and G.

- A. Zielinski, 1997, The Holocene Younger Dryas transition recorded at Summit, Greenland: *Science*, v. 278, p. 825-827.
- Taylor, M. P., M. G. Macklin, and K. Hudson-Edwards, 2000, River sedimentation and fluvial response to Holocene environmental change in the Yorkshire Ouse Basin, northern England: *Holocene*, v. 10, p. 201-212.
- Tebbens, L. A., and A. Veldkamp, 2001, Exploring the possibilities and limitations of modelling Quaternary fluvial dynamics: a case study of the River Meuse: *River Basin Sediment Systems: Archives of Environmental Change*, p. 469-484.
- Trilita, M. N., N. Anwar, D. Legono, and B. Widodo, 2010, Dividing Streamline Formation Channel Confluences by Physical Modeling: *The Journal for Technology and Science*, v. 21, p. 7.
- Tucker, G., S. Lancaster, N. Gasparini, and R. Bras, 2001, The Channel-Hillslope Integrated Landscape Development model (CHILD)  
Landscape erosion and evolution modeling, v. New York, NY, Kluwer Academic/Plenum Publishers, 349-388 p.
- Tucker, G. E., 2009, CHILD Users Guide, Version R9.4.0, Boulder, Colorado, Cooperative Institute for Research in Environmental Sciences,  
<http://csdms.colorado.edu/wiki/Model:CHILD>.
- Tucker, G. E., L. Arnold, R. L. Bras, H. Flores, E. Istanbuluoglu, and P. Solyom, 2006, Headwater channel dynamics in semiarid rangelands, Colorado high plains, USA: *Geological Society of America Bulletin*, v. 118, p. 959-974.
- Tucker, G. E., and D. N. Bradley, 2010, Trouble with diffusion: Reassessing hillslope erosion laws with a particle-based model: *Journal of Geophysical Research-Earth Surface*, v. 115.
- Tucker, G. E., and G. R. Hancock, 2010, Modelling landscape evolution: *Earth Surface Processes and Landforms*, v. 35, p. 28-50.
- Tucker, G. E., and R. Slingerland, 1997, Drainage basin responses to climate change: *Water Resources Research*, v. 33, p. 2031-2047.
- Vail, P. R., 1977, AAPG-SEG School on Stratigraphic Interpretation of Seismic Data: *Geophysics*, v. 42, p. 189-189.
- Van Wagoner, J. C., 1992, Sequence stratigraphy and facies architecture of the incised-valley fills in the lower Sego Sandstone, Book Cliffs in eastern Utah and western Colorado: *Annual Meeting Expanded Abstracts - American Association of Petroleum Geologists*, v. 1992, p. 134.
- Vandenbergh, J., 1995, Timescales, climate and river development: *Quaternary Science Reviews*, v. 14, p. 631-638.
- Vandenbergh, J., 2003, Climate forcing of fluvial system development: an evolution of ideas: *Quaternary Science Reviews*, v. 22, p. 2053-2060.
- Vandenbergh, J., and D. Maddy, 2001, The response of river systems to climate change: *Quaternary International*, v. 79, p. 1-3.
- Vargha, A. M., 1948, Le problème de l'hydraulique agricole et de l'irrigation en Iran, Paris-Sorbonne, 348 p.
- Veldkamp, A., and J. J. van Dijke, 1998, Modelling long-term erosion and sedimentation processes in fluvial systems; a case study for the Allier/Loire system: *Palaeohydrology and environmental change*: Chichester, John Wiley & Sons, 53-66 p.
- Wegmann, K. W., and F. J. Pazzaglia, 2002, Holocene strath terraces, climate change, and active tectonics: The Clearwater River basin, Olympic Peninsula, Washington State: *Geological Society of America Bulletin*, v. 114, p. 731-744.
- Weimer, R. J., 1984, Relation of unconformities, tectonics, and sea-level changes, Cretaceous of Western Interior, U.S.A: *AAPG Memoir*, v. 36, p. 7-35.
- Willgoose, G., R. L. Bras, and I. Rodrigueziturbe, 1991, Results from a New Model of River Basin Evolution: *Earth Surface Processes and Landforms*, v. 16, p. 237-254.

- Willgoose, G. R., and S. Sharmeen, 2006, A One-dimensional model for simulating armouring and erosion on hillslopes: I. Model development and event-scale dynamics: *Earth Surface Processes and Landforms*, v. 31, p. 970-991.
- Yalin, M. S., 1992, *River mechanics*, Oxford ;New York, Pergamon Press, p. xv, 219 p.
- Yatsu, E., 1955, On the longitudinal profile of the graded river: *Transactions - American Geophysical Union*, v. 36, p. 655-663.
- Zachos, J., M. Pagani, L. Sloan, E. Thomas, and K. Billups, 2001, Trends, rhythms, and aberrations in global climate 65 Ma to present: *Science*, v. 292, p. 686-693.

## BIOGRAPHICAL INFORMATION

Ron Tingook holds B.Sc. and M.Sc. degrees in geology from the University of Hawaii, Hilo, and the Colorado School of Mines, respectively. His work and research interests revolve around the creation of models that strive to accurately depict the distribution of the various types of sedimentary rocks in the subsurface.